2010

Forced-Exercise Alleviates Neuropathic Pain in Experimental Diabetes: Effects on Voltage-Gated Calcium Channels

Sahadev A. Shankarappa
Loyola University Chicago

LOYOLA UNIVERSITY CHICAGO

FORCED-EXERCISE ALLEVIATES NEUROPATHIC PAIN IN EXPERIMENTAL DIABETES: EFFECTS ON VOLTAGE-GATED CALCIUM CHANNELS

A DISSERTATION SUBMITTED TO

THE FACULTY OF THE GRADUATE SCHOOL

IN CANDIDACY FOR THE DEGREE OF

DOCTOR OF PHILOSOPHY

PROGRAM IN NEUROSCIENCE

BY

SAHADEV A SHANKARAPPA

CHICAGO, ILLINOIS

MAY 2010

ACKNOWLEDGEMENTS

Firstly, I would like to acknowledge Dr. Evan B. Stubbs, Jr., who has been my graduate advisor, mentor, and racquetball teacher, for his guidance in helping me to understand, critically think, and do science in an organized and logical manner. I sincerely thank Dr. Erika S. Piedras-Rentería, who has been my second mentor, for all her help, suggestions, and guidance for the electrophysiology component of this dissertation. I also thank the members of my graduate committee, Dr. Edward J. Neafsey, Dr. Morris Fisher and Dr. Gwendolyn Kartje, for their valuable suggestions and encouragement.

I acknowledge the Arthur J Schmitt foundation for awarding me the Schmitt fellowship, and the Veteran Affairs department of rehabilitation services for the financial assistance, that made this study possible.

I would like to thank my colleagues, Dr. Jason Sarkey, Dr. Cynthia Von ee and Mr. Michael Richards, for their assistance, advice and encouragement during my graduate career.

I thank my mother, Gowthami; my father, Shankar; and my sister, Parvathi; for their unrelenting emotional support throughout my career. I thank my wife Shivanee, and my daughter Aarika without whom I would not have come this far.

“To my lovely wife Shivanee and my beautiful daughter Aarika

TABLE OF CONTENTS

LIST OF TABLES

LIST OF FIGURES

LIST OF ABBREVIATIONS

AGE Advanced Glycated End product

CDC Center for Disease Control

BBB Blood Brain Barrier

BNB Blood Nerve Barrier

CMAP Compound Muscle Action Potential

DAG Diacylglycerol

DHP Dihydropyridines

DPN Diabetic Polyneuropathy

DM Diabetes Mellitus

DRG Dorsal Root Ganglion

GLUT Glucose Transporter

HEK Human Embryonic Kidney

HHS Hyperglycemic Hyperosmolar State

HVA High Voltage Activated

JNK C-Jun B-terminal kinase

LVA Low Voltage Activated

MNCV Motor Nerve Conduction Velocity

NAD Nicotinamide Adenine Dinucleotide

PKC Protein Kinase C

RAGE Receptor for Advanced Glycated End product

RDNS Rochester Diabetic Neuropathy Study

SNCV Sensory Nerve Conduction Velocity

SSI Steady State Inactivation

STZ Streptozotocin

VGCC Voltage Gated Calcium channels

WHO World Health Organization

τ_{On} Tau On

τ_{Off} Tau Off

ABSTRACT

Diabetes mellitus (DM) is a metabolic disorder that affects an estimated 171 million people world wide. DM and its related complications are among the leading cause of adult blindness and renal failure in the developed nations. Equally alarming, greater than half of all patients with long-standing diabetes develop polyneuropathy, a debilitating progressive deterioration of peripheral and autonomic nerves. Currently, diabetic polyneuropathy (DPN) is untreatable. Maintenance of euglycemia as an indirect means of delaying the development of diabetic complications is the recommended therapeutic approach. Innovative treatment strategies designed to prevent or delay peripheral nerve injury in the diabetic patient are critically needed. Moderate exercise is a safe and integral approach to the management of patients with diabetes. Recent clinical studies suggest that exercise may help in the treatment of DPN. However, the mechanism by which exercise protects against diabetes-induced nerve dysfunction is unknown. In this dissertation we hypothesized that forced-exercise protects against experimental DPN by preventing glucose-associated alterations of voltage-gated calcium currents (VGCC) in small diameter dorsal root ganglion (DRG) neurons. Using behavioral, nerve-electrophysiology and patch-clamp methodology we examined the functional consequences of forced-exercise (treadmill, 5.4 km/week) on VGCC in dissociated small diameter DRG neurons from rats conferred diabetic by streptozotocin (STZ) treatment. Vehicle treated rats were used as controls. Exercised-STZ, rats in comparison to

sedentary-STZ, rats demonstrated a 4 week delay in the onset of tactile hyperalgesia that was independent of changes in blood glucose levels. Interestingly, forced-exercise induced protection against diabetes-induced tactile hyperalgesia was reversed in a dose dependent manner by the opioid antagonist, naloxone. Forced-Exercise also prevented peripheral nerve conduction deficits in STZ–treated rats. Small diameter DRG neurons harvested from hyperglycemic sedentary-STZ rats with demonstrated hyperalgesia exhibited 2-fold increase in peak high-voltage activated (HVA) Ca^{2+} current density and low-voltage activated (LVA) Ca^{2+} current component. The steady-state inactivation (SSI) (measure of channel availability) of LVA currents demonstrated a rightward shift in the sedentary-STZ rats (+7.5 mV shift; V_{50} = -50.9 ± 0.6 mV; vehicle treated rats V_{50} = -58.4 ± 0.9 mV). Forced-exercise prevented the increase in both, peak HVA Ca^{2+} current density and LVA SSI shift (V_{50} = -58.2 ± 1.4 mV), but did not alter LVA current component. We conclude that forced-exercise delayed the onset of diabetic tactile hyperalgesia by preventing the alteration of VGCCs in small diameter DRG neurons, possibly by decreasing total calcium influx and dampening neuronal over-excitability.

CHAPTER ONE

INTRODUCTION

STATEMENT OF PROBLEM

Diabetes mellitus (DM) is a group of metabolic disorders sharing hyperglycemia as a common phenotype that, when poorly managed, results in debilitating retinal, renal, and neurologic complications (Nathan, 1996). The prevalence of DM and its hyperglycemic-related complications are at near epidemic proportions in the U.S., affecting approximately 24 million Americans, or greater than 8% of the population (Center for Disease Control, 2005). In 2007, almost 25% of the population aged 60 years and above had diabetes. In addition, another 57 million people are estimated to have pre-diabetes, a condition that increases the risk of developing DM. (Center for Disease Control, 2008). Strikingly, DM is the seventh leading cause of death in the United States and globally 5% of all deaths are attributed to DM. Complications of DM, which include heart diseases, blindness, kidney failure, and lower limb amputations pose a significant financial burden on the health care system. The direct and indirect costs in the U.S. for medical services and lost productivity due to DM is approximately 132 billion dollars (Hogan et al., 2003).

Greater than half of all patients with DM develop neurological complications (Pirart, 1977). Although varied, the most common neurologic complication seen among

DM patients includes distal symmetric polyneuropathy (DPN), a progressive deterioration of the peripheral and autonomic nerves. DPN is causally associated with greater than 200,000 cases of diabetic foot ulcers and 71,000 amputations per year (Center for Disease Control, 2008). The primary risk factor for DPN is hyperglycemia (Perkins et al., 2001). Independent secondary risk factors include cigarette smoking, hypercholesterolemia, alcohol consumption and hypertension (Adler et al., 1997). Clinically, DPN is characterized by chronic peripheral pain described as a burning, pricking or tingling sensation with symmetric stocking glove distribution. Several pathogenic mechanisms have been proposed to explain the development of DPN, including activation of the polyol pathway secondary to hyperglycemia, accumulation of advanced glycation end products, vascular insufficiency, neurotrophic factor deficiency, and neuronal membrane ion channel dysfunction (Gooch and Podwall, 2004).

Current therapeutic interventions for the treatment of DPN are largely limited to pain management and strict glycemic control. Gabapentin, tricyclic antidepressants, duloxetine (serotonine-norepinephrine reuptake inhibitor), opioids, and topical capsaicin cream are currently prescribed, with mixed results. Results from clinical trials using nerve growth factor therapy, aldose reductase inhibitors, or acetyl carnitine have experienced limited success (Ziegler and Luft, 2002). Innovative interventional or preventive strategies are required to address the needs of the ever growing DPN patient population.

Exercise training, in combination with pharmacological intervention, is now

recognized as a cornerstone of treatment for DM. Aerobic exercise without or with resistance training has shown to have beneficial effects in DM (Castaneda et al., 2002). Previous studies have shown that long term aerobic exercise can modify the natural history of DPN in diabetic patients (Balducci et al., 2006). Physical exercise, in addition to improving blood glucose control, also exerts protective effects on cardiovascular and endothelial function (Maiorana et al., 2001; Fuchsjager-Mayrl et al., 2002). Less, however, is known about the effects of exercise on the onset and progression of diabetes associated complications including DPN (Tesfaye et al., 1992; Richardson et al., 2001).

Patients with DPN often exhibit hyperalgesia or enhanced sensitivity to pain (Baron et al., 2009), which contributes to the morbidity in diabetes. The cause of impaired pain tolerance remains unclear. Early experimental studies suggest that intermittent hyperglycemia damages sensory neurons and increases spontaneous C-fiber firing, resulting in neuropathic pain (Chen and Levine, 2001). Evidence to support a protective effect of moderate aerobic exercise against the development of neuropathic complications in diabetic patients is mounting (Balducci et al., 2006), raising interest in aerobic exercise as a putative therapeutic intervention for the management of pain in diabetic neuropathy. The cellular mechanism(s) by which neuropathic pain develops in the diabetic patient is poorly understood, but may involve remodeling of voltage- or ligand-gated ion channels (Hall et al., 1995; Cao, 2006; Jagodic et al., 2007), resulting in abnormal enhancement of sensory neuron excitability (Ikeda and Dunlap, 2007).

Little is known about the effect of exercise on the functioning of ion channels. Modulation of voltage gated calcium channels (VGCC) in response to exercise has been recently reported in swine coronary smooth muscle cells (Bowles, 2000) and treadmill trained rat ventricular myocytes (Wang et al., 2008). However, there have been no studies to date describing the effect of exercise on neuronal VGCC's associated with neuropathic pain.

In this dissertative research study, we examined whether exercise attenuates the onset and progression of diabetic neuropathy in an animal model of DM. Further, we examined whether forced-exercise can prevent or delay the onset of neuropathic pain by attenuating diabetes-associated increased functioning of voltage-gated calcium channels in the dorsal root ganglion neurons.

HYPOTHESIS

Forced-exercise will protect against the onset of tactile hyperalgesia in streptozotocin-induced hyperglycemic rats by preventing the over-activity of voltage-gated calcium channels in the small diameter dorsal root ganglion neurons.

SPECIFIC AIMS

This hypothesis will be tested using the following three Specific aims:

Specific Aim 1.

We will determine the effect of forced-exercise on the onset and progression of peripheral nerve injury in STZ-induced diabetic rats, as quantitated by evoked-response electrophysiology, tactile withdrawal threshold, and thermal-evoked hind-paw

withdrawal latency response times. Vehicle- and STZ-treated non-exercised rats will be included as sedentary controls for comparison.

Specific Aim 2.

We will determine the effect of forced-exercise on high- and low-voltage activated Ca^{2+} current densities and low-voltage activated Ca^{2+}channel steady state properties in small diameter dorsal root ganglion neurons harvested from STZ-treated rats, as quantitated by whole cell patch-clamp electrophysiology. Non-exercised veh-and STZ-treated rats will be used as controls.

Specific Aim 3.

We will determine the effect of high D-glucose on current densities, channel kinetics and steady state properties from HEK-293 cells stably transfected with the $Ca_V3.2$ α_{1H} channel subunit, using whole cell patch-clamp electrophysiology.

LITERATURE REVIEW

DIABETES MELLITUS

Insulin, produced by the β cells in the islets of Langerhans of the endocrine pancreas, is responsible for glucose uptake into cells of the liver, muscle and fat. Dysregulation of insulin production, secretion, or action results in abnormalities of blood glucose homeostasis, resulting in diabetes mellitus (DM). The syndrome of DM comprises a group of chronic disorders, sharing hyperglycemia as a common phenotype (Table 1). Overtime patients with long term DM develop multi-organ complications affecting the eye, kidney and peripheral/autonomic nerves (Nathan, 1996). The hallmark of DM is a sustained increase in blood glucose levels, with clinical diagnosis primarily based on blood glucose level measurements (Table 2).

DM is classified into several types (Table 1), of which DM type 1 and 2 (Himsworth, 1949) are more common. DM type 1 occurs as a result of autoimmunity that ultimately destroys the insulin- producing pancreatic β cells (Mandrup-Poulsen, 1996), leading to the development of severe hypoinsulinemia. The autoimmune processes are likely to be initiated by unknown environmental triggers in genetically susceptible individuals (Donner et al., 1997). In contrast, DM type 2 is a multi-factorial disease with genetic and life-style choices (poor eating habits, physical inactivity, chronic stress) playing a major role (Anderson et al., 2003). Type 2 DM in its initial phase exhibits enhanced insulin levels secondary to cellular insulin resistance and eventually demonstrates insulin deficiency (Reaven, 1988; Mahler and Adler, 1999). Increased

glucose production and decreased glycogen storage, secondary to insulin resistance in the liver, further contribute to the development of hyperglycemia in type 2 DM. Insulin resistance of adipocytes leads to enhanced free fatty acid flux from adipose tissue, which in turn increases liver lipid and triglyceride production resulting in dyslipidemia (Dennis L. Kasper, 2010).

	Primary Pathology	**Etiology**
Type 1 Diabetes Mellitus	β cell destruction leading to insulin deficiency	Auto immune mediated, Idiopathic
Type 2 Diabetes Mellitus	Peripheral resistance to insulin	Genetic, Life-style choices
Gestational Diabetes Mellitus	Reduced insulin secretion Enhanced insulin resistance	Idiopathic

Other types of Diabetes Mellitus:

Genetic defects in beta cell function and insulin action- Maturity onset diabetes of the young (MODY), Lipodystrophy syndromes

Disorders of the exocrine pancreas- Pancreatitis, Cystic fibrosis

Endocrinopathies – Acromegaly, Cushing's, Glucagonoma

Iatrogenic- Glucocorticoids, Clozapine, Thiazides

Table 1. Classification of Diabetes Mellitus

	Fasting	2 hr post prandial
Normal	< 100 mg/dL	< 140 mg/dL
Pre diabetes	100 – 125 mg/dL	140 – 200 mg/dL
Diabetes	≥ 126 mg/dL	≥ 200 mg/dL

Table 2. Clinical classification of glucose tolerance based on plasma glucose levels.

Epidemiology of DM

The prevalence of DM and its related complications are at near epidemic proportions. According to the World Health Organization, the prevalence for all age groups worldwide is 2.8% and is predicted to increase up to 4.4% by 2030 (Wild et al., 2004). In the U.S., DM affects an estimated 8% of the population (Center for Disease Control, 2005). In addition to human morbidity and mortality, DM and its complications represent a substantial economic burden on the health care system.

Complications of DM

Chronic complications of DM involve multiple organs and are responsible for the majority of mortality associated with diabetes. The incidence of complications increases along with the duration of hyperglycemia (U.K.prospective-diabetes-study, 1995), hence chronic complications are more common during the second decade of DM (Powers, 2006). Chronic complications of DM can be classified into non-vascular and vascular disorders. Vascular disorders affect both macro- and micro-vascular blood vessels leading to a host of pathological conditions involving the vasculature of the heart

(coronary artery disease), brain (cerebrovascular disease), eye (retinopathy), kidney (nephropathy), and nerves (neuropathy) (Mahler and Adler, 1999).

Acute complications of DM include ketoacidosis and hyperglycemic hyperosmolar state (HHS). Diabetic ketoacidosis and HHS are both potentially serious conditions characterized by severe hyperglycemia, blood electrolyte abnormalities, progressing to unconsciousness and if untreated, death (Umpierrez and Kitabchi, 2003; Kitabchi and Nyenwe, 2006).

DIABETIC NEUROPATHY

It is estimated that more than half of all patients with DM develop diabetic neuropathy. The prevalence varies from 1% within the first year of diagnosis of DM to more than 50% after 25 years (Pirart, 1977). The Rochester Diabetic Neuropathy Study found that approximately 66% of insulin-dependent DM patients and 59% of non-insulin dependent DM patients had some forms of diabetic neuropathy (Dyck et al., 1993).

The 'syndrome' of diabetic neuropathy is a microvascular complication of DM affecting the sensory, motor and autonomic nerves. Patients with diabetic neuropathy present with a wide range of symptoms from altered tactile sensations to cardiac arrhythmias. Table 3 summarizes the features of different types of diabetic neuropathies. Of the various types, symmetrical polyneuropathy, usually referred as diabetic polyneuropathy (DPN), is more common among the diabetic population. DPN patients exhibit altered perception to vibratory, tactile, pressure hot and cold stimuli along with slower nerve conduction velocity (Lipnick and Lee, 1996). DPN is associated with more than 71,000 foot amputations per year and 200,000 foot ulcers (CDC, 2007).

Pathogenic mechanisms of diabetes-associated nerve injury

Neurons, unlike muscle, liver, and fat, do not require insulin for glucose uptake (Greene and Winegrad, 1979). However, glucose is actively transported across the blood brain barrier (BBB) and the blood nerve barrier (BNB) for its metabolism (Rechthand et al., 1985; Kumagai et al., 1994). The endothelium of these vascular barriers uses the insulin-insensitive GLUT-1 transporter to facilitate glucose transport (Pardridge et al.,

1990). The absence of insulin-regulation in neurons makes these cells more prone to hyperglycemic insult (Thorburn et al., 1990).

Type	Primary Signs and Symptoms
Distal symmetric polyneuropathy	Paresthesias, numbness, hyperesthesias, ataxia
Diabetic polyradiculopathy	Severe disabling pain in the distribution of the affected nerve roots, with motor weakness
Diabetic mononeuropathy	Dysfunction of an isolated cranial nerve or peripheral nerve. Features include diplopia (III nerve is commonly affected), facial weakness and pain
Autonomic neuropathy	Cardiac arrhythmia, orthostasis, impotence and constipation

Table 3. Types, symptoms, and signs of diabetic neuropathy.

After its facilitated entry into the cell, D-glucose undergoes hexokinase mediated phosphorylation as it enters the glycolytic pathway. In contrast, the increased blood glucose load in diabetes saturates the hexokinase enzyme system. Rising intra-cellular glucose concentrations approach the K_m of aldose reductase, an enzyme that channels excess glucose into the polyol pathway (Oates, 2002). The main byproducts of the polyol pathway are sorbitol and fructose.

Sorbitol is a poorly permeable intracellular osmolyte that enables cells to maintain interstitial osmotic pressure. Accumulation of sorbitol results in osmotic disturbances within the cell which de-stabilizes the uptake of carrier proteins for other osmolytes like

myo-inositol and taurine (Bagnasco et al., 1986). Impaired *myo*-inositol-dependent phosphoinositide signaling pathway leads to reduced activity of the Na^+/K^+ ATPase, necessary for the maintenance of nerve action potential propagation and nerve conduction velocity (Nishimura et al., 1987). In neurons, activation of aldose reductase compromises the recycling of the antioxidant glutathione, by depletion of NADPH, resulting in the generation of damaging hydroxyl free radicals and concurrently altering the redox state of the cell.

Non-enzymatic glycation is another mechanism implicated in development of diabetic neuropathy. Reducing sugars like glucose and fructose non-enzymatically react with free amino groups of lipids, proteins and nucleic acids to form Schiff bases, ketamines, and Amadori products, which undergo slow spontaneous molecular arrangement (Amadori rearrangement) forming stable advanced glycation end-products (AGE) (Singh et al., 2001; Jakus and Rietbrock, 2004). Activation of AGE receptors (RAGE) leads to a variety of detrimental affects, including activation of pro-inflammatory cascades, sustained cellular dysfunction and tissue destruction (Ahmed et al., 2003; Haslbeck et al., 2007). Table 4 summarizes diabetes mediated cellular mechanisms that are implicated in nerve injury.

Mechanism	Key features
Polyol pathway	Increased sorbitol and fructose production Decreased NADPH Decreased glutathione Decreased myoinositol
Oxidative stress	Hydrogen peroxide formation DNA strand breakage
Glycation of proteins	Formation of advance glycated end-products (AGE) Activation of receptors for AGE (RAGE)
Dysfunctional intra-cellular signaling	Aberrant activation of MAP kinases
Reduced trophic support	Nerve growth factor, insulin like growth factor-1, brain derived trophic factor

Table 4. Mechanisms of diabetes induced nerve injury.

Neuropathic pain in diabetic neuropathy

Up to 20% of diabetic patients with neuropathy describe abnormal peripheral sensations (Boulton et al., 1983; Partanen et al., 1995), including spontaneous pain, exaggerated perception of pain to mildly noxious (hyperalgesia) or innocuous stimuli (allodynia), and the feeling of pins and needles (paresthesia). Painful diabetic neuropathy is extremely disabling and greatly affects the quality of life.

Altered nociception is reported in patients with either insulin dependent or insulin resistant DM, suggesting that the onset of pain is not entirely resultant from insulin

deficiency. Interestingly, healthy non-diabetic subjects show marked decreases in pain thresholds in response to glucose infusions (Morley et al., 1984). In some cases, diabetic patients demonstrate alleviation of neuropathic symptoms upon improved glycemic control (DCCT, 1995). However in some cases, pain persists for many years even after strict glycemic control (Calcutt, 2002). These findings suggest that blood glucose control alone is insufficient to prevent the development of altered nociception in DM.

Experimental animal models of diabetic neuropathy

Experimental animal models that demonstrate similar pathological features of DM and its associated complications are vital in understanding the pathogenesis of DPN. Animal models of DPN provide opportunities to design and test new treatment options for improved management of the neuropathic diabetic patient. As in human insulin-dependent diabetes, type 1 animal models of DM demonstrate characteristic features including insulitis (Zuccollo et al., 1999), pancreatic β cell death (Yang et al., 2003), and the involvement of immunological (Kay et al., 2000; Eizirik and Mandrup-Poulsen, 2001) and Major Histocompatability Complex (MHC) in disease development (Hashimoto et al., 1994; Martin et al., 1999). By comparison, the type 2 animal models, (Table 5) demonstrate insulin resistance and beta cell failure along with prominent characteristics similar to human type 2 DM, including obesity (Zhang et al., 1994), dyslipidaemia, and hypertension (Marquie et al., 1991; Ziv et al., 1999).

Animal Models of Type 1 DM	Animal Models of Type 2 DM
Drug induced • Streptozotocin, Alloxan Spontaneously insulin-dependent • Non-obese diabetic mouse (NOD) • Bio breeding rat (BB) • Long-Evans Tokushima lean rat • Keeshond dog • New Zealand white rabbit • Macaca Nigra	• ob/ob mouse (Leptin-deficient) • db/db mouse (Leptin-receptor deficient) • fa/fa Zucker rat (Obesity phenotype) • KK mouse • Goto Kakizaki rat (Non-obese) • NSY mouse • Israeli sand rat (Leptin-resistant) • Fat-fed streptozotocin-treated rat • Diabetic Torri rat (Non-obese) • New Zealand obese mouse • Otsuka LE Tokushima fatty rat

Table 5. Animal models of DM and its subtypes, modified from (Rees and Alcolado, 2005)

Streptozotocin (STZ)-induced DM

Streptozotocin [N-(methylnitrosocarbamoyl)-α-D-glucosamine] is an antineoplastic antibiotic produced from the gram positive bacteria, *Streptomyces achromogenes* (Brian Rodrigues, 1999). STZ is used mainly in the treatment of pancreatic islet cell tumors (Kouvaraki et al., 2004). While the diabetogenic property of STZ was first reported by Upjohn laboratories, Rakieten *et al*. first described the β-cell necrosis property of STZ (Rakieten et al., 1963).

The chemical structure of STZ comprises of a glucose molecule with a cytotoxic nitrosourea side chain. The glucose moiety directs the STZ molecule to the insulin producing pancreatic beta cells (Johansson and Tjalve, 1978), where it is selectively

taken up by GLUT-2 for transport into the pancreatic β cell (Kawada et al., 1987; Schnedl et al., 1994). Once inside, the nitroso moiety decomposes to form a highly reactive carbonium ion that causes DNA breaks by alkylating DNA bases (Uchigata et al., 1982). DNA damage activates poly (ADP-ribose) synthetase, a nuclear enzyme essential for DNA repair. NAD^+ is used as a substrate by poly (ADP-ribose) synthetase, and following STZ treatment, depletion of NAD^+ occurs within 20 minutes (Wilson et al., 1984). In addition to the DNA alkylating property of STZ, oxidative stress due to the production of hydrogen peroxide (Robbins et al., 1980) and nitric oxide have been proposed (Turk et al., 1993; Kwon et al., 1994).

Changes in blood glucose and insulin levels follow a triphasic pattern within the first 24h upon *in vivo* STZ administration. Initial hyperglycemia lasting for approximately 1h is followed by marked hypoglycemia (~6 h) due to the secondary release of pancreatic insulin, resultant from β cell degranulation (Junod et al., 1969). Stable hyperglycemia develops within 24h to 48 h and remains elevated three to four times the normal blood glucose level. Even though the STZ treated animals are insulin deficient, they neither develop diabetic ketoacidosis nor do they require exogenous insulin for survival (Junod et al., 1969; Brian Rodrigues, 1999). However complications similar to that seen in human DM do develop, including cardiac (Litwin et al., 1990), vasculature (Hill and Ege, 1994), retina (Bensaoula and Ottlecz, 2001), kidney (Okada et al., 1992) and the nervous system (Duran-Jimenez et al., 2009) abnormalities.

STZ-induced diabetic polyneuropathy

The STZ-treated rodent model used in this study develops peripheral nerve complications that closely mimic some of the changes seen human DPN. STZ-treated animals develop hyperalgesia to tactile (Ahlgren and Levine, 1993; Calcutt et al., 1996), thermal (Forman et al., 1986; Lee and McCarty, 1990), and chemical noxious stimuli (Courteix et al., 1993; Malmberg et al., 1993), defined here as neuropathic pain. Nerve morphological changes seen in STZ-induced DPN include decreased axonal fiber size (Medori et al., 1988; Yagihashi et al., 1990a), nodal swelling, and segmental demyelination (Sima et al., 1988b; Yagihashi et al., 1990b) with concomitant decreased nerve conduction velocity. Axonal degeneration and fiber loss, consistent findings in human diabetic neuropathy, however, is not observed in the STZ diabetic model (Malcangio and Tomlinson, 1998).

Treatment options in diabetic neuropathy

Current therapeutic interventions for the treatment of DPN are less than satisfactory. Strict glycemic control is still the mainstay of treatment, but blood glucose control alone does not prevent development or progression of DPN. Gabapentin, tricyclic antidepressants, duloxetine (serotonin-norepinephrine reuptake inhibitor), opioids and topical capsaicin are currently prescribed, with mixed results. Clinical trials using nerve growth factor replacement therapy, aldose reductase inhibitors, and acetyl carnitine supplementation have been largely disappointing. ***Innovative interventional or preventive strategies are critically needed to advance the care of patients with DPN.***

Exercise as a therapeutic strategy

Exercise has numerous beneficial effects that promote protection, both at the level of central and peripheral nervous system. In the central nervous system, exercise facilitates recovery from traumatic brain injury by normalizing the levels of myelin derived growth inhibitory molecules like MAG (myelin-associated glycoprotein) and Nogo-A, and promotes axonal growth (Chytrova et al., 2008). In spinal-cord injury (SCI) models, exercise promotes functional motor recovery by inducing axonal growth and synapse formation (Doyle and Roberts, 2004; Goldshmit et al., 2008). Exercise has also been used in combination with a wide variety of therapeutic measures including stem cells therapy (Carvalho et al., 2008; Foret et al., 2010), melatonin therapy (Park et al., 2010) and neurotrophin therapy (Nothias et al., 2005) in SCI animal models. Improvements in cognition and memory have been observed with exercise in animal models of aging and dementia (Kramer et al., 2006; Nichol et al., 2009). Exercise protects against diabetes-associated decreases in LTP (long-term potentiation) induction (Reisi et al., 2010), suggesting a facilitative role in synaptic plasticity. Overall, growing evidence supports a more than passive role of exercise in protection of neuronal function against a wide array of physiological and non-physiological CNS insults.

Moderate exercise is now considered a well established, safe, and integral approach to the management of patients with DM (Lynch et al., 1996; Knowler et al., 2002; Tanasescu et al., 2003). Recent studies have demonstrated that aerobic exercise significantly decreases the complications arising from DM induced microvascular lesions (Estacio et al., 1998). Therapeutic interventions such as aerobic exercise may enhance

blood flow to the peripheral nerves and improve outcome measures of diabetic neuropathy (Fisher et al., 2007). Exercise attenuates tactile hyperalgesia in a spinal cord injury model (Hutchinson et al., 2004). Smith *et al.* observed decreased diabetes-induced neuropathic pain and improved sural nerve responses with diet and exercise-mediated life style intervention. *There is however no mechanistic or observational data addressing the protective effect of exercise on neuropathic pain in experimental diabetes.*

Exercise and voltage-gated calcium channels

Voltage-gated Ca^{2+} channels (VGCC) are protein complexes present in the plamsa membrane of virtually all excitable cells. Plasma membrane depolarization triggers the opening of VGCC's, resulting in the rapid influx of extracellular Ca^{2+} which is known to be involved in various cellular processes including neurotransmitter release and cellular excitability. Recent studies have demonstrated that VGCC's play an important role in pain signaling. The cellular mechanism(s) by which neuropathic pain develops in the diabetic patient is poorly understood, but may involve remodeling of voltage- or ligand-gated ion channels (Carbone and Lux, 1984; Nowycky et al., 1985; Cao, 2006) leading to abnormal enhancement of sensory neuron excitability (Ikeda and Dunlap, 2007) and altered neurotransmitter release.

The impact of exercise on the function of voltage-gated ion channels remains unclear. Experimental exercise has been shown to *increase* L-type peak calcium current density in swine arterial smooth muscles (Bowles, 2000). In contrast, ventricular myocytes from swim-trained rats demonstrate *reduced* peak L-type Ca^{2+} current density, compared to sedentary controls (Wang et al., 2008). However, there is a deficit of

reported studies examining the effect of exercise on neuronal VGCC's associated with diabetes-induced neuropathic pain.

VOLTAGE GATED CALCIUM CHANNELS

The plasma membranes of virtually all excitable cells, including neurons express voltage gated calcium channels (VGCC). VGCC's are oligomeric protein complexes consisting of different central pore-forming α_1 subunit isoforms (Table 6), surrounded by several auxiliary subunits (β, $\alpha_2\delta$ and γ) which serve to modulate the function of the α_1 subunit (Castellano et al., 1993; Felix, 1999) (Figure 1B). The complex consists of four distinct domains (I-IV), each exhibiting six (S1-S6) helical membrane spanning regions. The S4 helices in each of the four domains are enriched with positively charged amino acid residues that allow the VGCC's to detect changes in membrane potential. The selective hydrophilic pore is formed by the coalescence of the reentrant p-loops between S5 and S6 of each of the four domains. Plasma membrane depolarization triggers the opening of VGCC's, resulting in the rapid influx of extracellular Ca^{2+} involved in various cellular processes including neuronal excitability and neurotransmitter release (Catterall, 2000; Cao, 2006) (Table 6).

There are several distinct families of VGCC's defined by various molecular, pharmacological, and genetic criteria (Tsien et al., 1988; Bean, 1989). In general, VGCC's can be characterized by their activation range into two basic categories, high-voltage (HVA) and low-voltage (LVA) activated Ca^{2+} channels. The HVA Ca^{2+} channels open in response to large change in membrane potentials and include the Ca_V1(L) and Ca_V2 (P, Q, N, R) families of calcium channels. The LVA Ca^{2+} channels open in response to small changes in membrane potential and include the Ca_V3 (T) family of Ca^{2+} channels.

Ca^{2+} Channel	α1 subunit	Gene	Current	Blocker	Localization	Function
$Ca_V1.1$	α_{1S}	CACNA1S	L	dyhdropyridine	Skeletal muscle	Calcium homeostasis, gene expression and excitation – contraction coupling
$Ca_V1.2$	α_{1C}	CACNA1C	L	dyhdropyridine	Cardiac muscle Neurons Endocrine cells	Excitation-contraction coupling, hormone secretion, gene regulation
$Ca_V1.3$	α_{1D}	CACNA1D	L	dyhdropyridine	Neurons, Endocrine cells	Hormone secretion and gene regulation
$Ca_V1.4$	α_{1F}	CACNA1F	L		Retina	Neurotransmitter release
$Ca_V2.1$	α_{1A}	CACNA1A	P/Q	ω-agatoxin 1Va	Nerve terminals Dendrites	Neurotransmitter release, dendritic Ca^{2+} transients
$Ca_V2.2$	α_{1B}	CACNA1B	N	ω-conotoxin-GVIA		Neurotransmitter release, dendritic Ca^{2+} transients
$Ca_V2.3$	α_{1E}	CACNA1E	R	SNX-482	Cell bodies, dendrites nerve terminals	Ca^{2+} dependent AP's neurotransmitter release, dendritic Ca^{2+} transients
$Ca_V3.1$	α_{1G}	CACNA1G	T	nickel ethosuximide mibefradil	Cardiac muscle Skeletal muscle Neuron	Action potential generation Rhythm pattern generation
$Ca_V3.2$	α_{1H}	CACNA1H	T	mibefradil	Cardiac muscle Neuron	Action potential generation Rhythm pattern generation
$Ca_V3.3$	α_{1I}	CACNA1I	T		Neuron	Rhythm pattern generation

Table 6. Pharmacology and function of the α1 Ca^{2+} channel subunit.

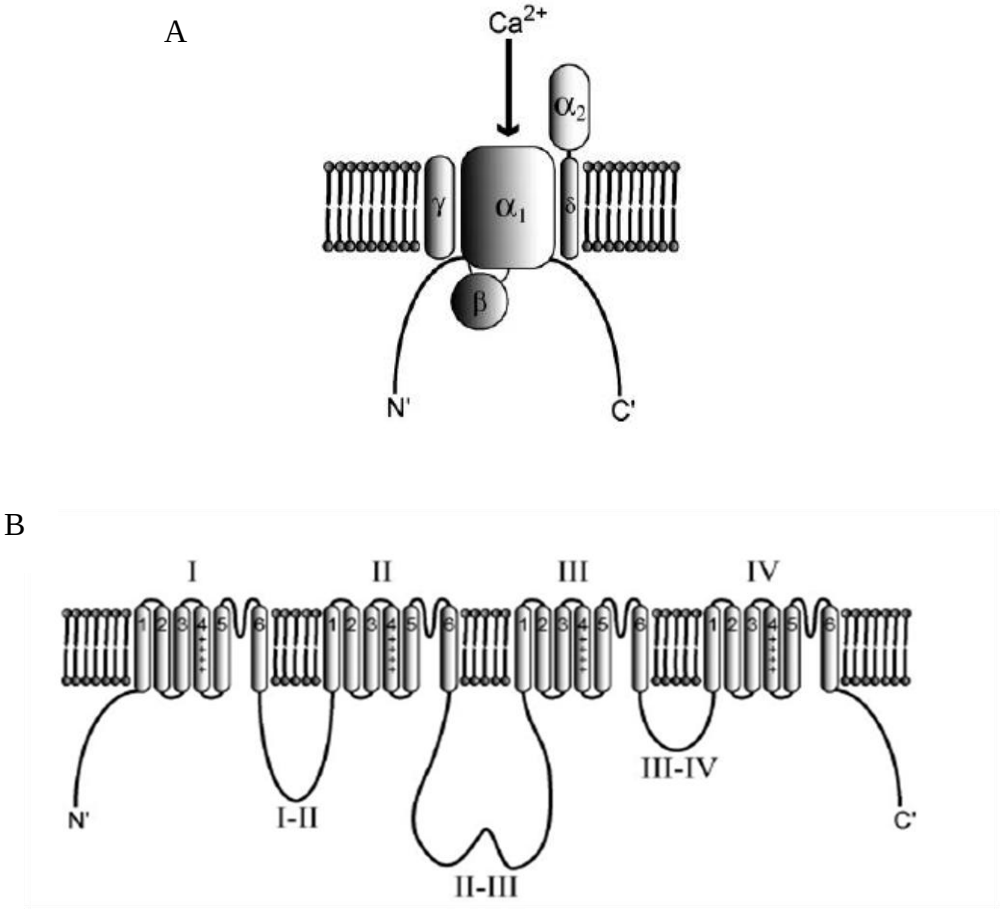

Figure 1. Schematic of voltage-gated calcium channel.

(A) Cartoon depicting the various subunits of the voltage-gated Ca^{2+} channel and (B) structural features of the central pore-forming α_1 subunit. Figure reproduced from (Tedford and Zamponi, 2006).

High-voltage activated Ca^{2+} channel isoforms

HVA Ca^{2+} channels activate in response to large changes in membrane potentials (Fox et al., 1987). Opening of some HVA Ca^{2+} channel types facilitates neurotransmitter release, excitation-contraction coupling, and secretion. The different HVA Ca^{2+} channels are described below.

Ca_V 1 (L- type) family of Ca^{2+} channels

L type currents are predominant in cardiac, smooth, skeletal muscles and brain. They are also present in endocrine cells, where they are known to play a role in hormone secretion (Milani et al., 1990). Ca_V 1 channels located on the cell body and dendrites of nerves regulate gene expression and integrate synaptic inputs (Bean, 1989). L type currents are distinguished by their high voltage dependence of activation, slower voltage dependent inactivation, relatively large single channel conductance, regulation by cAMP–dependent phosphorylation pathways, and sensitivity to dihydropyridines, phenylalkylamines and benzothiazepines (Reuter, 1983; Hadley and Lederer, 1991).

Ca_V 2 (P/Q, N, R - type) family of Ca^{2+} channels

Ca_V 2.1 (P/Q) Ca^{2+} channels are prominently expressed on the dendrites and pre-synaptic nerve terminal of neurons. Currents from the P – type Ca^{2+} channels were first recorded in the cerebellar Purkinje neuron (Llinas et al., 1989) and are characterized by high affinity binding of ω- agatoxin IVA (Mintz et al., 1992). In comparison the Q-type Ca^{2+} currents present in the cerebellar granule cells (Randall and Tsien, 1995) exhibit a lower affinity binding to ω- agatoxin IVA (Stea et al., 1994). P/Q-type channel currents are

primarily regulated by G protein coupled pathways (Hille, 1994) and are functionally involved in initiating synaptic transmission (Catterall, 2000).

The $Ca_V2.2$ (N-type) Ca^{2+} channels are expressed exclusively in the nervous system, with primary afferent sensory neurons and the superficial layer of the dorsal horn showing high expression levels (Bourinet and Zamponi, 2005). N-type currents are distinguished by their intermediate voltage dependence and a rate of inactivation which is more negative and faster than L-type currents but more positive and slower than T-type currents. The cone-snail peptide, ω-conotoxin GVIA irreversibly inhibits $Ca_V2.2$ Ca^{2+} channels and has been used as a primary tool to distinguish N-type from other Ca^{2+}currents. Modulation of $Ca_V2.2$ channel function is primarily through GPCR mediated pathways (Ikeda, 1996; Ikeda and Dunlap, 1999). Recently, Ca_V 2.2 channels have been implicated in pain signaling. In the superficial layer of the dorsal horn, Ca_V 2.2 Ca^{2+} channels regulate the release of the nociceptive neurotransmitters including glutamate and neuropeptides (Smith et al., 2002). Accordingly, Ca_V 2.2 channel knockout mice do not develop inflammatory or neuropathic pain associated mechanical hyperalgesia, suggesting a role for $Ca_V2.2$ channels in nociception (Kim et al., 2001; Saegusa et al., 2001).

The $Ca_V2.3$ (R-type) Ca^{2+} channel currents are known to be resistant to most Ca^{2+} channel blockers. These channels have been thought to play a crucial role in regulating the release of neurotransmitters (Wu et al., 1998; Albillos et al., 2000). Also, they may

participate in Ca^{2+} influx in response to action potentials (Magee and Johnston, 1995; Sabatini and Svoboda, 2000).

Low-voltage activated Ca^{2+} channels

Ca_V3 family (T-type) Ca^{2+} channels

The Ca_V3 family of calcium channels are activated by small depolarization of the cell membrane, hence commonly referred to as – low-voltage activated calcium channels. The Ca_V3 family comprises of three isoforms based on biophysical and pharmacological properties, namely $Ca_V3.1$ α_{1G}, $Ca_V3.2$ $\alpha_{1H,}$ and $Ca_V3.3$ α_{1I} (Cribbs et al., 1998; Perez-Reyes et al., 1998). The first recording of low-voltage activated calcium currents was made in mouse neuroblastoma cell line (N1E-115) (Moolenaar and Spector, 1978). T-type calcium channels are expressed in the nervous system (Carbone and Lux, 1984), the heart (Nilius et al., 1985), kidneys (Gordienko et al., 1994), endocrine organs, smooth muscles (Brueggemann et al., 2005) and sperm (Arnoult et al., 1996). They have been reported to be involved in the pathophysiology of cardiac arrhythmias (Satoh, 1995), sleep disorders (McCormick and Bal, 1997), epilepsy (Tsakiridou et al., 1995), nociception (Kim et al., 2003), and fertilization (Talavera and Nilius, 2006). Biologically, these channels modulate vital cellular functions including excitability (Chemin et al., 2002), secretion (Bhattacharjee et al., 1997), differentiation (Bijlenga et al., 2000), proliferation (Lory et al., 2006) and excitation-contraction coupling (Zhou and January, 1998).

T-type Ca^{2+} currents have several unique electrophysiological characteristics that separate them from the high-voltage activated calcium channels. T-type Ca^{2+} channels begin to activate after small depolarization of the cell membrane and exhibit rapidly inactivating transient currents in response to sustained depolarization. Upon repolarization, they close slowly resulting in the generation of tail currents with slow deactivation time constant. (Perez-Reyes, 2003). T-type Ca^{2+} channels open at small voltage ranges, but do not inactivate completely, resulting in window currents which may be essential for regulating intracellular Ca^{2+} concentration (Bijlenga et al., 2000).

Role of voltage-gated Ca^{2+} channels in neuropathic pain

Modulation and transmission of painful stimuli from the periphery to the CNS is mediated at the level of DRG by a variety of ion channels including the persistent Na^{+} channels, inward rectifying K^{+} channels and voltage gated Ca^{2+} channels (Woolf and Mannion, 1999; Julius and Basbaum, 2001). Recent studies have demonstrated that VGCC's play an important role in pain signaling. VGCC's modulate key aspects of pain transmission by regulating neuronal properties such as excitability, generation and propagation of action potential and release of nociceptive neurotransmitters in sensory neurons.

Voltage activated N-, T- and to some extent, P/Q-type Ca^{2+} channels are established mediators of pain signaling (Zamponi et al., 2009), while the role of L- and R-type in nociception is uncertain (Altier and Zamponi, 2004; Cao, 2006; Gribkoff, 2006). The N-type Ca^{2+} channels control the release of glutamate and substance P at the

pre-synaptic nerve terminals in the dorsal horn of the spinal cord (Smith et al., 2002), thereby supporting pain transmission from the periphery to the CNS. Moreover, engineered mice lacking N-type channels demonstrate decreased behavioral response to neuropathic pain stimuli suggesting their role in nociception (Hatakeyama et al., 2001; Saegusa et al., 2001). Recent studies have demonstrated the existence of multiple isoforms of the N-type channel, derived from alternative splicing of N-type mRNA (Pan and Lipscombe, 2000; Lin et al., 2004). Among the multiple isoforms, the e37a isoform is markedly expressed in nociceptive DRG neurons and is specifically required for the onset and maintenance of thermal and tactile hyperalgesia (Altier et al., 2007).

Neuromodulators/neurotransmitters such as endogenous opioids, endo-cannabinoids or GABA have been shown to regulate N-type calcium currents through G protein-coupled receptor signaling (Holz et al., 1986; Polo-Parada and Pilar, 1999). N-type channel inhibition occurs, in some cases, through direct interaction of the $G_{\beta\gamma}$ subunit with the intracellular loop between domains I and II (Figure 1) of the N-type α_1 subunit (De Waard et al., 1997; Herlitze et al., 1997). Although the $G_{\beta\gamma}$ subunits play a primary role in N-type Ca^{2+} channel regulation, there is evidence to suggest that other synapse associated proteins such as syntaxin1 may also regulate channel function (Stanley and Mirotznik, 1997).

Unlike the HVA N-type channels, the LVA T-type Ca^{2+} channels regulate the *excitability* of the sensory neurons (Catterall, 2000; Perez-Reyes, 2003) and play a key role in the generation of acute peripheral nociceptive signals (Bourinet et al., 2005;

Nelson and Todorovic, 2006). T-type channel modulation of neuronal activity results in enhanced neurotransmission and amplification of sensory afferent signals, along with increased pain perception (Perez-Reyes, 2003; Todorovic and Jevtovic-Todorovic, 2007). There is increasing experimental evidence to support a role for T-type Ca^{2+} channels in the development of neuropathic pain associated with peripheral nerve injury (Dogrul et al., 2003) and, more recently, with painful diabetic neuropathy (Jagodic et al., 2007; Messinger et al., 2009b).

T-type channels are typically resistant to modulation by conventional analgesic compounds. However, recent molecular, genetic and electrophysiological studies have described novel methods of T-type channel regulation that could have important implications in neuropathic pain management. Specifically, T-type channels are regulated by a number of cellular mechanisms including redox modulation. Reducing agents such as dithiothreitol and L-cysteine (L-cys) selectively enhance LVA calcium currents in small diameter DRG neurons. L-cys, DTT and other thiol containing L-cys analogs produce hyperalgesia when experimentally introduced into peripheral receptive fields. These agents are thought to sensitize C-type nociceptors that express T-type currents. Furthermore, agents that are capable of chelating zinc ions mimic and occlude the effects of L-cys and DTT whereas cysteine-modifying agents do not prevent the effects of reducing agents on T-currents in DRG neurons. These effects can be completely abolished by single-point mutations of histidine 191 to glutamine (H191Q) without affecting channel kinetics (Zamponi et al., 2009). The H191Q mutation disrupts high-

affinity zinc inhibition of $Ca_V3.2$ T-channel, suggesting that the effects of reducing agents may occur indirectly by dis-inhibition of the channels endogenous zinc ions.

The $Ca_V3.2$ T-channel isoform that is predominately expressed in nociceptive neurons is inhibited by the activation of G protein-coupled receptor signaling involving selective interaction of $G_{\beta 2\gamma 2}$ subunits to the channel α_1 subunit (Wolfe et al., 2003; DePuy et al., 2006). The $Ca_V3.2$ T-channel isoform has also been reported to be modulated by various compounds such as nitrous oxide (Todorovic et al., 2001), phenytoin (Todorovic and Lingle, 1998), certain neuroactive steroids (Pathirathna et al., 2005), endocannabinoids (Ross et al., 2009) and by the actin binding protein, Kelch-like 1 (Aromolaran et al., 2010). The exact molecular determinants of the T-type channel that is involved in this regulation is however, still unknown.

CHAPTER TWO

FORCED-EXERCISE ALLEVIATES NEUROPATHIC PAIN IN EXPERIMENTAL DIABETES: EFFECTS ON VOLTAGE-GATED CALCIUM CHANNELS

ABSTRACT

Exercise is now established as an integral adjunct to the management of diabetes. Diabetic polyneuropathy, a painful complication of diabetes, remains untreatable, emphasizing a critical need for improved therapeutic strategies. Recent evidence suggests that exercise may facilitate recovery of peripheral nerve function in the diabetic neuropathic patient. The mechanism by which exercise protects against peripheral nerve dysfunction in diabetes is unknown, but may involve correction of glucose-associated alterations of voltage-gated calcium currents (VGCC) in DRG neurons. Here, using a combination of behavioral and patch clamp methodology, we examined the functional consequences of exercise on VGCC in DRG neurons from streptozotocin (STZ)-induced diabetic rats. Compared to vehicle control, STZ-treated sedentary rats developed marked tactile hyperalgesia within two weeks of induction that was sustained for the 10-week duration of study. STZ-treated rats subjected to forced-exercise (treadmill, 5.4 km/week), by comparison, exhibited a significant delay in the onset of tactile hyperalgesia independent of changes in blood glucose control. Addition of the non-selective opiate receptor antagonist naloxone dose-dependently reversed the analgesic effect of forced-

exercise in STZ-treated rats. Compared to sedentary vehicle-treated rats, the dose-response to naloxone in exercised animals was rightward shifted. Small diameter DRG neurons harvested from STZ-treated sedentary hyperalgesic rats exhibited a 2-fold increase in peak high-voltage activated (HVA) calcium current density with a 10 mV rightward shift; the low-voltage activated (LVA) calcium current component was similarly enhanced 2-fold. Forced-exercise attenuated the diabetes-associated increase in HVA peak current density. Moreover, the observed shift in HVA peak current density by diabetes was normalized with forced-exercise. Steady-state inactivation (SSI) properties of LVA calcium channels in DRG neurons from STZ-treated sedentary hyperalgesic rats demonstrated a significant rightward shift (+8 mV; V_{50} = -50.9 ± 0.6 mV) that was prevented by forced-exercise (V_{50} = -58.2 ± 1.4 mV; vehicle-treated control rats SSI V_{50} = -58.4 ± 0.9 mV). However, diabetes-associated increase in LVA current component was unaffected by forced-exercise. These findings demonstrate that acute hyperglycemic-hypoinsulinemic insult elicits marked tactile hyperalgesia in the STZ-diabetic sedentary rat by enhancing calcium influx in small diameter nociceptive DRG neurons. This may occur, in part, by a mechanism that increases LVA calcium channel availability and enhances both HVA and LVA Ca^{2+} channel currents. Forced-exercise was found to significantly delay the onset of tactile hyperalgesia largely by preventing diabetes-associated changes in HVA and LVA channel functions.

INTRODUCTION

Poorly controlled diabetes often leads to impaired function of central, peripheral, and/or autonomic nerves (Emerick et al., 2005). As a result, nerve dysfunction associated with diabetes is best realized clinically as a heterogeneous disease that encompasses a wide range of neurologic abnormalities. Distal symmetrical polyneuropathy, the most common form of diabetic polyneuropathy, is particularly debilitating, affecting both large and small nerve fibers and altering a patient's stability, sensorimotor function, gait, and quality of life (Menz et al., 2004). The development of neuropathic pain including hyperalgesia/allodynia, burning, tingling, and/or numbness sensations in a length-dependent distribution, is prominent among diabetic patients and is strongly suggestive of small nerve fiber impairment (Tavee and Zhou, 2009). Approximately a third of patients with painful sensory neuropathy, and nearly half with otherwise idiopathic small fiber neuropathy, experience some form of impaired glucose tolerance or metabolic dysregulation (Singleton et al., 2001).

Lifestyle intervention designed to improve blood glucose control through weight management with diet and exercise significantly reduced by 58% the incidence of type 2 diabetes in high risk patients (Knowler et al., 2002). In a small cohort of pre-diabetic patients, Smith *et al.* (Smith et al., 2006) observed that lifestyle intervention similarly improved impaired glucose tolerance with significant preservation of intra-epidermal nerve fiber density, increased foot sweat volume (autonomic tone), and decreased neuropathic pain. The cause of neuropathic pain associated with impaired glucose tolerance, or with frank diabetes, remains unclear. Early experimental studies suggest that

intermittent hyperglycemia damages sensory neurons and increases spontaneous C-fiber firing, resulting in neuropathic pain (Chen and Levine, 2001).

The analgesic effect of exercise has been previously reported (Willow et al., 1980; Janal, 1996; O'Connor and Cook, 1999). Rats subjected to swimming exercise, demonstrate an attenuated response to inflammatory neuropathic pain (Kuphal et al., 2007). Mice subjected to treadmill running exhibited increased tail flick latencies to a heat stimulus (Blustein et al., 2006). Evidence supporting a protective effect of moderate aerobic exercise against the development of neuropathic complications in diabetic patients is mounting (Balducci et al., 2006), raising interest in aerobic exercise as a putative therapeutic intervention for the management of painful diabetic neuropathy. In a preliminary study, (Fisher et al., 2007) report that aerobic exercise statistically improves some measures of peripheral nerve function in diabetic patients with established length-dependent neuropathy.

The cellular mechanism(s) by which neuropathic pain develops in the diabetic patient is poorly understood, but may involve remodeling of voltage- or ligand-gated ion channels (Carbone and Lux, 1984; Nowycky et al., 1985; Cao, 2006) leading to abnormal enhancement of sensory neuron excitability (Ikeda and Dunlap, 2007). Voltage gated N- and T-type Ca^{2+} channels are established mediators of pain signaling and processing in afferent neurons (Zamponi et al., 2009). N-type Ca^{2+} channels are activated by large changes in membrane potential and regulate neurotransmitter release. By comparison, T-type Ca^{2+} channels are activated by small changes in membrane potential, thereby

regulating the excitability of the sensory neuron (Catterall, 2000; Perez-Reyes, 2003) and playing a key role in the generation of acute peripheral nociceptive signals (Bourinet et al., 2005; Nelson and Todorovic, 2006). There is increasing experimental evidence to support a role for T-type Ca^{2+} channels in the development of neuropathic pain associated with peripheral nerve injury (Dogrul et al., 2003) and, more recently, with painful diabetic neuropathy (Jagodic et al., 2007; Messinger et al., 2009b).

Given the potential application of moderate intensity exercise to be of therapeutic value for the management of painful nerve dysfunction in patients with DM, we investigated in this study the consequence of forced-exercise on voltage gated Ca^{2+} channel function in nociceptive (small-diameter) DRG neurons from streptozotocin-induced hyperalgesic rats. A preliminary account of these findings have been previously reported (Shankarappa et al., 2007; Shankarappa et al., 2009). The present chapter addresses the proposed first and second specific aims of this dissertation.

MATERIALS AND METHODS

Animal care

This study was conducted using protocols approved by the Edward Hines Jr. VA Hospital Institutional Animal Care and Use Committee in accordance with the principles of laboratory animal care (National Institutes of Health Publ. 86-23, 1985). All animals were housed in pairs, allowed standard rat diet and water *ad libitum*, and maintained on a 10h/14h light/dark cycle. Adult male Sprague-Dawley rats (initial body weight 200 g) were randomly divided into two treatment groups (vehicle-control or STZ-induced diabetes) and a subset of each group subjected to daily 1h-sessions of either exercise or sedentary inactivity for up to 10 weeks.

Induction of experimental diabetes mellitus

Streptozotocin (STZ) was used in this study to induce experimental DM, a well established animal model of painful diabetic neuropathy. Non-fasted ketamine (100 mg/kg)-xylazine (5 mg/kg) anesthetized rats received a single intraperitoneal injection of freshly prepared streptozotocin (STZ, 60 mg/kg body wt; Sigma-Aldrich, St. Louis, MO) dissolved in citrate buffer (100 mmol/l; pH 4.5). Non-diabetic control, gender and age-matched rats received an equal volume of intraperitoneally injected, freshly prepared citrate buffer (100 mmol/l; pH 4.5). Non-fasting blood glucose levels were determined before vehicle or STZ was administered and at regular weekly intervals throughout the study. Blood samples were obtained by tail prick, and glucose content was quantified

using a calibrated commercial glucometer (MediSense Precision QID glucometer, Abbot Laboratories, Bedford, MA). STZ-treated rats exhibiting blood glucose levels <300 mg/dl (<16.6 mmol/L) at 48h post treatment were considered to be non-diabetic and were excluded from further study. Animals were weighed daily to monitor disease progression and severity.

Experimental exercise regimens

Experimentally, there are two categories of exercise regimens that can be utilized to study the effect of exercise. Animals can be subjected to either a voluntary or forced exercise regimen. To determine the optimal exercise regimen for this study, rats were assigned either to the forced-exercise or the voluntary running groups.

Voluntary-exercise: In the voluntary running group, rats were housed individually at night, for 16h (5 Pm to 9 Am) in an enclosed glass chamber (11.5 X 14.2 X 7.5, inches) with a running wheel (37 inches in circumference) fitted with a standard cyclometer. Animals had unrestricted access to food and water within the glass chamber. Rats were allowed to explore and adapt to the running wheel for 2 weeks prior to STZ treatment. Upon STZ treatment, rats were allowed to run 5 nights a week for a period of 4 weeks. Distance run was recorded daily. Animals were returned to their home cages every morning.

Forced-exercise: Prior to vehicle- or STZ-treatment, rats assigned to the forced-exercise group were acclimated (5-day training period) to a motorized treadmill (Exer 3/6 Open treadmill, Columbus Instruments, Columbus, OH) equipped with a motivational shock

grid set to emit an innocuous 8mA electric shock to the plantar surface. Training involved a gradual transition at zero grade inclination toward a constant velocity (18 m/min) and duration (60 min/day). On the fifth day, after training, rats received either vehicle- or STZ-treatment. Rats were run between 9:00h-13:00h for 60 min/day x 5 days a week for 10 weeks. Rats subjected to this regimen showed no evidence of foot trauma or callus formation. Vehicle- or STZ-treated rats assigned to the sedentary groups were allowed to explore an identical sized environment for the same duration of time (including the training period), but without receiving an exercise challenge or shock incentive.

Tactile-responsiveness to Von-Frey filaments

Tactile responsiveness was measured separately on all animals at 0-, 2-, 4-, 6-, 8-, and 10-weeks post vehicle- or STZ-treatment. Tactile responsiveness was measured using logarithmically calibrated Semmes Weinstein monofilaments (Stoelting Co, Wood Dale, IL) and semi-quantified by the Up-Down method of Dixon as previously described (Chaplan et al., 1994). Following acclimation to a wire mesh bottom, the mid plantar surface of both hind feet of each rat were separately probed at right angle for 8s with sufficient force to cause slight buckling of the monofilament. Paw withdrawal occurring within the 8s stimulus duration was considered a positive response. Testing began with a 2g-force equivalent monofilament followed by hairs with greater or lesser mass-force depending on the previous paw response. In the event of a positive paw withdrawal to the initially selected filament, the next lesser mass-force filament was presented. Similarly, in the event of an absent paw withdrawal response, the next higher mass-force filament was presented. A total of six consecutive critical data points were considered starting from

one data point prior to the first positive withdrawal response. The withdrawal threshold, defined as the filament mass-force (grams) required to elicit a 50% response rate, was calculated using the formula (Chaplan et al., 1994):

$$\frac{10^{[X+k\delta]}}{10{,}000}$$

where x = the value of the last filament used, in log units, k = a tabular value for the pattern of positive and negative response generated and δ = the mean mass-force difference (log units) between filaments (0.224). Recordings were repeated twice per animal and the mean considered as the withdrawal threshold. Thresholds generated in this manner were considered to have a non-parametric distribution.

In a separate experiment, the role of opioids in mediating forced-exercise induced affect on diabetes-associated tactile hyperalgesia was determined. Tactile responsiveness was measured in 2 week post veh- or STZ- treated rats, subjected to either forced-exercise or sedentary regimens. Prior to withdrawal threshold testing, rats received 0, 5 or 10 mg/kg of naloxone (Sigma, St Louis, MO), administered *via* the intraperitoneal route. Saline was used as vehicle. Withdrawal threshold recordings were performed 8 minutes after naloxone administration.

Thermal responsiveness to infra-red heat stimulus

Thermal responsiveness was quantified using a microprocessor-controlled infrared Ugo Basile Thermal Plantar Analgesia Instrument (Stoelting Co, Wood Dale, IL). Briefly, rats placed on a temperature-controlled (23-24°C) glass platform were

allowed to acclimate x 30 min. After the acclimation period, the infrared lamp with a pre-set intensity (Figure 6C) was positioned directly beneath the rat's hindpaw and manually activated. Upon paw withdrawal, latencies were automatically recorded to the nearest 0.1s. Mean of three trials was considered as the withdrawal latency.

Peripheral nerve conduction studies

Evoked compound muscle action potential (CMAP) amplitudes and latencies of peripheral nerves were quantified at week 0 and again at week 8 post vehicle- or STZ-treatment as previously described (Lawlor et al., 2002). Briefly, sciatic nerves of ketamine (100 mg/kg)-xylazine (5 mg/kg) anesthetized rats were stimulated at the sciatic notch or at the ankle (tibial nerve) with unipolar pin electrodes using supramaximal stimuli (25 mA, 0.05-ms duration) at high frequency (1 Hz) for the direct measurement of motor nerve (M-wave) responses (Figure 2). Unipolar pin recording electrodes were used to record the evoked potentials from the plantar muscles of the left hind foot. Individual responses were amplified and recorded using a TECA Synergy electromyograph system. For each animal, the M-wave was measured as an average of 25 individual evoked responses, repeated in triplicate. Motor nerve conduction velocity was calculated as the distance from notch-to-ankle divided by the difference of the M-wave latency (notch–ankle). A heating pad was used to maintain the body temperature of the rat at 37°C.

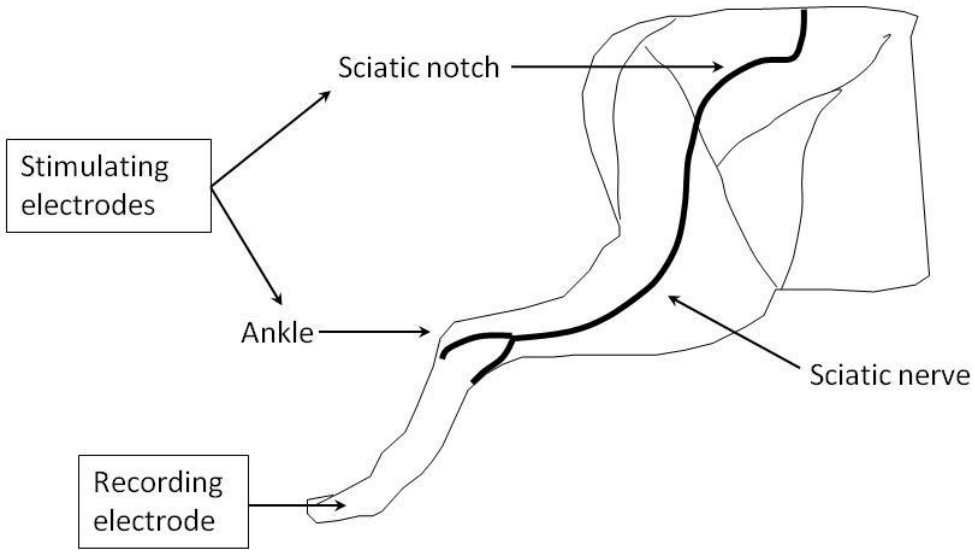

Figure 2. Evoked compound muscle action potential recording from the rat sciatic nerve

For recording sensory nerve conduction velocity (SNCV), the tail nerve was stimulated (6 mA, 0.01 ms) 6 cm and 10 cm distal to the recording ring electrode with unipolar pin electrodes. The recording ring electrode was placed at the base of the tail, with the reference electrode placed 1cm proximal to the recording electrode. A series of 8 individual responses were evoked at a frequency of 1 Hz, with each series being repeated three times. SNCV was calculated as the distance between the proximal and the distal stimulation points (4 cm) on the tail divided by the difference in nerve action potential latency.

Dissociation of dorsal root ganglia neurons

Vehicle- or STZ-treated rats were euthanized by CO_2 asphyxiation, a lumbar laminectomy was performed, and lumbar (L4-L5) dorsal root ganglia were extracted and quickly immersed in ice-cold Ca^{2+} and Mg^{2+} free Hank's Balanced Salt Solution (HBSS, Invitrogen, Carlsbad, CA). DRG neurons were isolated using a modified procedure, based on a previously reported method (Scroggs and Fox, 1992). Briefly, DRG neurons were prepared by dissociation at 37ºC x 30min in the presence of collagenase (2 mg/ml; type I, Sigma-Aldrich, St. Louis, MO) and dispase (5 mg/ml; type II, Invitrogen, Carlsbad, CA). Dissociated DRG neurons were washed in HBSS supplemented with 20% fetal bovine serum (FBS, Invitrogen, Carlsbad, CA) and subsequently plated on uncoated glass coverslips in preparation for whole-cell voltage-clamp recordings as previously described (Aromolaran et al., 2007). Small, medium, and large diameter DRG neurons were typically present in our dissociated preparations (Figure 8). Since neuropathic pain transmission is largely facilitated by small-diameter DRG neurons, only cells with soma diameters less than 30μm (i.e., <30pF) were patched. In all cases, dissociated small diameter DRG neurons were used within 6 h of harvest.

Voltage clamp electrophysiology

Ca^{2+} currents were recorded in acutely dissociated small diameter DRG neurons lacking visible processes. Soma were continuously perfused with an external solution (300 mOsm) containing (mM): 2 $CaCl_2$, 140 tetraethylammonium (TEA)-Cl, 10 HEPES (pH 7.4), and 10 glucose (Aromolaran et al., 2007). Electrodes were pulled from borosilicate glass microcapillary tubes (Warner Instruments, LLC, Hamden, CT) and had

a resistance from 2-4 MΩ when filled with an internal solution (280 mOsm) containing (mM): 108 $CsMeSO_3$, 4 $MgCl_2$, 1 Cs-EGTA, 9 HEPES (pH 7.4), 5 ATP-Mg, 1 GTP-Li, 15 phosphocreatine-TRIS. Whole-cell somatic Ca^{2+} currents were recorded using an Axopatch 200B patch-clamp amplifier (Molecular Devices, Palo Alto, CA) at 23 ºC and digitized using a Digidata 1322A converter interfaced with pClamp Software. Cell capacitance was measured from a transient current evoked by a 5 mV depolarizing pulse from a holding potential (V_h) of -90 mV. Currents were low-pass filtered at 1 kHz. Series resistance and capacitance values were obtained after electronic subtraction of capacitive transients. Voltage clamp recordings were obtained by patching small diameter DRG neurons with uncompensated series resistance of <20 MΩ and cell capacitance <30 pF (Table 2). LVA and HVA currents were elicited from V_h = -90mV. HVA currents were recorded in isolation from LVA currents using V_h = -50mV, a voltage that completely inactivates LVA currents (Carbone and Lux, 1984; Bean, 1992). In each case, soma were depolarized for 250 ms to test potentials (V_t) = -80 to +50 mV, with 10 mV increments. The net LVA current contribution was determined by using current subtraction at different V_h (Fig. 4B). Currents recorded from V_h = -50mV were subtracted from those obtained using V_h = - 90mV for each V_t from -70mV to -20mV as previously described (Xu and Best, 1992). Steady-state inactivation (SSI) of LVA Ca^{2+} channels was assessed using an established double-pulse protocol. DRG neurons held at -90mV received a series of pre-conditioning pulses (-110mV to +10mV; 10 mV increments, 1.5s duration) followed by a depolarizing test pulse to -30mV in order to evoke Ca^{2+} channel opening

(Aromolaran et al., 2007). Data were analyzed by Clampfit (Molecular Devices) and fitted to a single Boltzmann distribution

$$\frac{I_{max}}{1 + \frac{\exp\,(V_{50} - V)}{k}}$$

where I_{max} is the maximal current amplitude, V_{50} is the voltage at which half of the current is inactivated, *k* is the voltage dependence (slope) of the function.

Statistical analysis

Data are expressed as the mean ± SEM of *N* observations unless noted otherwise. Statistical significance between multiple experimental groups was determined by one-way or two-way ANOVA with a Bonferroni multiple comparison post-hoc analysis. In each case, $p < 0.05$ was considered statistically significant.

RESULTS

Streptozotocin-induced diabetes and voluntary-exercise

Rats given access to voluntary running wheels ran ~ 0.6 Km/night (16h, 16:00 to 09:00) prior to vehicle or STZ administration (Figure 3). Upon STZ-treatment, the average daily running distance gradually decreased over the study period. At the end of 4 weeks, STZ-treated rats ran 0.09 ± 0.01 Km/night as compared to the vehicle-treated rats which maintained a running distance of 0.5 ± 0.04 Km/night. This decreased voluntary running behavior of STZ-diabetic rats lead us to adopt forced treadmilling as the exercise intervention of choice.

Streptozotocin-induced diabetes and forced-exercise

Administration of freshly prepared streptozotocin (STZ) to adult male SD rats produced a marked elevation of non-fasting blood glucose levels (>16.7 mmol/L) that was sustained throughout this 10-week study (Figure 4A). Rats forced to run continuously on a zero grade treadmill (forced-exercise; 18m/min x 60min/day for 5 days/week) exhibited nearly identical sustained increases in blood glucose (Figure 4A). Previously, we demonstrated that subcutaneous implantation of insulin pellets at 4 weeks reversed the observed hyperglycemic effects of STZ and normalized blood glucose levels to near physiological concentrations in sedentary SD rats (Emerick et al., 2005), consistent with the experimental induction of insulin-dependent DM. By comparison, control rats receiving an equal volume of citrate buffer (100 mmol/L; pH 4.5) maintained

non-fasting blood glucose levels near 6 mmol/L (Figure 4A). Blood glucose levels were similarly unaffected by continuous forced-exercise in vehicle-treated control rats.

The body weights of the vehicle-treated (non-diabetic) rats steadily increased over the course of study (Figure 4B). By comparison, STZ-induced diabetic rats exhibited a steady decline in the rate of body weight gain. Vehicle-treated rats undergoing continuous forced-exercise exhibited a delay in the rate of body weight gain resulting in 20-25% less overall weight gain. A similar, but more exaggerated delay was observed with STZ-induced diabetic rats undergoing forced-exercise (Figure 4B). At no time throughout the course of this study, did sedentary or forced-exercises STZ-induced diabetic rats lose body weight, suggesting that complications secondary to diabetes-induced cachexia was negligible.

Forced-exercise protects against STZ-induced diabetes-associated nerve conduction deficits

We next determined the effect of forced-exercise on peripheral nerve function in vehicle- and STZ-treated rats by evoked-response electrophysiology (Emerick et al., 2005; Sarkey et al., 2007). Despite exhibiting marked and sustained hyperglycemia, STZ-treated rats (8-weeks) maintained near normal evoke-response sciatic/tibial nerve conduction amplitudes when compared with vehicle-treated non-diabetic controls or pre-treatment (baseline) measures (Table 7). In contrast, calculated motor nerve conduction velocities (MNCV) in STZ-treated (8-weeks) rats were slowed by approximately 23%, consistent with previous reports (Manschot et al., 2003). Forced-exercise did not alter the

calculated MNCV in vehicle-treated non-diabetic rats when compared with sedentary vehicle-treated non-diabetic rats (Table 7). By comparison, calculated MNCV in STZ-treated rats undergoing forced-exercise were statistically indistinguishable from vehicle-treated forced-exercise non-diabetic control rats or pre-treatment (baseline) measures (Table 7).

SNCV (32.4 ± 1.3 m/s), recorded from the tail nerve of STZ-treated rats was not however significantly different from vehicle treated controls (35 ± 3 m/s) (Table 8). Similarly, forced-exercise did not affect SNCV in vehicle- (30.0 ± 0.5 m/s) or STZ-treated rats (31.5 ± 1.3 m/s) (Table 8). These data suggest that, unlike the sciatic nerve, the tail nerve is spared from STZ-induced diabetes associated conduction deficits.

Forced-exercise delays onset of diabetes-associated hyperalgesia

To assess whether forced-exercise alters STZ-induced diabetes-associated nociception *in vivo,* we determined behavior response thresholds to tactile and thermal stimuli as a function of time (0-10 weeks). Vehicle-treated sedentary non-diabetic rats exhibited tactile withdrawal threshold sensitivities of 12.8 ± 0.6 g (n = 8) that were maintained over the 10-week course of study (Figure 5A). Forced-exercise vehicle-treated rats responded similarly to tactile stimulation, suggesting that the forced-exercise regimen used in this study does not significantly alter tactile sensitivity. Within 2-weeks, STZ-treated hyperglycemic sedentary rats developed an enhanced sensitivity to tactile stimuli that was sustained throughout the 10-week course of study (Figure 5B). This is consistent with the development of neuropathic hyperalgesia/allodynia in STZ-treated

rats as previously reported (Malcangio and Tomlinson, 1998). By comparison, forced-exercise significantly ($p<0.05$) delayed by approximately 4-weeks the onset of tactile hyperalgesia in STZ-treated hyperglycemic rats (Figure 5B) without altering blood glucose levels (Figure 4A). Moreover, statistical evaluation between sedentary and forced-exercise STZ-treated rats by two-way ANOVA found that the treatment-time interaction was highly significant ($F(5, 72) = 6.21$, $p<0.0001$).

Responsiveness to thermal stimulus is not altered by forced-exercise

To assess whether forced-exercise similarly affects thermal responsiveness, thermal withdrawal latencies were determined using a modified Hargreaves method (Hargreaves et al., 1988) in response to a infrared heat source of specified intensity (Figure 6C). Thermal withdrawal latencies (10.9 ± 0.5s, n = 22) obtained from naïve euglycemic rats were not significantly different from those of vehicle-treated sedentary non-diabetic rats (10.1 ± 0.5s, n = 4; 10-weeks) (Figure 6A). A significant, but modest, reduction in thermal withdrawal latency (8.3 ± 0.1s, n = 7; 10-weeks,) was seen in STZ-treated hyperglycemic rats (Figure 6B). Earlier timed points (2, 4, 6, and 8-weeks), however, were not statistically different from vehicle-treated controls. Ten-weeks of forced-exercise did not alter thermal withdrawal latencies in vehicle-treated control rats (12.0 ± 1.2s, n = 4). STZ-treated hyperglycemic rats undergoing 10-weeks of forced-exercise had thermal withdrawal latencies (10.5 ± 1.0s, n = 7) that were statistically indistinguishable ($p = 0.3$) from vehicle or naïve control values.

Naloxone reverses forced-exercise induced analgesia

To determine the mechanism by which forced-exercise protects against the development of diabetes-associated tactile hyperalgesia, we assessed hind-paw withdrawal thresholds after administration of naloxone hydrochloride, a non-selective opiate receptor antagonist. In vehicle-treated sedentary rats, naloxone reduced hind-paw withdrawal thresholds in a dose-dependent manner (Fig. 6.). Naloxone (5 mg/kg) in vehicle-treated sedentary rats decreased the mean withdrawal threshold to 3.3 ± 1.3 g. In contrast, exercised vehicle-treated animals demonstrated a significant rightward shift in the naloxone dose-response curve (11.0 ± 1.9 g in response to 5 mg/kg naloxone). This data suggests the presence of increased endogenous opioids in non-diabetic vehicle-treated rats subjected to forced-exercise. In comparison, STZ-treated exercised rats exhibited a similar dose-response profile (10.4 ± 2.0 g in response to 5 mg/kg naloxone) as the exercised vehicle-treated group. Both, vehicle- and STZ-treated exercised groups demonstrated reduced withdrawal thresholds with 10 mg/kg naloxone (veh-exe: 3.1 ± 0.7 g and STZ-exe: 4.1 ± 0.2 g). STZ-treated sedentary rats exhibited a withdrawal threshold of 3.3 ± 0.4 g, and were not challenged with naloxone.

Forced-exercise prevents diabetes associated alteration in Ca^{2+} current densities

To determine the mechanism by which forced-exercise protects against the early development of tactile hyperalgesia in STZ-induced diabetic rats, we measured Ca^{2+} current densities in small diameter (21.4 ± 0.9 μm) DRG neurons (Figure 8A) harvested from vehicle- or STZ-treated sedentary or STZ-treated force-exercised rats. Confirmation

of tactile responsiveness was determined in all rats prior to tissue harvest and voltage-clamp analysis. DRG neurons have been previously reported to co-express several types of Ca^{2+} channels, including low-voltage activated (LVA) T-type and high-voltage activated (HVA) N-, L-, and P/Q-Type channels (Scroggs and Fox, 1992). Passive membrane properties between voltage-clamped DRG neurons harvested from vehicle, STZ, and forced-exercise STZ groups were not significantly different (Table 9). Inward Ca^{2+} currents elicited from a V_h = -50 mV (V_t = 0 mV) exhibited prolonged inactivation characteristic of HVA currents (Figure 9A). DRG neurons from vehicle-treated sedentary rats exhibited HVA Ca^{2+} currents that peaked at 0 mV, with a maximum current density of -8.2 ± 1.0 pA/pF (Figure 9B). DRG neurons from STZ-treated sedentary hyperalgesic rats, by comparison, demonstrated significant enhancement (>2.5-fold) of HVA Ca^{2+} current density whose peak (-26.3 ± 2.8 pA/pF) was rightward shifted to +10 mV (Figure 9B). In contrast, DRG neurons from STZ-treated rats undergoing forced-exercise displayed HVA Ca^{2+} currents with an intermediate density (-16.8 ± 2.3 pA/pF) that peaked at 0 mV, identical to sedentary vehicle controls. Moreover, current-voltage curves obtained from DRG neurons of sedentary or forced-exercise diabetic rats exhibited an atypical shoulder near -30 mV (Figure 9B) that is suggestive of the emergence of LVA T-type Ca^{2+} currents in these neurons.

Inward Ca^{2+} currents elicited from a V_h = -90 mV exhibited rapid (~100 ms) inactivation properties consistent with the presence of LVA ‘T-type’ currents in diabetic DRG neurons (Figure 10A). Compared to HVA currents, the peak density of the observed LVA component was modest, as expected for these currents. However, at a V_t =

-30mV, peak LVA Ca^{2+} current density in diabetic DRG neurons was enhanced approximately 2-fold compared to vehicle controls (Figure 10B). In contrast to HVA currents, however, forced-exercise did not alter diabetes-associated increases in LVA Ca^{2+} current density (Fig. 4B) or the net LVA Ca^{2+} current component (Figure 10C).

Diabetes-associated changes in LVA Ca^{2+} current steady-state inactivation

The presence of LVA currents elicited from V_h = -50mV (Figure 11A) indicates altered voltage-dependent inactivation properties. As shown in Figure 11, steady-state inactivation (SSI) properties of LVA Ca^{2+} currents in DRG neurons from STZ-treated diabetic rats exhibited a significant ($p<0.05$) rightward depolarizing shift (7.5 mV; V_{50} = -50.9 ± 0.6 mV) that occurred in parallel with the early development of tactile hyperalgesia. In contrast, LVA Ca^{2+} currents in neurons from forced-exercised STZ-treated rats displayed V_{50} values that were indistinguishable (V_{50} = -58.2 ± 1.4 mV) from vehicle-treated controls (V_{50} = -58.4 ± 0.9 mV). The slope (k) of the SSI curves did not differ significantly among vehicle (-7.5 ± 0.8), sedentary STZ (-6.1 ± 0.6), or forced-exercise STZ-treated (-7.3 ± 1.2) groups.

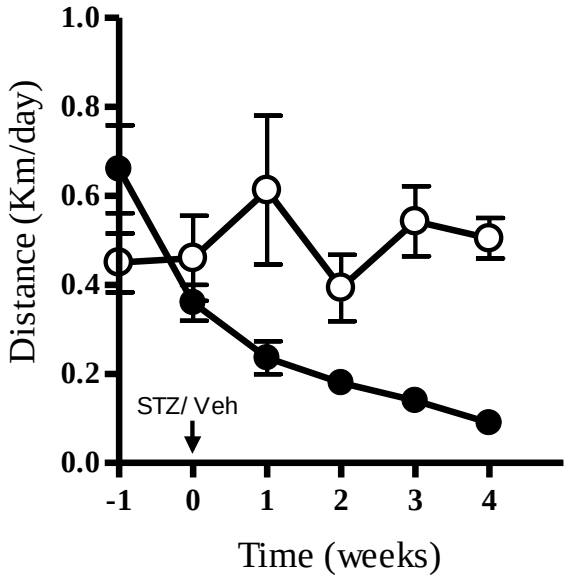

Figure 3. Effect of STZ-treatment on voluntary wheel running in SD rats.

Comparative changes in nocturnal running distance (Kms) in vehicle-treated rats (open circles, n=3), compared to STZ-treated rats (closed circles, n=3). Animals were given access to running wheels starting one week prior to vehicle or STZ administration. Data shown are means ± SEM.

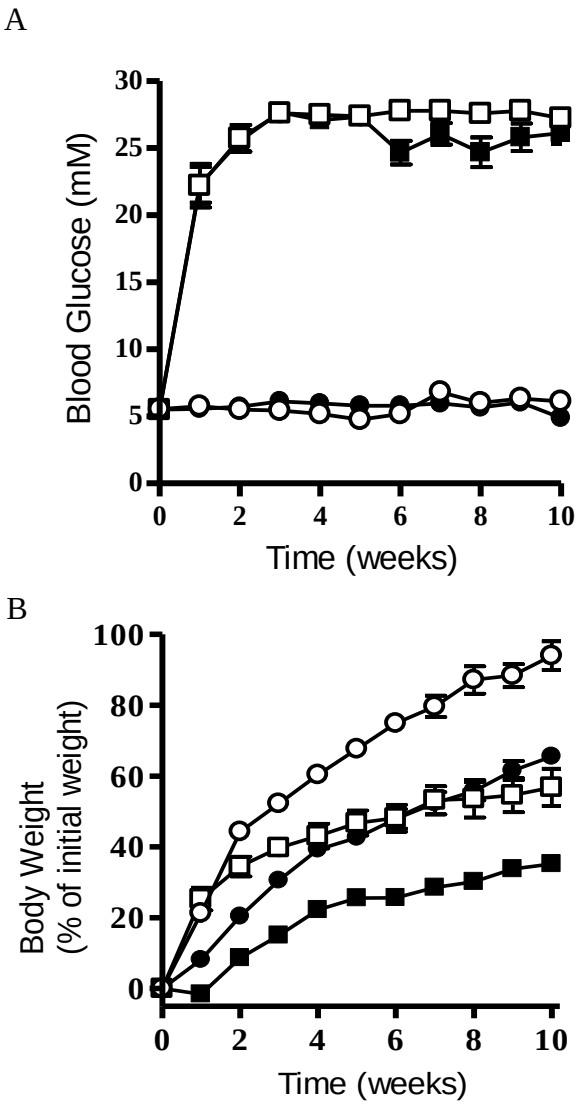

Figure 4. Effect of forced-exercise on progression of experimental diabetes.

Comparative changes in **(A)** blood glucose concentration and **(B)** body weight gain (expressed as a percentage of initial body weight) in vehicle- (*circles*) and STZ-treated (*squares*) sedentary (*open symbols*) or forced-exercise (*closed symbols*) rats. Data shown are the means ± SEM (vehicle, n=4; STZ, n=7).

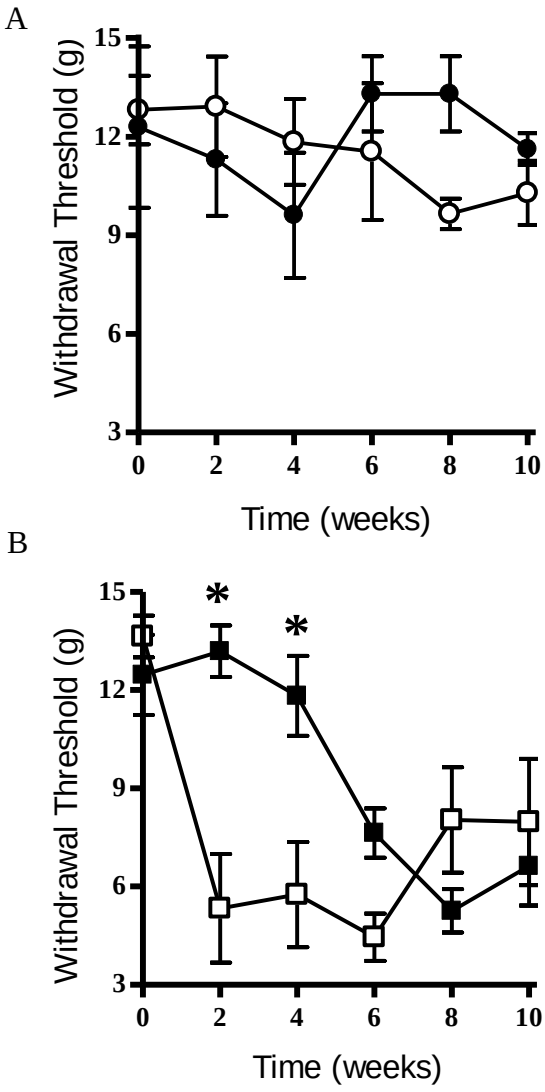

Figure 5. Effect of forced-exercise on the onset and progression of tactile hypersensitivity in STZ-treated rats.

Withdrawal thresholds to von Frey filaments in **(A)** vehicle- (*circles*) or **(B)** STZ-treated (*squares*) sedentary (*open symbols*) or forced-exercise (*closed symbols*) rats. Data shown are the means ± SEM (vehicle, n=4; STZ, n=7). *, $p < 0.05$; two-way repeated measures ANOVA with post-hoc Bonferonni multiple comparison analysis.

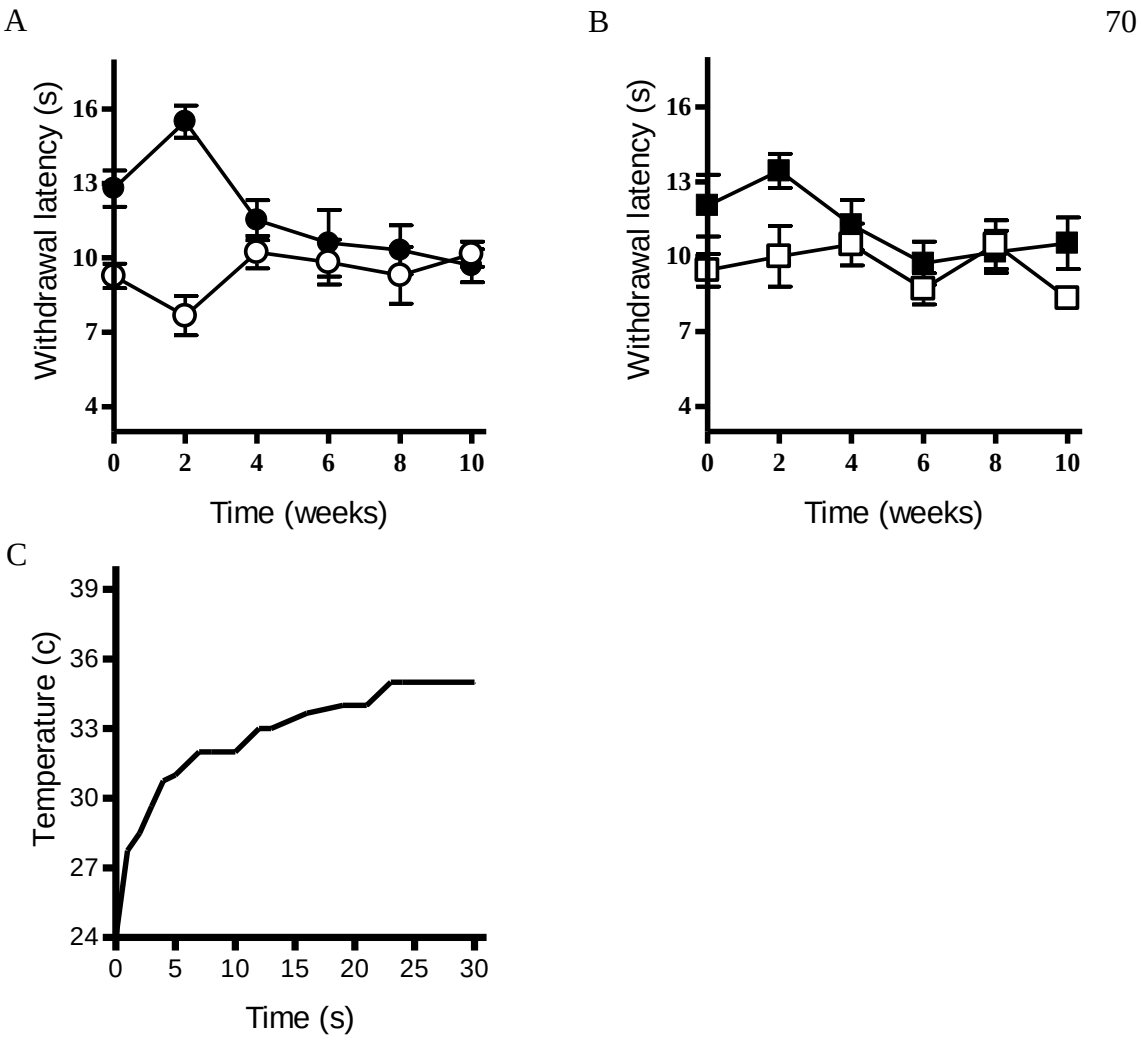

Figure 6. Effect of forced-exercise on thermal responsiveness in STZ-treated rats.

Hind-paw withdrawal latency from **(A)** vehicle-(*circles*) or **(B)** STZ-treated (*squares*) sedentary (*open symbols*) or forced-exercised (*closed symbols*) rats are shown. Data shown are the means ± SEM (vehicle, n=4; STZ, n=7). (**C**) Rate of change in thermal intensity (°C) from the infra-red lamp used to measure withdrawal latency in (A) and (B).

CMAP Amplitude (mV)	Sedentary		Forced-Exercise	
	Vehicle	STZ	Vehicle	STZ
Baseline				
Notch	2.2 ± 0.4	3.9 ± 0.5	4.2 ± 0.5	3.1 ± 0.3
Ankle	3.3 ± 0.3	4.5 ± 0.3	4.9 ± 0.3	4.1 ± 0.3
Notch/Ankle Ratio	0.7	0.9	0.9	0.8
8-week				
Notch	5.2 ± 1.2	3.6 ± 0.7	4.6 ± 0.4	3.4 ± 0.2
Ankle	6.5 ± 1.1	4.9 ± 0.8	5.5 ± 0.4	4.6 ± 0.5
Notch/Ankle Ratio	0.8	0.7	0.8	0.7
Conduction Velocity (m/s)	**Sedentary**		**Forced-Exercise**	
	Vehicle	STZ	Vehicle	STZ
Baseline	44.4 ± 3.5	53.5 ± 4.1	45.0 ± 3.3	46.1 ± 2.4
8-week	50.9 ± 1.9	**41.3 ± 3.1***	53.1 ± 5.3	51.0 ± 1.3

Table 7. Evoked compound muscle action potential response from the sciatic nerve of STZ-diabetic rats subjected to sedentary or forced-exercise.

Compound muscle action potential amplitudes and conduction velocity were evoked and quantified at baseline (week 0) and again at week 8 from vehicle (n = 4)- or STZ (n = 7) -treated rats subjected to a sedentary or forced-exercise regimen as described in methods. Data shown are the means ± SEM; *, $p<0.05$ Student's t-test.

Conduction Velocity (m/s)	Sedentary		Forced-Exercise	
	Vehicle	STZ	Vehicle	STZ
Baseline	25.0 ± 0.7	23.3 ± 0.8	21.6 ± 0.3	25.4 ± 1.2
8-week	30.5 ± 1.3	32.4 ± 1.3	30.0 ± 0.5	31.5 ± 1.3

Table 8. Conduction velocity calculated from the tail nerve in diabetic rats subjected to forced-exercise.

Tail nerve action potential were evoked and conduction velocity calculated at baseline (week 0) and again at week 8 from vehicle (n = 4) - or STZ (n = 8) -treated rats subjected to a sedentary or forced-exercise regimen as described in methods. Data shown are the means ± SEM.

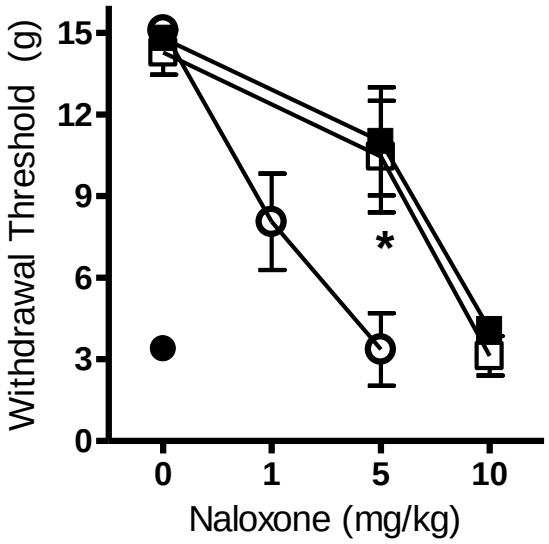

Figure 7. Effect of naloxone on forced-exercise induced analgesia.

Hind-paw withdrawal threshold from vehicle- (*open symbols*) and STZ- (*closed symbols*) treated forced exercise (*square*) and sedentary (*circles*) rats. Data are mean ± SEM of (4) observations per group. *, $p < 0.05$; One way ANOVA.

A

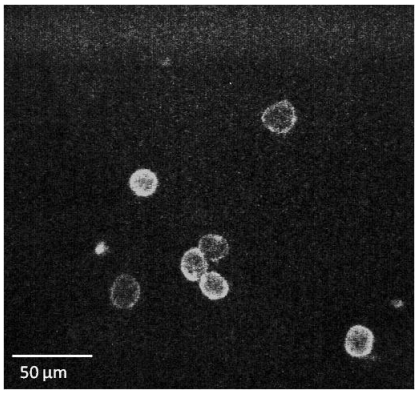

B

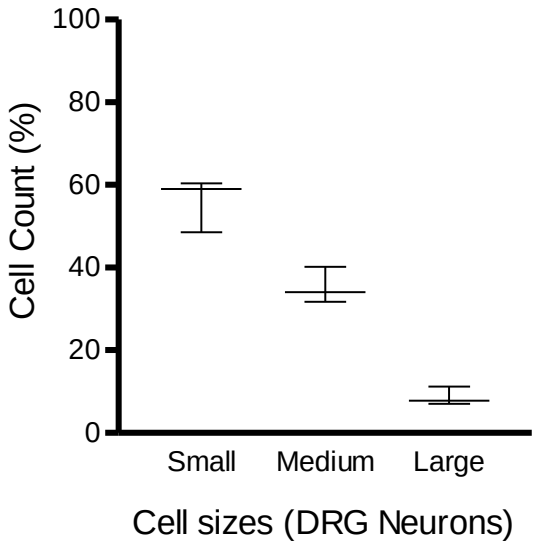

Figure 8. Percentage of small, medium and large diameter DRG neurons harvested from naïve adult rat.

Dissociated DRG neurons were classified into small, medium and large cells based on their cellular diameter as described in methods **(A)** Dissociated small diameter DRG neurons and **(B)** Box and whisker plot showing the percentage size distribution of neurons in the DRG.

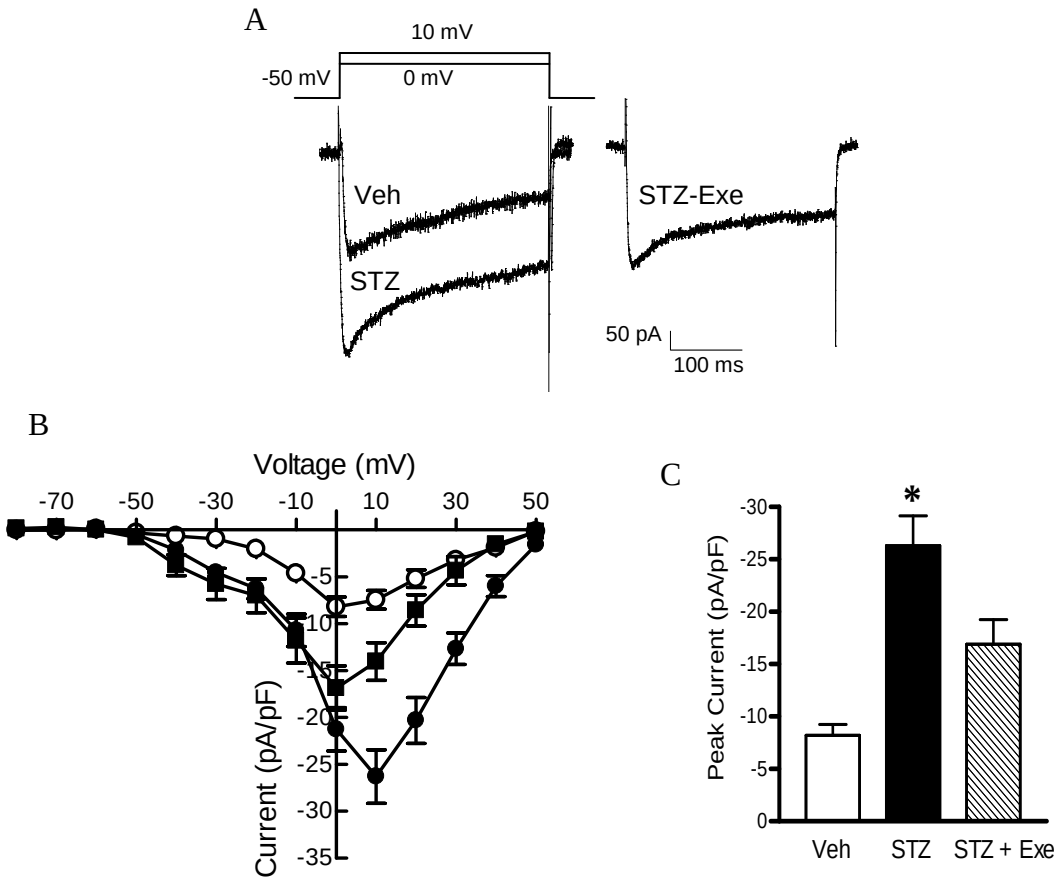

Figure 9. Forced-exercise attenuates diabetes-associated enhancement of HVA Ca^{2+} current density in dissociated small diameter DRG neurons.

(A) Representative current tracings elicited from a holding potential of -50mV to peak test pulses. **(B)** Current-voltage curves from sedentary vehicle-treated (*open circles*, n=9), STZ-treated (*closed circles*, n=15), or forced-exercise STZ-treated (*closed squares*, n=6) rats. Currents shown are normalized to cell size (capacitance) and are expressed as the means ± SEM. **(C)** Quantitative comparison of peak current density between sedentary vehicle (veh), streptozotocin (STZ), and forced-exercised streptozotocin-treated (STZ + Exe) rats. Data shown are means ± SEM of N observations indicated in (B). *, $p<0.05$; one-way ANOVA with post-hoc Bonferonni multiple comparison analysis.

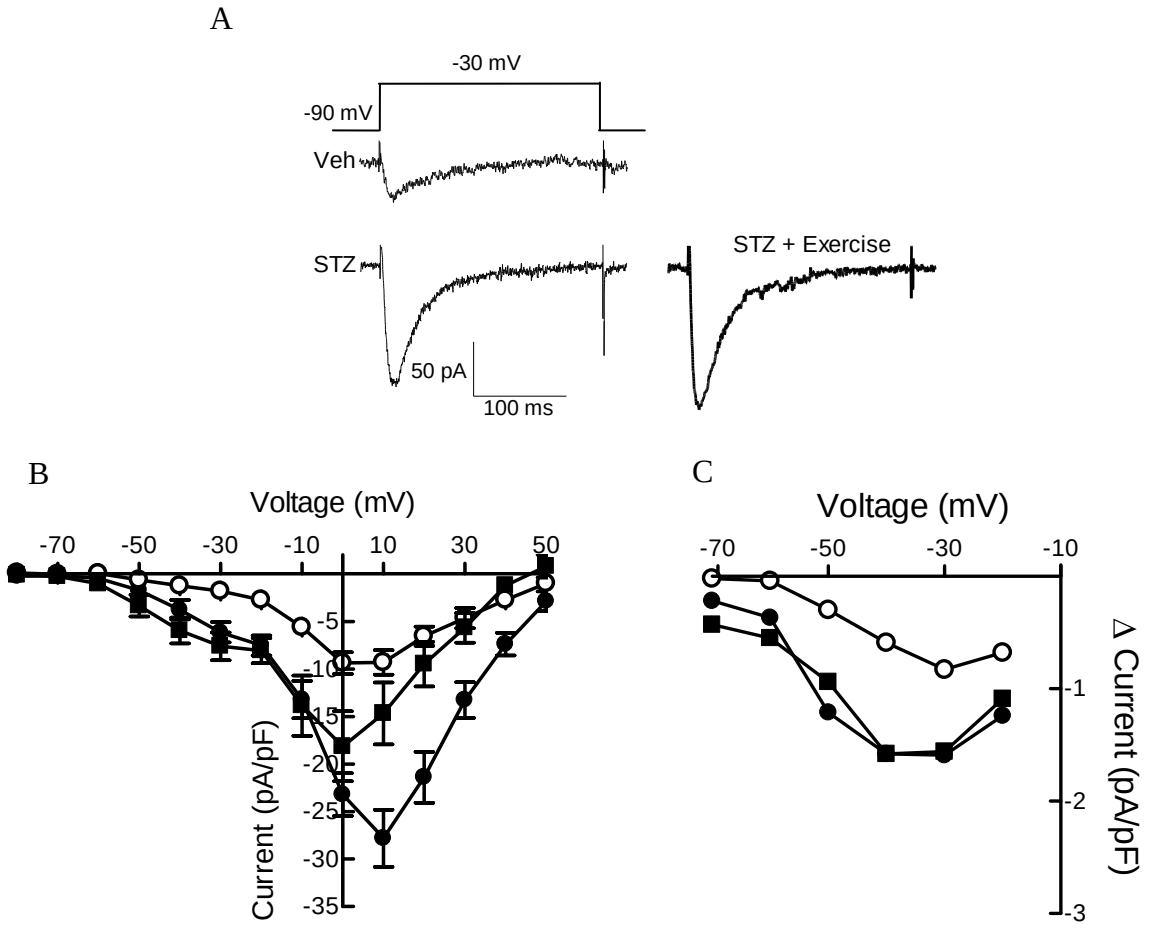

Figure 10. Effect of forced-exercise on LVA Ca^{2+} current density in dissociated small diameter DRG neurons.

(A) Representative current tracings elicited from a holding potential of -90mV at a test pulse of -30 mV. **(B)** Current-voltage curve from sedentary vehicle-treated (*open circles*, n=8), STZ-treated (*closed circles*, n=17), or forced-exercise STZ-treated (*closed squares*, n=7) rats. Currents shown are normalized to cell size (capacitance) and are expressed as the means ± SEM. **(C)** Net LVA Ca^{2+} current components obtained by trace subtraction of currents shown in Figure 9 from V_t = -70mV to -20mV.

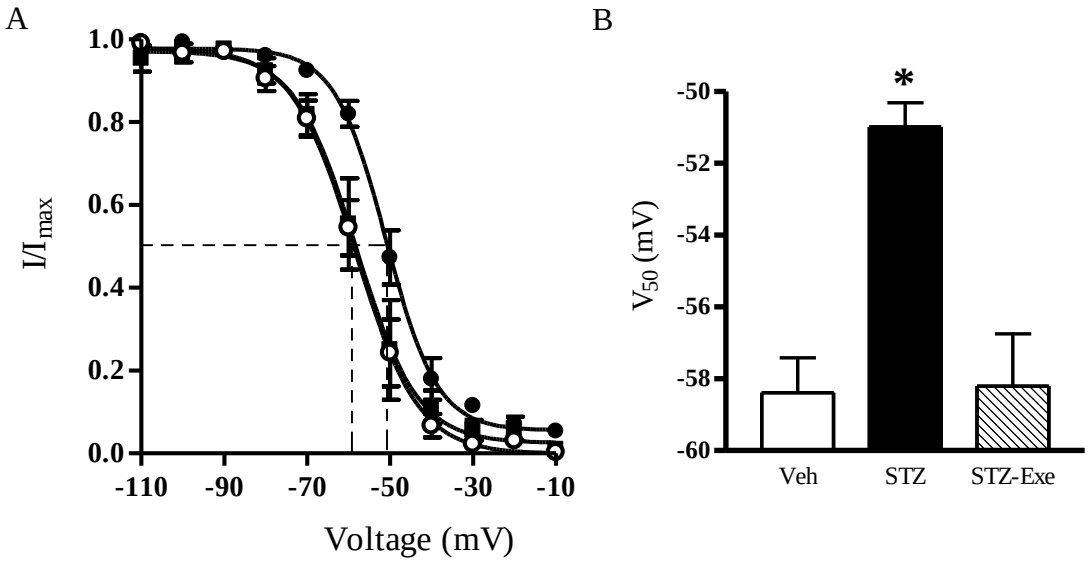

Figure 11. Forced-exercise prevents diabetes-associated increase in LVA Ca^{2+} channel availability.

(A) Steady-state inactivation of LVA Ca^{2+} channels in small diameter DRG neurons from sedentary vehicle-treated (*open circles*, n=6), STZ-treated (*closed circles*, n=6), and forced-exercise STZ-treated (*closed squares*, n=5) rats. (B) Quantitative comparison of V_{50} values derived from A. Data shown are the means of N observations. *, $p<0.05$; one-way ANOVA with post-hoc Bonferonni multiple comparison analysis.

DRG Source	Series Resistance (MΩ)	Capacitance (pF)
Sedentary Vehicle (9)	17.5 ± 2.6	20.0 ± 2.2
Sedentary STZ (14)	13.0 ± 1.7	17.1 ± 1.4
Force-Exercise STZ (7)	10.3 ± 1.1	15.6 ± 1.1

Table 9. Passive membrane properties of dissociated small diameter DRG neurons.

Data shown are the means ± SEM from (N) DRG neurons harvested from sedentary vehicle-, sedentary STZ-, or force-exercised STZ-treated rats.

DISCUSSION

This is the first study to demonstrate that forced-exercise markedly delays the onset of tactile hyperalgesia, a semi-quantitative behavioral measure of painful neuropathy, in experimentally-induced diabetic rats. The protective effects of forced-exercise occurred independent of blood glucose control. Diabetes-associated changes in HVA Ca^{2+} current density in small-diameter dorsal root ganglia (DRG) sensory neurons were significantly attenuated by forced exercise. Steady-state inactivation (SSI, a measure of channel availability and an indicator of neuronal excitability) of LVA Ca^{2+} channels in diabetic DRG neurons revealed a significant depolarizing (sensitizing) shift that was prevented by forced-exercise. We propose that forced-exercise delays the development of painful neuropathy in experimental diabetes, in part, by preventing diabetes-associated remodeling/modulation of Ca^{2+} channels in DRG sensory neurons.

Painful diabetic polyneuropathy is untreatable in humans. Current management of affected patients primarily involves alleviation of discomfort and glycemic control (DCCT, 1993). Early clinical studies reveal a significant independent association between the occurrence of diabetic complications, including neuropathy, and declining exercise capacity among diabetic patients (Estacio et al., 1998). The application of exercise has since then been established as a safe and effective integral approach to the management of diabetes (Lynch et al., 1996; Knowler et al., 2002). The question of whether exercise protects against the development and progression of diabetic neuropathic complications, however, remains unresolved. Recent preliminary studies with small cohorts of neuropathic diabetic patients support a beneficial effect of exercise on some measures of

peripheral nerve function (Richardson et al., 2001; Fisher et al., 2007). Exercise (Balducci et al., 2006), or lifestyle intervention strategies that include an exercise component (Smith et al., 2006), may even delay or protect against the development of diabetic peripheral nerve complications.

It is well established that the peripheral nerve damage develops in diabetes in close association with poorly-controlled chronic hyperglycemia. Numerous thesis have been proposed to explain the association between prolonged hyperglycemia and nerve dysfunction, including alterations in voltage-gated ion channel function (Tomlinson and Gardiner, 2008). Sustained periods of hyperglycemia are reported to reduce nodal $Na_v1.6$ peak current density in myelinated neurons (Wittmack et al., 2005), possibly contributing to well described diabetes-associated deficits in nerve conduction velocity (Table 1). By comparison, acute periods of hyperglycemia may precipitate neuropathic pain. Pain thresholds are markedly decreased following glucose administration to healthy volunteers (Morley et al., 1984) and to experimental animals (Lee et al., 1990). Moreover, direct application of hyperglycemic solutions to DRG neurons *in vivo* reduces mechanical pain thresholds (Dobretsov et al., 2001). In this study, we found that an acute period (2-week) of sustained hyperglycemia/hypoinsulinemia precipitated a selective hypersensitivity to mechanical stimuli (defined here as tactile hyperalgesia). In marked contrast, diabetic rats undergoing forced-exercise exhibited normal sensitivity to tactile stimuli despite elevated levels of blood glucose. The protective effect of forced-exercise was transient, however, with diabetic rats developing tactile hyperalgesia by the sixth week of sustained hyperglycemia/hypoinsulinemia. The mechanism by which forced-exercise delays the

development of tactile hyperalgesia was unrelated to glycemic control. Insulin content, while not measured in this study, was not expected to change with forced exercise in STZ-treated animals (Howarth et al., 2009), since blood glycemic index, which is a reflection of insulin activity remained unchanged in both groups.

Previous studies have suggested the role of altered opioid-mediated analgesia in diabetes (Simon and Dewey, 1981; Kamei et al., 1992). Reduced potency of morphine (Chen and Pan, 2003), and decreased endogenous opioid levels in diabetic animals (Williams et al., 2008) are thought to contribute towards a lowered opioidergic tone, resulting in an enhanced pain state. Opioid receptor expression and receptor binding in neurons from the dorsal horn and the DRG of diabetic animals remain unchanged (Hall et al., 2001; Chen and Pan, 2003). In this study, naloxone reversed the analgesic effect of forced-exercise in diabetic animals and showed similar elevation of pain thresholds in both, vehicle- and STZ- treated forced-exercised animals. This observation may be due to exercise induced increase in endogenous opioids. Exercise mediated increase in pain threshold due to enhanced release of endogenous opioids is well documented in both human and animal studies (Koltyn, 2000). Alternatively, previous studies also indicate, that exercise-facilitated neuroprotection may be mediated by changes in neurotrophic support (Hutchinson et al., 2004).

A slowing of nerve conduction velocity is a well established feature of diabetic neuropathy (Greene et al., 1999; Patel and Tomlinson, 1999; Zotova et al., 2007). Functional abnormality of neuronal transmembrane ion gradients with altered distribution

of nodal ion channels (Cherian et al., 1996) has been previously reported. Structural changes in the form of segmental demyelination in the vicinity of the node of Ranvier (Jakobsen, 1976; Sima et al., 1988a) along with mild axonal atrophy (Sugimura et al., 1980) are present in nerves from STZ-induced diabetic rats. In our study, the motor nerve conduction velocity of the sciatic nerve from sedentary STZ-induced diabetic animals was decreased by approximately 20-30%. Sensory nerve conduction velocity of the tail nerve from the same animals, however, remained unaltered. One possible explanation for this observation could be the difference in the number of myelinated axons present within these nerves. The sciatic nerve comprises of approximately 30% myelinated axons (Schmalbruch, 1986), as compared to 11% in the tail nerves (Govindaraju et al., 2007). Demyelination of sciatic nerve axons results in decreased conduction velocity. However, since tail nerve has relatively low myelinated axon population, it may only develop slight decrease in conduction velocity.

Altered distribution of ion channels, including at the node of ranvier in the myelinated axons is another possibility for the slower conduction velocity in the sciatic nerve but not in the tail nerve. In this study, forced-exercise protected against diabetes associated decreases in motor nerve conduction velocity.

Voltage gated Ca^{2+} currents are enhanced in DRG neurons from chronic diabetic rats (Hall et al., 1995), raising a possible role for these channels in the development of painful diabetic neuropathy. Both HVA and LVA T-type Ca^{2+} channels are expressed in sensory neurons and appear quite sensitive to acute periods of hyperglycemia. Also, the

function of these channels are enhanced in parallel with the development of hyperalgesia (Jagodic et al., 2007). We found a similar enhancement of LVA (T-type) and HVA Ca^{2+} current densities in small diameter DRG sensory neurons from diabetic hyperalgesic rats. Moreover, SSI of LVA Ca^{2+} channels in diabetic DRG neurons was found to be rightward shifted, indicating enhanced channel availability for activation at physiological resting membrane potentials. This finding is similar to those previously reported in medium sized DRG neurons from STZ-treated rats (Jagodic et al., 2007). Forced-exercise not only diminished diabetes-associated increases in HVA Ca^{2+} current densities but also prevented changes in LVA Ca^{2+} channel SSI. Forced-exercise did not, however appear to alter the LVA current component in diabetic DRG neurons, suggesting selectivity of protection.

It is well established that voltage gated Ca^{2+}channels are modulated by ligands, such as endogenous opioids, that signal through G protein coupled receptors (Catterall, 2000). Decreased levels of endogenous opioids (Williams et al., 2008) and impaired opioid mediated GPCR signaling (Chen and Pan, 2003) have been reported in neurons from diabetic animals. In this study, the observed partially normalizing effect of exercise on HVA current densities of Ca^{2+} channels could result from minimizing diabetes-associated loss of opioidergic signaling. Modulation of LVA Ca^{2+} currents by opioids has not been reported. However, recent studies have implicated G protein signaling in the inhibition of LVA channels (Wolfe et al., 2003; DePuy et al., 2006).

Alternatively ligand-mediated enhancement of Ca^{2+} current density in diabetic sensory neurons may result from altered phosphorylation of Ca^{2+} channels (Iftinca and Zamponi, 2009; Trimarchi et al., 2009) or perhaps increased expression of distinct channel isoforms (Zhong et al., 2006). We would anticipate, however, that messenger-mediated changes in channel function would be rapid, giving rise to hyperalgesia within days, rather than weeks, of hyperglycemic onset. Rapid enhancement of Ca^{2+} current density remains a possibility, since DRG neurons from diabetic rats were not evaluated within this short time frame.

Based on this study, we conclude that forced-exercise delays the development of painful neuropathy in experimental diabetes, in part, by preventing diabetes-associated remodeling/modulation of Ca^{2+} channels in DRG sensory neurons possibly through an opioid mediated mechanism. However, the basic question of whether glucose directly plays a role in Ca^{2+} channel modulation remains to be elucidated.

CHAPTER THREE

D-GLUCOSE DEPENDENT MODULATION OF $Ca_V3.2$ α_{1H} CHANNEL FUNCTION

ABSTRACT

The low-voltage activated (LVA) Ca_V3 (T type) family of calcium channels modulate neuronal activity, and play a crucial role in the control of cellular excitability. We and others have previously reported alteration of LVA Ca^{2+} channel function in an experimental animal model of diabetic polyneuropathy. In this study, the effects of high glucose concentration on $Ca_V3.2$ $\alpha_{1H,}$ channel subunit properties were investigated. T type Ca^{2+} currents from $Ca_V3.2$ α_{1H} subunits stably transfected in HEK-293 cells were recorded using whole-cell voltage clamp electrophysiology. HEK-293 cells cultured for 24h in high-glucose (25 mM) containing media demonstrated a significant increase in peak $Ca_V3.2$ current density (29.7 ± 2.8 pA/pF) , compared to peak current density (21.8 ± 1.7 pA/pF) obtained from HEK-293 cells cultured in media containing normal glucose (5.6 mM). Kinetics of activation was altered by high glucose, while the channel inactivation and deactivation time constants, and steady state properties remained unaffected. Addition of the aldose-reductase inhibitor statil did not attenuate high-glucose induced enhancement of $Ca_V3.2$ currents. These data suggest that high-glucose induced increase in $Ca_V3.2$ channel function involves a mechanism that is independent of D-

glucose metabolism through the polyol pathway. These preliminary data support a direct role of D-glucose in altering LVA $Ca_V3.2$ channel function.

INTRODUCTION

Ca_V3 (T type) family of calcium channels are low-voltage activating channels present in various tissues such as cardiac muscle, skeletal muscle, and neurons (Catterall, 2000). T type channels play a crucial role in the control of cellular excitability in various physiological and pathological states (Huguenard, 1996; Llinas and Ribary, 2001). In the nervous system, these channels modulate neuronal activity, resulting in increased transmission efficiency and signal amplification (Perez-Reyes, 2003). T channels have been reported to be involved in the pathophysiology of cardiac arrhythmias (Satoh, 1995), sleep disorders (McCormick and Bal, 1997), epilepsy (Tsakiridou et al., 1995), fertilization (Talavera and Nilius, 2006), and nociception (Kim et al., 2003). Specifically, mutations in the gene encoding the $Ca_V3.2$ isoform of the T-type Ca^{2+} channel resulting in decreased channel activity has been associated with autism spectrum disorders (Splawski et al., 2006). In comparison, mutations that enhanced T channel activity were associated with seizure disorders (Heron et al., 2007) and altered nociception (Bourinet et al., 2005).

In situ hybridization studies have shown a wide distribution of $Ca_V3.2$ α_{1H} gene expression in the central and peripheral nervous system (Talley et al., 1999). Interestingly, subsets of small and medium sized DRG neurons, as well as sensory neurons in the superficial lamina of the dorsal horn show expression of $Ca_V3.2$ (Talley et al., 1999), suggesting a possible role in nociception (Shin et al., 2003). In addition, peripheral pain behavior was attenuated in the $Ca_V3.2$ knockout mice (Choi et al., 2007)

but not in the $Ca_V3.1$ knockouts (Kim et al., 2003). In a recent study, silencing of the $Ca_V3.2$ channels in sensory neurons alleviated hyperalgesia associated with STZ-induced diabetes (Messinger et al., 2009a). As previously reported, STZ-induced diabetes is associated with significant enhancement of T-type currents (Jagodic et al., 2007; Latham et al., 2009). The mechanism by which this occurs is unknown. Increased glucose concentration has been reported to effect the functioning of voltage gated ion channels in the rat coronary artery (Liu et al., 2001) and mesangial cells (Seal et al., 1995). However, whether D-glucose has a direct effect on $Ca_V3.2$ channels is not clear. In this study, we investigate the effects of high D-glucose concentration on the biophysical properties of $Ca_V3.2$ $\alpha_{1H,}$ a T type Ca^{2+} channel subunit stably transfected in HEK-293 cells.

MATERIALS AND METHODS

Cell culture

HEK-293 cells, stably transfected with $Ca_V3.2\alpha_{1H}$, were cultured in minimum essential medium (Hyclone, MA) containing 5.6 mM (normal) or 25 mM (high) D-glucose (Table 10), supplemented with 10% fetal bovine serum (Cellgro, Herndon , VA), 100 U/ml penicillin, 100 μg/ml streptomycin (Cellgro, Herndon, VA) and 600 mg/ml of G418 sulfate. Cells were plated onto 12 mm round glass coverslips (Warner instruments, Hamden, CT) and incubated in a humidified atmosphere of 5% CO_2/95% air at 37º C. Osmolarity of normal and high-glucose containing media was measured using a Vapro osmometer (Wescor Biomedical Systems, Logan, Utah) (Table 11).

To determine whether elevated levels of D-glucose contribute to the observed changes in calcium current densities by increased flux through the polyol pathway, HEK-293 cells were cultured for 24h in high-glucose containing media in the absence (veh, 0.1% DMSO) or presence (50 or 200 μM) of the aldose reductase inhibitor statil (Tocris, UK).

Voltage Clamp Electrophysiology

Ca^{2+} currents elicited from HEK cells were recorded using an Axopatch 200B amplifier (Axon Instruments, Union City, CA) at 23 ºC. Data was acquired at 1 kHz using the Digidata 1322A analog-to-digital converter. Ca^{2+} currents were recorded from HEK cells bathed in extracellular solution containing (in mM) 5 $CaCl_2$, 140 TEA-Cl, 10

Hepes and 10 glucose (pH 7.4, 300 mOsm). Borosilicate glass (Warner Instruments, Hamden, CT) patch pipettes were drawn using a microelectrode puller (Sutter Instrument, Novato, CA). Resulting patch electrodes had a resistance of 2-4MΩ, when filled with intracellular solution containing (in mM) 108 $CsMeSO_{3,}$ 4 $Mgcl_{2,}$ 1 Cs-EGTA, 9 HEPES, 5 ATP-Mg, 1 GTP-Li, 15 phosphocreatine-TRIS (pH 7.4, 280 mOsm). Cell capacitance was measured from a transient current evoked by a 5 mV depolarizing pulse from a holding potential (V_h) of -90 mV. Only patched HEK cells with capacitance of < 20 pF and series resistance (Rs) of < 10 MΩ were used. Rs was compensated online (>80%).

Currents were elicited from V_h = -90 mV and depolarized for 250 ms to test potentials (V_t) = -90 to +50 mV, with 10 mV increments. Activation time constants (τ_{on}) were determined using V_t = -70 mV to + 70 mV from V_h = -90 mV. Rising phase of the elicited currents were fitted with a single exponential equation. Kinetics of current inactivation was assessed using V_t = -70 mV to + 70 mV from V_h = -90 mV. Inactivation time constants (τ_{off}) were determined by fitting the decay phase of the current with a single exponential equation. Deactivation kinetics were assessed with a 12 ms duration depolarizing prepulse from V_h= -90 mV to V_t= -30 mV, followed by repolarizing pulses from -140 mV to -60 mV with 10 mV increments. Resulting tail currents were best fitted with a single exponential function at all potentials.

Steady state inactivation (SSI) was determined by first stepping the membrane potential from V_h = -90 mV to pre-pulse voltage levels (V_{pre}: -110 mV to +10 mV, with 10 mV increments) for 1.5 second duration, immediately followed by a depolarizing test

pulse from -90 mV to -30 mV to evoke T type channel opening. Data were analyzed by Clampfit (Molecular Devices) and fitted to a single Boltzmann distribution:

$$\frac{I_{max}}{1 + \frac{\exp\,(V_{50} - V)}{k}}$$

where I_{max} is the maximal current amplitude recorded, V_{50} is the voltage at which half of the current is inactivated, *k* is the voltage dependence (slope) of the function. Steady state activation curves were obtained using Vt = -90 mV to 0 mV from V_h = -90 mV, immediately followed by repolarization to -100 mV to evoke inward tail currents that were then fitted with a single Boltzmann equation.

Statistical Analysis

Data are expressed as the mean ± SEM of *N* observations unless noted otherwise. Statistical significance between experimental groups was determined by unpaired Students t test. $p < 0.05$ was considered statistically significant.

RESULTS

D-Glucose induced enhancement of T-type currents in HEK-293 cells

To determine whether D-glucose alters T-type calcium channel function or properties, HEK-293 cells stably expressing $Ca_V3.2$ channels were cultured overnight (24h) in media containing normal (5.6 mM, NGM) or high (25 mM, HGM) concentrations of D-glucose. Calcium currents elicited from HEK-293 cells cultured in NGM exhibited a peak current density of -21 ± 1.9 pA/pF (n=18). By comparison, calcium currents elicited from HEK-293 cells cultured in HGM exhibited a significantly ($p < 0.05$) higher peak current density of -29.6 ± 2.5 pA/pF (n=13) (Figure 12). Transformed mammalian cells are typically cultured in media containing high glucose (>25 mM). However, calcium currents elicited from HEK-293 cells cultured chronically (14 days) in NGM exhibited a peak Ca^{2+} current density (-17.3 ± 1.4 pA/pF) that was statistically indistinguishable from acute (24h) exposure conditions (Figure 13). These data support an acute effect of D-glucose on T-type calcium channel function in these cells.

D-glucose induced alteration of $Ca_V3.2$ channel gating properties

The rate of $Ca_V3.2$ channel opening, measured as the activation time constant (τ_{on}), was significantly faster in HEK-293 cells cultured for 24h in HGM, compared to cells cultured in NGM (Figure 14B). In contrast, the inactivation time constant (τ_{off}), a measure of channel inactivation, was not significantly altered by elevated D-glucose concentrations (Figure 15B). Similarly, the deactivation time constant ($\tau_{deactivation}$), a

measure of channel closing, remained statistically unaltered by elevated concentrations of D-glucose (Figure 16B).

Effect of D-glucose on $Ca_V3.2$ channel steady state properties

The probability of calcium channel opening or the willingness of channels to open, measured as the steady state activation (SSA), was not significantly altered by elevated D-glucose concentrations. Specifically, SSA curves obtained from HEK-293 cells cultured for 24h in either NGM (V_{50} = -31.9 ± 0.6 mV, k = 6.8 ± 0.6) or HGM (V_{50} = -33.5 ± 0.5 mV, k = 6.5 ± 0.4) were statistically indistinguishable (Figure 18B). Calcium channel availability, measured as the steady state inactivation (SSI), was also similarly unaffected by elevated concentrations of D-glucose (NGM, V_{50} = -59.3 ± 1.1 mV, k = -6.7 ± 0.9; HGM, V_{50} = -60.2 ± 1.0 mV, k = -7.6 ± 0.9) (Figure 17B).

Aldose reductase inhibition does not alter D-glucose induced enhancement of $Ca_V3.2$ currents

To determine whether elevated levels of D-glucose contribute to the observed changes in calcium current densities by increasing flux through the polyol pathway, HEK-293 cells were cultured for 24h in high-glucose containing media in the absence (veh, 0.1% DMSO) or presence (50 or 200 μM) of the aldose reductase inhibitor statil (Tocris, UK). Vehicle- or statil (50 μM)-treated cells exhibited similar peak current densities of -28.4 ± 4.3 pA/pF or -29.5 ± 2.7 pA/pF, respectively. Increasing statil concentrations to 200 μM did not further alter peak current density (-34.2 ± 2.4 pA/pF).

These data suggest that D-glucose induced elevation in peak current density occurs by a mechanism that is independent of the polyol pathway.

Media	Glucose concentration*	SD Rats	Blood glucose levels
Normal Glucose	5.6 mM	**Euglycemic**	5.7 ± 0.1 mM
High Glucose	25 mM	**Diabetic**	27.3 ± 0.2 mM

Table 10. Comparison of in vitro and in vivo glucose concentrations.
(* As reported by the manufacturer)

Media	Osmolarity (mOsm)
Normal Glucose	329 ± 3.7
High Glucose	331.3 ± 0.8

Table 11. Osmolarity measurements of normal and high-glucose containing media.
(Measurements are means of 3 media samples)

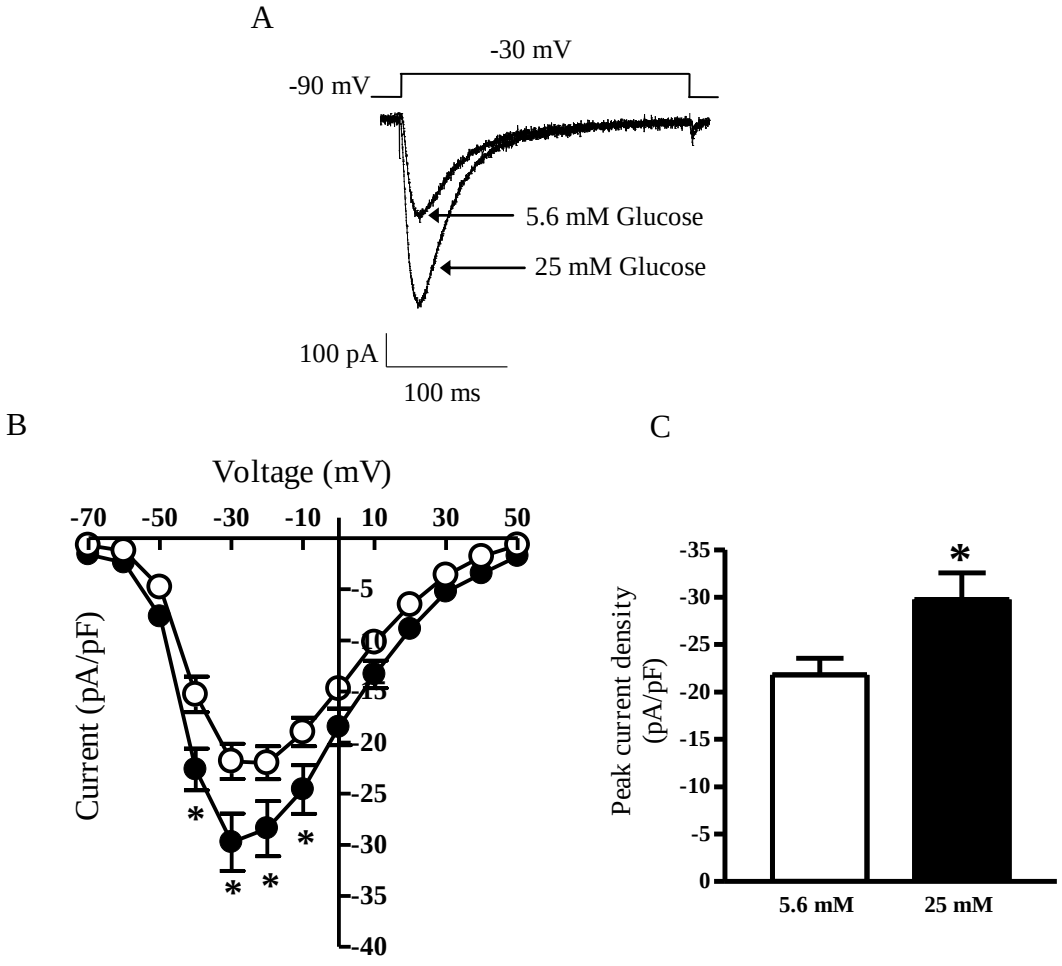

Figure 12. D-glucose enhances $Ca_V3.2$ current densities in HEK-293 cells.

(A) Representative Ca^{2+} current traces evoked by a 250 ms depolarizing pulse from V_h= -90 mV to a V_t= -30 mV from HEK-293 cells cultured 24h in 5.6 mM or 25 mM D-glucose containing media. **(B)** Current-voltage relationships from HEK-293 cells cultured in media containing 5.6 mM (open circles, n= 18) and 25 mM D-glucose (closed circles, n=13). **(C)** Bar graph comparing peak current densities from B. Data shown in B and C are the means ± SEM.*, $p < 0.05$; unpaired Students t test.

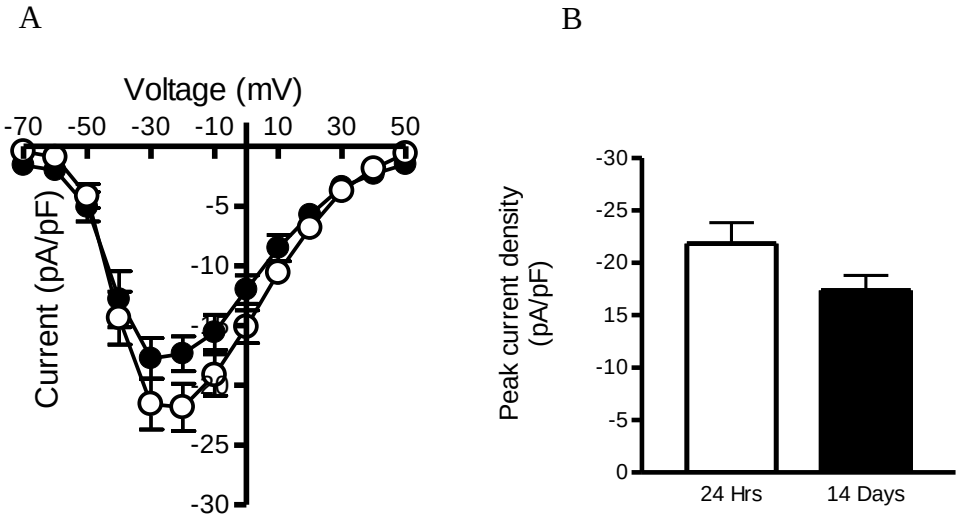

Figure 13. $Ca_V3.2$ current densities from HEK-293 cells cultured for 14 days in normal-glucose containing media.

(A) Current-voltage relationships of $Ca_V3.2$ channels from HEK-293 cells incubated overnight (open circles, n= 13) or 14 days (closed circles, n=5) in media containing 5.6 mM D-glucose. **(B)** Bar graph showing peak current density. Data shown in A and B are the means ± SEM. In each case, $p > 0.05$; unpaired Students t test.

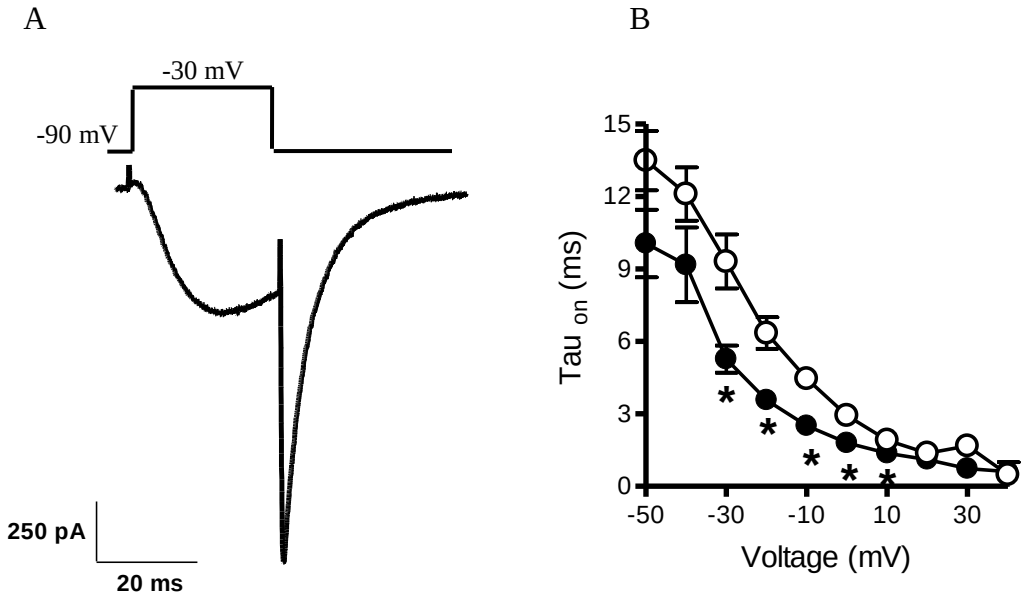

Figure 14. D-glucose enhances activation kinetics of $Ca_V3.2$ channels in HEK-293 cells.

(A) Representative trace showing a calcium current elicited from a V_h = -90 mV to a V_t = -30 mV. **(B)** Activation time constants (τ_{on}) from HEK-293 cells cultured in media containing 5.6 mM (open circles, n=12) or 25 mM (closed circles, n=9) D-glucose. Data shown are the means ± SEM.*, $p < 0.05$; unpaired Students t test.

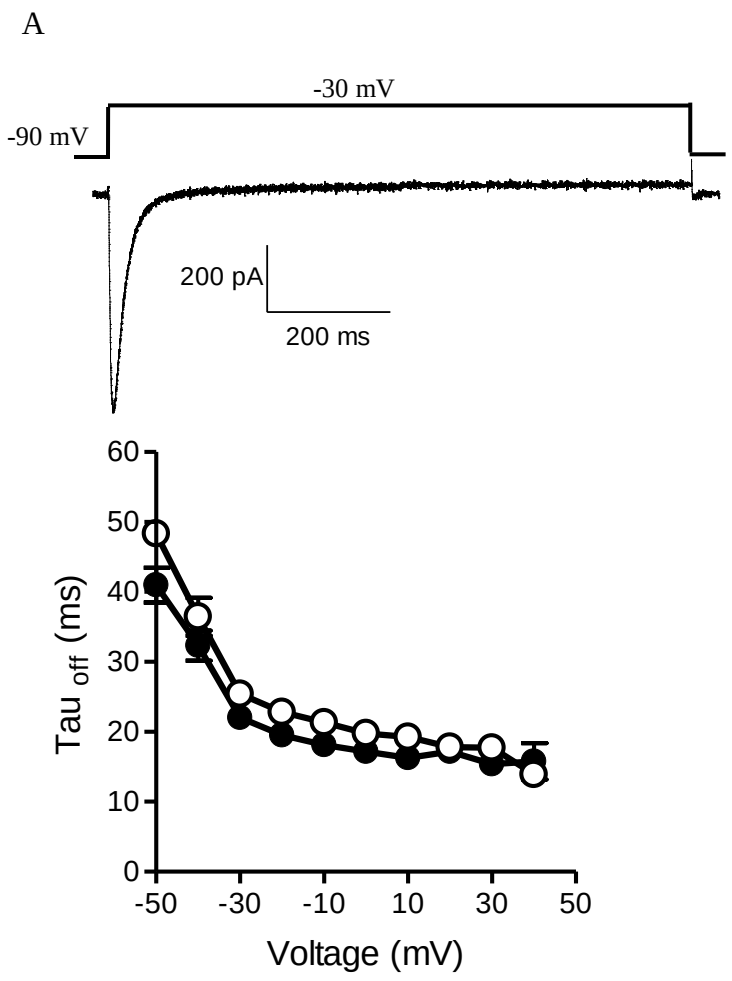

Figure 15. Effect of D-glucose on inactivation kinetics of $Ca_V3.2$ channels in HEK-293 cells.

(A) Representative trace showing a calcium current elicited from a V_h = -90 mV to a V_t = -30 mV. **(B)** Inactivation time constants (τ_{off}) from HEK-293 cells cultured in media containing 5.6 mM (open circles, n=10) or 25mM D-glucose (closed circles, n=9). Data shown are the means ± SEM. In some case, standard errors are less than symbol size. Observed differences between groups were not statistically significant (unpaired Student's *t-test*).

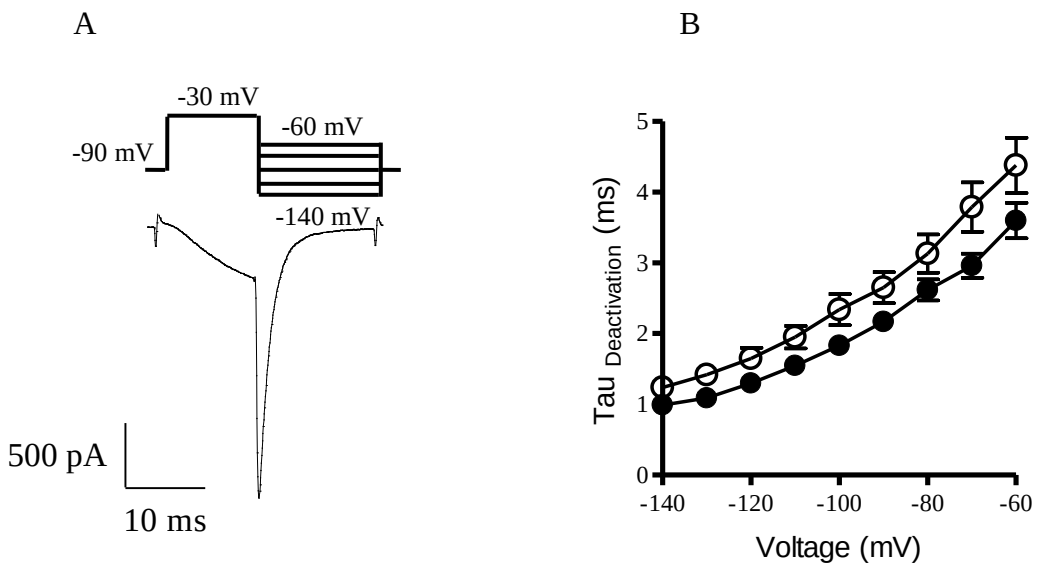

Figure 16. Effect of D-glucose on deactivation kinetics of $Ca_V3.2$ channels in HEK-293 cells.

(A) Representative trace showing a calcium current elicited from a V_h= -90mV to V_t= -30mV, followed by repolarizing pulses (-140 mV to -60 mV, as indicated). **(B)** Deactivation time constants ($\tau_{deactivation}$) from HEK-293 cells cultured in media containing 5.6 mM (open circles, n=10) or 25mM D-glucose (closed circles, n=9). Data shown are the means ± SEM. In some case, standard errors are less than symbol size. Observed differences between groups were not statistically significant (unpaired Student's *t-test*).

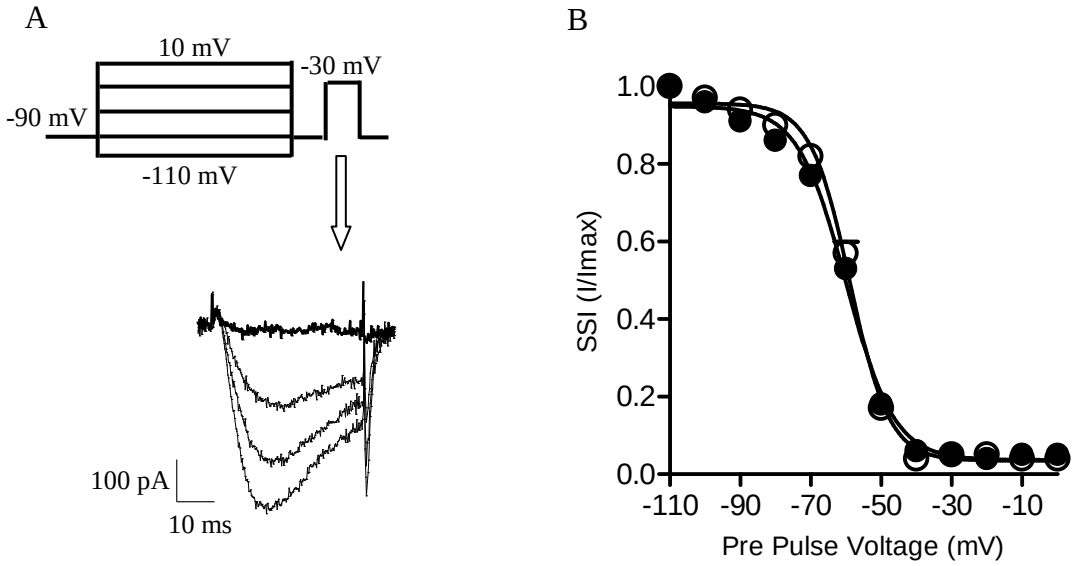

Figure 17. Effect of D-glucose on steady state inactivation of $Ca_V3.2$ channels in HEK-293 cells.

(A) Representative trace showing calcium currents elicited from a V_h = -90 mV to a Vt = -30 mV. Prior to the test pulse, cells were subjected to a prepulse voltage range from -110 mV to 10 mV, with 10 mV increments. **(B)** Steady state inactivation (SSI) curves obtained from HEK-293 cells cultured overnight in media containing 5.6 mM (open circles, n=12) and 25 mM (closed circles, n=7) D-glucose. Data shown are the means ± SEM. In some cases, standard errors are less than symbol size. Observed differences between groups were not statistically significant (unpaired Student's t-test).

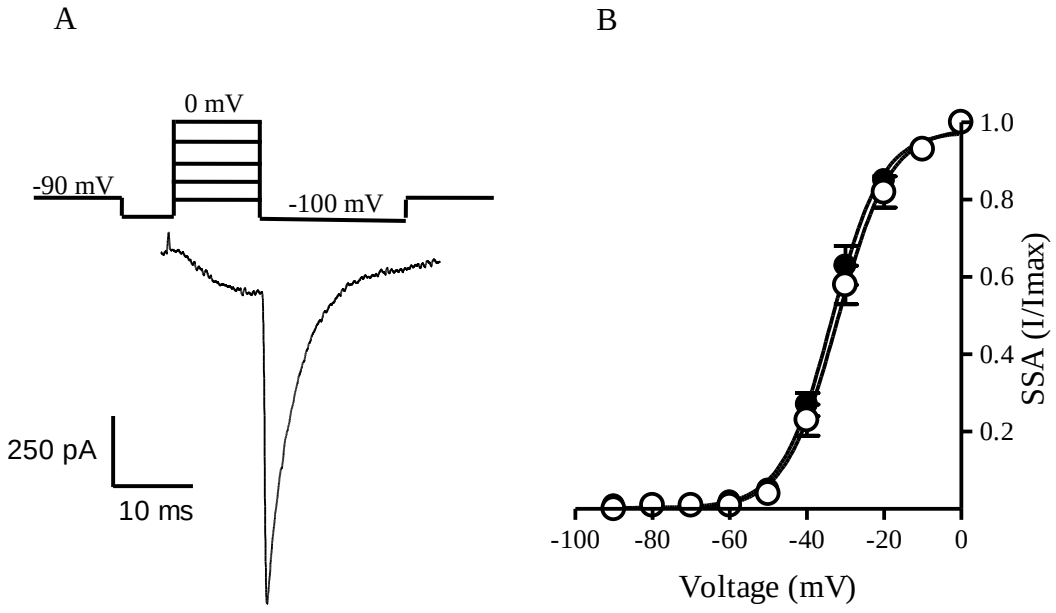

Figure 18. Effect of D-glucose on steady state activation of $Ca_V3.2$ channels in HEK-293 cells.

(A) Representative trace showing calcium currents elicited from a V_h = -90 mV to a Vt = -90 mV to 0 mV and repolarized to -100 mV to evoke inward tail currents. **(B)** Steady state activation (SSA) curves obtained from HEK-293 cells cultured in media containing 5.6 mM (open circles, n=11) and 25 mM D-glucose (closed circles, n=5). Data shown are the means ± SEM. In some cases, standard errors are less than symbol size. Observed differences between groups were not statistically significant (unpaired Student's t-test).

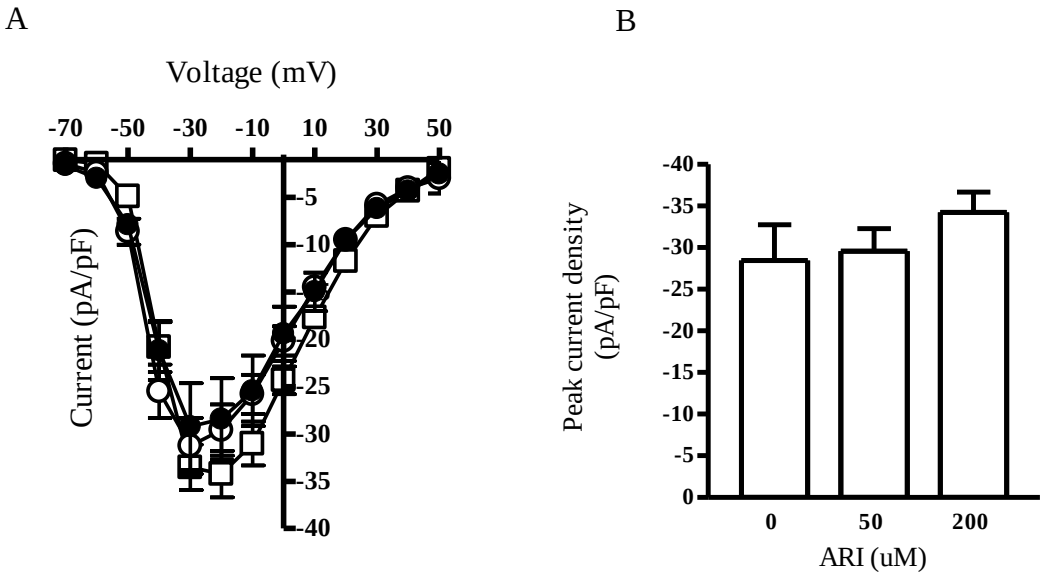

Figure 19. Effect of statil on D-glucose enhanced CaV3.2 current densities in HEK-293.

(A) Current-voltage relationship of $Ca_V3.2$ channels in HEK-293 cells cultured overnight in media containing 25 mM D-glucose in the absence (closed circle, n=3) or presence (50 μM, open circle (n=6) or 200 μM, open squares (n=5)) of statil, a potent aldose reductase inhibitor (ARI). **(B)** Bar graph comparing peak current densities shown in A. Data shown are the means ± SEM. Observed differences between groups were not statistically significant (one-way ANOVA, F(1.02), $p>0.05$).

DISCUSSION

LVA T type calcium currents are enhanced in sensory neurons of diabetic animals (Hall et al., 1995; Jagodic et al., 2007). However, there are limited studies examining the mechanism by with D-glucose may affect LVA channels. In this study, we show that elevated concentrations of D-glucose increase Ca^{2+} currents elicited from HEK-293 cells stably transfected with $Ca_V3.2_{\alpha 1H}$ channel subunit. The kinetics of channel opening was partially altered by elevated concentrations of D-glucose, while channel inactivation, deactivation, and steady state properties remained unaffected.

Enhanced T-type currents have been previously observed in rat neonatal cardiomyocytes cultured in high-glucose containing media (Li et al., 2005). Similarly, neuroblastoma cells cultured in high-glucose media demonstrate increased Na^+ currents with no changes in activation or inactivation kinetics (Wachtel et al., 1995). In this study, culturing cells overnight in high-glucose (25 mM) containing media enhanced by 30% peak $Ca_V3.2$ Ca^{2+} current density, compared to cells cultured in normal-glucose media. The rate of calcium channel activation was also faster in cells cultured for 24h in high-glucose media. However, elevated concentrations of D-glucose did not alter the kinetics of inactivation, deactivation or steady state channel properties, suggesting a mechanism(s) involving the regulation of channel opening.

Alternatively, D-glucose induced channel activation may not by itself explain the 30% enhancement of peak current density observed. This raises the possibility of increased channel number. However, HEK-293 cells used here stably express $Ca_V3.2$ α_{1H} channel subunits, free of regulatory control.

Under physiological conditions, extracellular D-glucose enters mammalian neurons by an insulin-independent facilitative transport mediated by GLUT 1 or GLUT 3 transporters where it is then metabolized by aerobic glycolysis. HEK-293cells used here similarly express insulin-independent GLUT 1 or GLUT 3 glucose transporters (Castro et al., 2008). In diabetes, where glucose homeostasis is disrupted, excess intraneuronal D-glucose is atypically shunted to the polyol pathway where it is reduced by aldose reductase to sorbitol and by sorbitol dehydrogenase to fructose. Glucose-dependent non-enzymatic glycation of intracellular proteins may alter calcium channel function. However, in this study, inhibition of the polyol pathway with the aldose reductase inhibitor statil did not prevent D-glucose induced increases in current densities in HEK-293 cells, suggesting an alternative mechanism of pathogenicity.

Conversely, enzymatic glycosylation is reported to alter gating properties in voltage activated sodium channels (Zhang et al., 1999; Stocker and Bennett, 2006). To address this possibility, studies designed to examine the effect of neuraminidase-associated deglycosylation of calcium channels in cultured HEK-293 cells are currently underway. We speculate that neuraminidase will reverse D-glucose induced enhancement of current density and normalize the rate of channel activation.

In some animal models of diabetes, aberrant elevation of diacylglycerol (DAG) with concomitant activation of protein kinase C (PKC) have been described (Koya and King, 1998). PKC activation, by its effects on cellular permeability, contractility, cell growth, apoptosis, cytokine activation, and cell adhesion is known to mediate various complications of diabetes (Sheetz and King, 2002). In many cell culture studies,

increasing the media glucose concentration from 5.6 mM to 22 mM results in elevated DAG levels and increased PKC activity (Ayo et al., 1991; Shiba et al., 1993). Recent studies have demonstrated that the $Ca_V3.2_{\alpha 1H}$ channel currents are enhanced by PKC stimulants (Park et al., 2003) as well as by activation of protein kinase A. However, there are conflicting reports regarding the ability of PKC isoforms to regulate Ca^{2+} T-currents (Perez-Reyes, 2003). In this study, PKC induced enhancement of T-currents remains a distinct possibility and further studies are needed to address the involvement DAG-PKC pathways in modulating Ca^{2+} currents from $Ca_V3.2$ α_{1H} channel subunits. Recent reports also suggest differential $Ca_V3.2$ channel behavior depending on the phosphorylation state of this channel (Hu et al., 2009; Perez-Reyes, 2009). Hyperglycemia-induced alteration of $Ca_V3.2$ α_{1H} subunit phosphorylation state remains another possibility to explain our observed effects.

SUMMARY

In this dissertation, we examined the effect of forced-exercise as a behavioral intervention in modulating the pathogenesis of tactile hyperalgesia in a rat model of type 1 diabetes mellitus. Diabetic rats that were forced to exercise demonstrated a delayed onset of pain intolerance in the form of tactile sensitivity, compared to non-exercised rats (Chapter 2). In addition, diabetes failed to induce nerve conduction deficits in rats subjected to forced exercise. The small diameter DRG neurons, which are generally associated with pain conduction, demonstrated increased high and low voltage activated Ca^{2+} currents in diabetic animals (Chapter 2). Enhanced HVA and LVA Ca^{2+} currents promote increased release of nociceptive neurotransmitters and increased cellular excitability respectively. Exercise partially prevented the diabetes-associated increase in HVA, but not LVA Ca^{2+} currents. In addition, diabetes induced depolarizing shift in LVA steady state inactivation property, indicative of increased cell membrane excitability, was normalized by forced-exercise (Chapter 2). *In-vitro* studies confirmed the role of high-glucose levels in the enhancement of LVA Ca^{2+} currents (Chapter 3). However, high-glucose did not change the LVA SSI *in vitro,* suggesting the presence of an additional factor(s) present in diabetes that are responsible for the observed SSI shift (see Figure 20). Forced-exercise protected against diabetes-induced changes in HVA and LVA Ca^{2+}channel functions, independent of blood glucose control.

The mechanism by which forced-exercise protects against diabetes associated neuropathic pain may involve dynamic changes in opiodergic tone. In this study, we

found that forced-exercise induced protection against diabetes-induced tactile hyperalgesia was reversed by naloxone, a non-selective opiate receptor antagonist (Chapter 2).

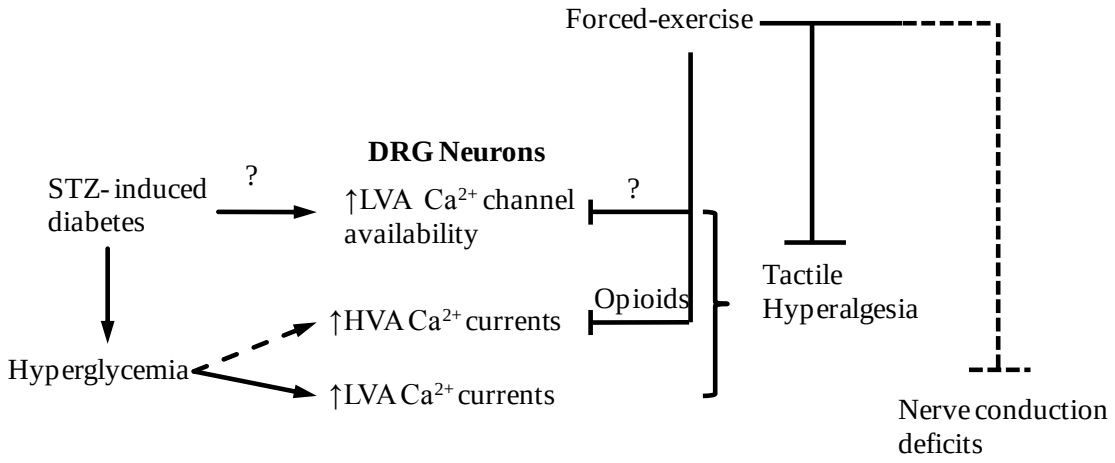

Figure 20. Working model to explain how forced-exercise may mediate its protection against diabetes-associated neuropathic pain

Consistent with these findings, previous studies have suggested a role of altered opioid-mediated analgesia in diabetes. Reduced potency of morphine and decreased endogenous opioid levels in diabetic animals are thought to contribute towards a lowered opioidergic tone, resulting in an enhanced pain state. Opioids inhibit HVA Ca^{2+} currents through their respective G protein-coupled receptors (μ, γ, δ). Of particular significance, opiate receptor activation does *not* affect LVA Ca^{2+} currents nor alter LVA Ca^{2+} channel steady state properties. Hence, in our study, the role of opioids in forced-exercise mediated

protection against diabetes-associated tactile hyperalgesia is most likely limited to their effects on HVA calcium channels. This suggests the presence of additional forced-exercise induced factors acting directly or indirectly with the LVA Ca^{2+} channels to delay the onset of diabetes associated tactile hyperalgesia.

One possibility may involve heterotrimeric G-protein mediated regulation of LVA Ca^{2+} channels. $Ca_V3.2$ predominately expressed in DRG nociceptive neurons is inhibited by the direct binding of $G_{\beta 2\gamma 2}$ to the channel α_1 subunit (Wolfe et al., 2003; DePuy et al., 2006). Alternatively, LVA Ca^{2+} channels are known to be modulated by nitrous oxide (Todorovic et al., 2001), phenytoin (Todorovic and Lingle, 1998), certain neuroactive steroids (Pathirathna et al., 2005), endocannabinoids (Ross et al., 2009) and by the actin binding protein, Kelch-like 1 (Aromolaran et al., 2010). However, the exact molecular determinants of LVA Ca^{2+} channel regulation remains unknown. Exercise-facilitated neuroplastic changes in pain management remains an exciting direction by which new neuroprotective therapeutic strategies can be tested.

This dissertative study raises awareness of the importance of exercise in the management of diabetic neuropathy. Even though our study did not show an effect of exercise on blood glucose control, exercise had a protective effect on diabetes-induced pain intolerance and nerve conduction deficits via a non-glucose dependent mechanism. This finding has several positive clinical implications. Many patients with diabetes suffer from nerve complications regardless of strict blood glucose control; exercise in these patients may be beneficial in managing their neurological symptoms. These findings also

add to the existing clinical literature about the need for supplementing pharmacological measures with physical exercise in the management of DM.

To the best of our knowledge, this is the first study to demonstrate the effect of forced-exercise on voltage gated calcium channels. Direct inhibition of VGCC as a clinical strategy for alleviation of painful symptoms in diabetic neuropathy is limited by the lack of available N- and T-type selective calcium channel blockers. It would be of interest to examine clinically the combined effect of exercise and conventional (L-type) calcium channel blockers on painful diabetic neuropathy. This research study also underscores the role of exercise in acute pain management. Many patients with painful conditions arising due to neuralgias, spinal cord trauma, and many forms of neuritis, have enhanced sensitivity to mildly painful stimuli. Based on this study, it would be worth exploring the benefits of exercise in these conditions as well.

REFERENCES

Adler AI, Boyko EJ, Ahroni JH, Stensel V, Forsberg RC, Smith DG (1997) Risk factors for diabetic peripheral sensory neuropathy. Results of the Seattle Prospective Diabetic Foot Study. Diabetes Care 20:1162-1167.

Ahlgren SC, Levine JD (1993) Mechanical hyperalgesia in streptozotocin-diabetic rats. Neuroscience 52:1049-1055.

Ahmed N, Thornalley PJ, Dawczynski J, Franke S, Strobel J, Stein G, Haik GM (2003) Methylglyoxal-derived hydroimidazolone advanced glycation end-products of human lens proteins. Invest Ophthalmol Vis Sci 44:5287-5292.

Albillos A, Neher E, Moser T (2000) R-Type Ca2+ channels are coupled to the rapid component of secretion in mouse adrenal slice chromaffin cells. J Neurosci 20:8323-8330.

Altier C, Zamponi GW (2004) Targeting Ca2+ channels to treat pain: T-type versus N-type. Trends Pharmacol Sci 25:465-470.

Altier C, Dale CS, Kisilevsky AE, Chapman K, Castiglioni AJ, Matthews EA, Evans RM, Dickenson AH, Lipscombe D, Vergnolle N, Zamponi GW (2007) Differential role of N-type calcium channel splice isoforms in pain. J Neurosci 27:6363-6373.

Anderson JW, Kendall CW, Jenkins DJ (2003) Importance of weight management in type 2 diabetes: review with meta-analysis of clinical studies. J Am Coll Nutr 22:331-339.

Arnoult C, Cardullo RA, Lemos JR, Florman HM (1996) Activation of mouse sperm T-type Ca2+ channels by adhesion to the egg zona pellucida. Proc Natl Acad Sci U S A 93:13004-13009.

Aromolaran KA, Benzow KA, Koob MD, Piedras-Renteria ES (2007) The Kelch-like protein 1 modulates P/Q-type calcium current density. Neuroscience 145:841-850.

Aromolaran KA, Benzow KA, Cribbs LL, Koob MD, Piedras-Renteria ES (2010) T-type current modulation by the actin-binding protein Kelch-like 1 (KLHL1). Am J Physiol Cell Physiol.

Ayo SH, Radnik R, Garoni JA, Troyer DA, Kreisberg JI (1991) High glucose increases

diacylglycerol mass and activates protein kinase C in mesangial cell cultures. Am J Physiol 261:F571-577.

Bagnasco S, Balaban R, Fales HM, Yang YM, Burg M (1986) Predominant osmotically active organic solutes in rat and rabbit renal medullas. J Biol Chem 261:5872-5877.

Balducci S, Iacobellis G, Parisi L, Di Biase N, Calandriello E, Leonetti F, Fallucca F (2006) Exercise training can modify the natural history of diabetic peripheral neuropathy. J Diabetes Complications 20:216-223.

Baron R, Tolle TR, Gockel U, Brosz M, Freynhagen R (2009) A cross-sectional cohort survey in 2100 patients with painful diabetic neuropathy and postherpetic neuralgia: Differences in demographic data and sensory symptoms. Pain 146:34-40.

Bean BP (1989) Classes of calcium channels in vertebrate cells. Annu Rev Physiol 51:367-384.

Bean BP (1992) Whole-cell recording of calcium channel currents. Methods Enzymol 207:181-193.

Bensaoula T, Ottlecz A (2001) Biochemical and ultrastructural studies in the neural retina and retinal pigment epithelium of STZ-diabetic rats: effect of captopril. J Ocul Pharmacol Ther 17:573-586.

Bhattacharjee A, Whitehurst RM, Jr., Zhang M, Wang L, Li M (1997) T-type calcium channels facilitate insulin secretion by enhancing general excitability in the insulin-secreting beta-cell line, INS-1. Endocrinology 138:3735-3740.

Bijlenga P, Liu JH, Espinos E, Haenggeli CA, Fischer-Lougheed J, Bader CR, Bernheim L (2000) T-type alpha 1H Ca2+ channels are involved in Ca2+ signaling during terminal differentiation (fusion) of human myoblasts. Proc Natl Acad Sci U S A 97:7627-7632.

Blustein JE, McLaughlin M, Hoffman JR (2006) Exercise effects stress-induced analgesia and spatial learning in rats. Physiol Behav 89:582-586.

Boulton AJ, Armstrong WD, Scarpello JH, Ward JD (1983) The natural history of painful diabetic neuropathy--a 4-year study. Postgrad Med J 59:556-559.

Bourinet E, Zamponi GW (2005) Voltage gated calcium channels as targets for analgesics. Curr Top Med Chem 5:539-546.

Bourinet E, Alloui A, Monteil A, Barrere C, Couette B, Poirot O, Pages A, McRory J, Snutch TP, Eschalier A, Nargeot J (2005) Silencing of the Cav3.2 T-type calcium

channel gene in sensory neurons demonstrates its major role in nociception. Embo J 24:315-324.

Bowles DK (2000) Adaptation of ion channels in the microcirculation to exercise training. Microcirculation 7:25-40.

Brian Rodrigues PP, Mary L. Battell, John H. McNeill (1999) Streptozotocin-Induced Diabetes: Induction, Mechanism(s), and Dose Dependency. In: Experimental Models of Diabetes (McNeil JH, ed), pp 3-18: CRC Press LLC.

Brueggemann LI, Martin BL, Barakat J, Byron KL, Cribbs LL (2005) Low voltage-activated calcium channels in vascular smooth muscle: T-type channels and AVP-stimulated calcium spiking. Am J Physiol Heart Circ Physiol 288:H923-935.

Calcutt NA (2002) Potential mechanisms of neuropathic pain in diabetes. Int Rev Neurobiol 50:205-228.

Calcutt NA, Jorge MC, Yaksh TL, Chaplan SR (1996) Tactile allodynia and formalin hyperalgesia in streptozotocin-diabetic rats: effects of insulin, aldose reductase inhibition and lidocaine. Pain 68:293-299.

Cao YQ (2006) Voltage-gated calcium channels and pain. Pain 126:5-9.

Carbone E, Lux HD (1984) A low voltage-activated, fully inactivating Ca channel in vertebrate sensory neurones. Nature 310:501-502.

Carvalho KA, Cunha RC, Vialle EN, Osiecki R, Moreira GH, Simeoni RB, Francisco JC, Guarita-Souza LC, Oliveira L, Zocche L, Olandoski M (2008) Functional outcome of bone marrow stem cells (CD45(+)/CD34(-)) after cell therapy in acute spinal cord injury: in exercise training and in sedentary rats. Transplant Proc 40:847-849.

Castaneda C, Layne JE, Munoz-Orians L, Gordon PL, Walsmith J, Foldvari M, Roubenoff R, Tucker KL, Nelson ME (2002) A randomized controlled trial of resistance exercise training to improve glycemic control in older adults with type 2 diabetes. Diabetes Care 25:2335-2341.

Castellano A, Wei X, Birnbaumer L, Perez-Reyes E (1993) Cloning and expression of a neuronal calcium channel beta subunit. J Biol Chem 268:12359-12366.

Castro MA, Angulo C, Brauchi S, Nualart F, Concha, II (2008) Ascorbic acid participates in a general mechanism for concerted glucose transport inhibition and lactate transport stimulation. Pflugers Arch 457:519-528.

Catterall WA (2000) Structure and regulation of voltage-gated Ca2+ channels. Annu Rev Cell Dev Biol 16:521-555.

CDC (2007) General information and national estimates on diabetes in the United States,2007. In: Department of Health and Human Services, Centers for Disease Control and Prevention,2008.

Center for Disease Control U (2005) National Diabetes Fact Sheet. In.

Center for Disease Control U (2008) General information and national estimates on diabetes in the United States,2008. In: Department of Health and Human Services, Centers for Disease Control and Prevention,2008.

Chaplan SR, Bach FW, Pogrel JW, Chung JM, Yaksh TL (1994) Quantitative assessment of tactile allodynia in the rat paw. J Neurosci Methods 53:55-63.

Chemin J, Monteil A, Perez-Reyes E, Bourinet E, Nargeot J, Lory P (2002) Specific contribution of human T-type calcium channel isotypes (alpha(1G), alpha(1H) and alpha(1I)) to neuronal excitability. J Physiol 540:3-14.

Chen SR, Pan HL (2003) Antinociceptive effect of morphine, but not mu opioid receptor number, is attenuated in the spinal cord of diabetic rats. Anesthesiology 99:1409-1414.

Chen X, Levine JD (2001) Hyper-responsivity in a subset of C-fiber nociceptors in a model of painful diabetic neuropathy in the rat. Neuroscience 102:185-192.

Cherian PV, Kamijo M, Angelides KJ, Sima AA (1996) Nodal Na(+)-channel displacement is associated with nerve-conduction slowing in the chronically diabetic BB/W rat: prevention by aldose reductase inhibition. J Diabetes Complications 10:192-200.

Choi S, Na HS, Kim J, Lee J, Lee S, Kim D, Park J, Chen CC, Campbell KP, Shin HS (2007) Attenuated pain responses in mice lacking Ca(V)3.2 T-type channels. Genes Brain Behav 6:425-431.

Chytrova G, Ying Z, Gomez-Pinilla F (2008) Exercise normalizes levels of MAG and Nogo-A growth inhibitors after brain trauma. Eur J Neurosci 27:1-11.

Courteix C, Eschalier A, Lavarenne J (1993) Streptozocin-induced diabetic rats: behavioural evidence for a model of chronic pain. Pain 53:81-88.

Cribbs LL, Lee JH, Yang J, Satin J, Zhang Y, Daud A, Barclay J, Williamson MP, Fox M, Rees M, Perez-Reyes E (1998) Cloning and characterization of alpha1H from human heart, a member of the T-type Ca2+ channel gene family. Circ Res 83:103-109.

DCCT (1993) The effect of intensive treatment of diabetes on the development and progression of long-term complications in insulin-dependent diabetes mellitus. The Diabetes Control and Complications Trial Research Group. N Engl J Med 329:977-986.

DCCT (1995) The effect of intensive diabetes therapy on the development and progression of neuropathy. The Diabetes Control and Complications Trial Research Group. Ann Intern Med 122:561-568.

De Waard M, Liu H, Walker D, Scott VE, Gurnett CA, Campbell KP (1997) Direct binding of G-protein betagamma complex to voltage-dependent calcium channels. Nature 385:446-450.

Dennis L. Kasper EB, Anthony S. Fauci, Stephen L. Hauser, Dan L. Longo, J. Larry Jameson, Kurt J. Isselbacher (2010) Powers Alvin C, "Chapter 338. Diabetes Mellitus" (Chapter). In: Harrison's Principles of Internal Medicine, "Chapter 338. Diabetes Mellitus", 17th Edition Edition.

DePuy SD, Yao J, Hu C, McIntire W, Bidaud I, Lory P, Rastinejad F, Gonzalez C, Garrison JC, Barrett PQ (2006) The molecular basis for T-type Ca2+ channel inhibition by G protein beta2gamma2 subunits. Proc Natl Acad Sci U S A 103:14590-14595.

Dobretsov M, Hastings SL, Stimers JR, Zhang JM (2001) Mechanical hyperalgesia in rats with chronic perfusion of lumbar dorsal root ganglion with hyperglycemic solution. J Neurosci Methods 110:9-15.

Dogrul A, Gardell LR, Ossipov MH, Tulunay FC, Lai J, Porreca F (2003) Reversal of experimental neuropathic pain by T-type calcium channel blockers. Pain 105:159-168.

Donner H, Rau H, Walfish PG, Braun J, Siegmund T, Finke R, Herwig J, Usadel KH, Badenhoop K (1997) CTLA4 alanine-17 confers genetic susceptibility to Graves' disease and to type 1 diabetes mellitus. J Clin Endocrinol Metab 82:143-146.

Doyle LM, Roberts BL (2004) Functional recovery and axonal growth following spinal cord transection is accelerated by sustained L-DOPA administration. Eur J Neurosci 20:2008-2014.

Duran-Jimenez B, Dobler D, Moffatt S, Rabbani N, Streuli CH, Thornalley PJ, Tomlinson DR, Gardiner NJ (2009) Advanced Glycation Endproducts in extracellular matrix proteins contribute to the failure of sensory nerve regeneration in diabetes. Diabetes.

Dyck PJ, Kratz KM, Karnes JL, Litchy WJ, Klein R, Pach JM, Wilson DM, O'Brien PC, Melton LJ, 3rd, Service FJ (1993) The prevalence by staged severity of various types of diabetic neuropathy, retinopathy, and nephropathy in a population-based cohort: the Rochester Diabetic Neuropathy Study. Neurology 43:817-824.

Eizirik DL, Mandrup-Poulsen T (2001) A choice of death--the signal-transduction of immune-mediated beta-cell apoptosis. Diabetologia 44:2115-2133.

Emerick AJ, Richards MP, Kartje GL, Neafsey EJ, Stubbs EB, Jr. (2005) Experimental diabetes attenuates cerebral cortical-evoked forelimb motor responses. Diabetes 54:2764-2771.

Estacio RO, Regensteiner JG, Wolfel EE, Jeffers B, Dickenson M, Schrier RW (1998) The association between diabetic complications and exercise capacity in NIDDM patients. Diabetes Care 21:291-295.

Felix R (1999) Voltage-dependent Ca2+ channel alpha2delta auxiliary subunit: structure, function and regulation. Receptors Channels 6:351-362.

Fisher MA, Langbein WE, Collins EG, Williams K, Corzine L (2007) Physiological improvement with moderate exercise in type II diabetic neuropathy. Electromyogr Clin Neurophysiol 47:23-28.

Foret A, Quertainmont R, Botman O, Bouhy D, Amabili P, Brook G, Schoenen J, Franzen R (2010) Stem cells in the adult rat spinal cord: plasticity after injury and treadmill training exercise. J Neurochem 112:762-772.

Forman LJ, Estilow S, Lewis M, Vasilenko P (1986) Streptozocin diabetes alters immunoreactive beta-endorphin levels and pain perception after 8 wk in female rats. Diabetes 35:1309-1313.

Fox AP, Nowycky MC, Tsien RW (1987) Kinetic and pharmacological properties distinguishing three types of calcium currents in chick sensory neurones. J Physiol 394:149-172.

Fuchsjager-Mayrl G, Pleiner J, Wiesinger GF, Sieder AE, Quittan M, Nuhr MJ, Francesconi C, Seit HP, Francesconi M, Schmetterer L, Wolzt M (2002) Exercise training improves vascular endothelial function in patients with type 1 diabetes. Diabetes Care 25:1795-1801.

Goldshmit Y, Lythgo N, Galea MP, Turnley AM (2008) Treadmill training after spinal cord hemisection in mice promotes axonal sprouting and synapse formation and improves motor recovery. J Neurotrauma 25:449-465.

Gooch C, Podwall D (2004) The diabetic neuropathies. Neurologist 10:311-322.

Gordienko DV, Clausen C, Goligorsky MS (1994) Ionic currents and endothelin signaling in smooth muscle cells from rat renal resistance arteries. Am J Physiol 266:F325-341.

Govindaraju SR, Curry BD, Bain JLW, Riley DA (2007) Nerve damage occurs at a wide range of vibration frequencies. International Journal of Industrial Ergonomics 38:687-692.

Greene DA, Winegrad AI (1979) In vitro studies of the substrates for energy production and the effects of insulin on glucose utilization in the neural components of peripheral nerve. Diabetes 28:878-887.

Greene DA, Arezzo JC, Brown MB (1999) Effect of aldose reductase inhibition on nerve conduction and morphometry in diabetic neuropathy. Zenarestat Study Group. Neurology 53:580-591.

Gribkoff VK (2006) The role of voltage-gated calcium channels in pain and nociception. Semin Cell Dev Biol 17:555-564.

Hadley RW, Lederer WJ (1991) Properties of L-type calcium channel gating current in isolated guinea pig ventricular myocytes. J Gen Physiol 98:265-285.

Hall KE, Sima AA, Wiley JW (1995) Voltage-dependent calcium currents are enhanced in dorsal root ganglion neurones from the Bio Bred/Worchester diabetic rat. J Physiol 486 (Pt 2):313-322.

Hall KE, Liu J, Sima AA, Wiley JW (2001) Impaired inhibitory G-protein function contributes to increased calcium currents in rats with diabetic neuropathy. J Neurophysiol 86:760-770.

Hargreaves K, Dubner R, Brown F, Flores C, Joris J (1988) A new and sensitive method for measuring thermal nociception in cutaneous hyperalgesia. Pain 32:77-88.

Hashimoto L, Habita C, Beressi JP, Delepine M, Besse C, Cambon-Thomsen A, Deschamps I, Rotter JI, Djoulah S, James MR, et al. (1994) Genetic mapping of a susceptibility locus for insulin-dependent diabetes mellitus on chromosome 11q. Nature 371:161-164.

Haslbeck KM, Neundorfer B, Schlotzer-Schrehardtt U, Bierhaus A, Schleicher E, Pauli E, Haslbeck M, Hecht M, Nawroth P, Heuss D (2007) Activation of the RAGE pathway: a general mechanism in the pathogenesis of polyneuropathies? Neurol Res 29:103-110.

Hatakeyama S, Wakamori M, Ino M, Miyamoto N, Takahashi E, Yoshinaga T, Sawada K, Imoto K, Tanaka I, Yoshizawa T, Nishizawa Y, Mori Y, Niidome T, Shoji S

(2001) Differential nociceptive responses in mice lacking the alpha(1B) subunit of N-type Ca(2+) channels. Neuroreport 12:2423-2427.

Herlitze S, Hockerman GH, Scheuer T, Catterall WA (1997) Molecular determinants of inactivation and G protein modulation in the intracellular loop connecting domains I and II of the calcium channel alpha1A subunit. Proc Natl Acad Sci U S A 94:1512-1516.

Heron SE, Khosravani H, Varela D, Bladen C, Williams TC, Newman MR, Scheffer IE, Berkovic SF, Mulley JC, Zamponi GW (2007) Extended spectrum of idiopathic generalized epilepsies associated with CACNA1H functional variants. Ann Neurol 62:560-568.

Hill MA, Ege EA (1994) Active and passive mechanical properties of isolated arterioles from STZ-induced diabetic rats. Effect of aminoguanidine treatment. Diabetes 43:1450-1456.

Hille B (1994) Modulation of ion-channel function by G-protein-coupled receptors. Trends Neurosci 17:531-536.

Himsworth HP (1949) The syndrome of diabetes mellitus and its causes. Lancet 1:465-473.

Hogan P, Dall T, Nikolov P (2003) Economic costs of diabetes in the US in 2002. Diabetes Care 26:917-932.

Holz GGt, Rane SG, Dunlap K (1986) GTP-binding proteins mediate transmitter inhibition of voltage-dependent calcium channels. Nature 319:670-672.

Howarth FC, Marzouqi FM, Al Saeedi AM, Hameed RS, Adeghate E (2009) The effect of a heavy exercise program on the distribution of pancreatic hormones in the streptozotocin-induced diabetic rat. Jop 10:485-491.

Hu C, Depuy SD, Yao J, McIntire WE, Barrett PQ (2009) Protein kinase A activity controls the regulation of T-type CaV3.2 channels by Gbetagamma dimers. J Biol Chem 284:7465-7473.

Huguenard JR (1996) Low-threshold calcium currents in central nervous system neurons. Annu Rev Physiol 58:329-348.

Hutchinson KJ, Gomez-Pinilla F, Crowe MJ, Ying Z, Basso DM (2004) Three exercise paradigms differentially improve sensory recovery after spinal cord contusion in rats. Brain 127:1403-1414.

Iftinca MC, Zamponi GW (2009) Regulation of neuronal T-type calcium channels. Trends Pharmacol Sci 30:32-40.

Ikeda SR (1996) Voltage-dependent modulation of N-type calcium channels by G-protein beta gamma subunits. Nature 380:255-258.

Ikeda SR, Dunlap K (1999) Voltage-dependent modulation of N-type calcium channels: role of G protein subunits. Adv Second Messenger Phosphoprotein Res 33:131-151.

Ikeda SR, Dunlap K (2007) Calcium channels diversify their signaling portfolio. Nat Neurosci 10:269-271.

Jagodic MM, Pathirathna S, Nelson MT, Mancuso S, Joksovic PM, Rosenberg ER, Bayliss DA, Jevtovic-Todorovic V, Todorovic SM (2007) Cell-specific alterations of T-type calcium current in painful diabetic neuropathy enhance excitability of sensory neurons. J Neurosci 27:3305-3316.

Jakobsen J (1976) Axonal dwindling in early experimental diabetes. II. A study of isolated nerve fibres. Diabetologia 12:547-553.

Jakus V, Rietbrock N (2004) Advanced glycation end-products and the progress of diabetic vascular complications. Physiol Res 53:131-142.

Janal MN (1996) Pain sensitivity, exercise and stoicism. J R Soc Med 89:376-381.

Johansson EB, Tjalve H (1978) Studies on the tissue-disposition and fate of [14C]streptozotocin with special reference to the pancreatic islets. Acta Endocrinol (Copenh) 89:339-351.

Julius D, Basbaum AI (2001) Molecular mechanisms of nociception. Nature 413:203-210.

Junod A, Lambert AE, Stauffacher W, Renold AE (1969) Diabetogenic action of streptozotocin: relationship of dose to metabolic response. J Clin Invest 48:2129-2139.

Kamei J, Ohhashi Y, Aoki T, Kawasima N, Kasuya Y (1992) Streptozotocin-induced diabetes selectively alters the potency of analgesia produced by mu-opioid agonists, but not by delta- and kappa-opioid agonists. Brain Res 571:199-203.

Kawada J, Okita M, Nishida M, Yoshimura Y, Toyooka K, Kubota S (1987) Protective effect of 4,6-O-ethylidene glucose against the cytotoxicity of streptozotocin in pancreatic beta cells in vivo: indirect evidence for the presence of a glucose transporter in beta cells. J Endocrinol 112:375-378.

Kay TW, Thomas HE, Harrison LC, Allison J (2000) The beta cell in autoimmune diabetes: many mechanisms and pathways of loss. Trends Endocrinol Metab 11:11-15.

Kim C, Jun K, Lee T, Kim SS, McEnery MW, Chin H, Kim HL, Park JM, Kim DK, Jung SJ, Kim J, Shin HS (2001) Altered nociceptive response in mice deficient in the alpha(1B) subunit of the voltage-dependent calcium channel. Mol Cell Neurosci 18:235-245.

Kim D, Park D, Choi S, Lee S, Sun M, Kim C, Shin HS (2003) Thalamic control of visceral nociception mediated by T-type Ca2+ channels. Science 302:117-119.

Kitabchi AE, Nyenwe EA (2006) Hyperglycemic crises in diabetes mellitus: diabetic ketoacidosis and hyperglycemic hyperosmolar state. Endocrinol Metab Clin North Am 35:725-751, viii.

Knowler WC, Barrett-Connor E, Fowler SE, Hamman RF, Lachin JM, Walker EA, Nathan DM (2002) Reduction in the incidence of type 2 diabetes with lifestyle intervention or metformin. N Engl J Med 346:393-403.

Koltyn KF (2000) Analgesia following exercise: a review. Sports Med 29:85-98.

Kouvaraki MA, Ajani JA, Hoff P, Wolff R, Evans DB, Lozano R, Yao JC (2004) Fluorouracil, doxorubicin, and streptozocin in the treatment of patients with locally advanced and metastatic pancreatic endocrine carcinomas. J Clin Oncol 22:4762-4771.

Koya D, King GL (1998) Protein kinase C activation and the development of diabetic complications. Diabetes 47:859-866.

Kramer AF, Erickson KI, Colcombe SJ (2006) Exercise, cognition, and the aging brain. J Appl Physiol 101:1237-1242.

Kumagai AK, Dwyer KJ, Pardridge WM (1994) Differential glycosylation of the GLUT1 glucose transporter in brain capillaries and choroid plexus. Biochim Biophys Acta 1193:24-30.

Kuphal KE, Fibuch EE, Taylor BK (2007) Extended swimming exercise reduces inflammatory and peripheral neuropathic pain in rodents. J Pain 8:989-997.

Kwon NS, Lee SH, Choi CS, Kho T, Lee HS (1994) Nitric oxide generation from streptozotocin. Faseb J 8:529-533.

Latham JR, Pathirathna S, Jagodic MM, Joo Choe W, Levin ME, Nelson MT, Yong Lee W, Krishnan K, Covey DF, Todorovic SM, Jevtovic-Todorovic V (2009) Selective

T-type calcium channel blockade alleviates hyperalgesia in ob/ob mice. Diabetes 58:2656-2665.

Lawlor MW, Richards MP, De Vries GH, Fisher MA, Stubbs EB, Jr. (2002) Antibodies to L-periaxin in sera of patients with peripheral neuropathy produce experimental sensory nerve conduction deficits. J Neurochem 83:592-600.

Lee JH, McCarty R (1990) Glycemic control of pain threshold in diabetic and control rats. Physiol Behav 47:225-230.

Lee JH, Cox DJ, Mook DG, McCarty RC (1990) Effect of hyperglycemia on pain threshold in alloxan-diabetic rats. Pain 40:105-107.

Li M, Zhang M, Huang L, Zhou J, Zhuang H, Taylor JT, Keyser BM, Whitehurst RM, Jr. (2005) T-type Ca2+ channels are involved in high glucose-induced rat neonatal cardiomyocyte proliferation. Pediatr Res 57:550-556.

Lin Y, McDonough SI, Lipscombe D (2004) Alternative splicing in the voltage-sensing region of N-Type CaV2.2 channels modulates channel kinetics. J Neurophysiol 92:2820-2830.

Lipnick JA, Lee TH (1996) Diabetic neuropathy. Am Fam Physician 54:2478-2484, 2487-2478.

Litwin SE, Raya TE, Anderson PG, Daugherty S, Goldman S (1990) Abnormal cardiac function in the streptozotocin-diabetic rat. Changes in active and passive properties of the left ventricle. J Clin Invest 86:481-488.

Liu Y, Terata K, Rusch NJ, Gutterman DD (2001) High glucose impairs voltage-gated K(+) channel current in rat small coronary arteries. Circ Res 89:146-152.

Llinas R, Ribary U (2001) Consciousness and the brain. The thalamocortical dialogue in health and disease. Ann N Y Acad Sci 929:166-175.

Llinas RR, Sugimori M, Cherksey B (1989) Voltage-dependent calcium conductances in mammalian neurons. The P channel. Ann N Y Acad Sci 560:103-111.

Lory P, Bidaud I, Chemin J (2006) T-type calcium channels in differentiation and proliferation. Cell Calcium 40:135-146.

Lynch J, Helmrich SP, Lakka TA, Kaplan GA, Cohen RD, Salonen R, Salonen JT (1996) Moderately intense physical activities and high levels of cardiorespiratory fitness reduce the risk of non-insulin-dependent diabetes mellitus in middle-aged men. Arch Intern Med 156:1307-1314.

Magee JC, Johnston D (1995) Characterization of single voltage-gated Na+ and Ca2+ channels in apical dendrites of rat CA1 pyramidal neurons. J Physiol 487 (Pt 1):67-90.

Mahler RJ, Adler ML (1999) Clinical review 102: Type 2 diabetes mellitus: update on diagnosis, pathophysiology, and treatment. J Clin Endocrinol Metab 84:1165-1171.

Maiorana A, O'Driscoll G, Cheetham C, Dembo L, Stanton K, Goodman C, Taylor R, Green D (2001) The effect of combined aerobic and resistance exercise training on vascular function in type 2 diabetes. J Am Coll Cardiol 38:860-866.

Malcangio M, Tomlinson DR (1998) A pharmacologic analysis of mechanical hyperalgesia in streptozotocin/diabetic rats. Pain 76:151-157.

Malmberg AB, Yaksh TL, Calcutt NA (1993) Anti-nociceptive effects of the GM1 ganglioside derivative AGF 44 on the formalin test in normal and streptozotocin-diabetic rats. Neurosci Lett 161:45-48.

Mandrup-Poulsen T (1996) The role of interleukin-1 in the pathogenesis of IDDM. Diabetologia 39:1005-1029.

Manschot SM, Gispen WH, Kappelle LJ, Biessels GJ (2003) Nerve conduction velocity and evoked potential latencies in streptozotocin-diabetic rats: effects of treatment with an angiotensin converting enzyme inhibitor. Diabetes Metab Res Rev 19:469-477.

Marquie G, Hadjiisky P, Arnaud O, Duhault J (1991) Development of macroangiopathy in sand rats (Psammomys obesus), an animal model of non-insulin-dependent diabetes mellitus: effect of gliclazide. Am J Med 90:55S-61S.

Martin AM, Blankenhorn EP, Maxson MN, Zhao M, Leif J, Mordes JP, Greiner DL (1999) Non-major histocompatibility complex-linked diabetes susceptibility loci on chromosomes 4 and 13 in a backcross of the DP-BB/Wor rat to the WF rat. Diabetes 48:50-58.

McCormick DA, Bal T (1997) Sleep and arousal: thalamocortical mechanisms. Annu Rev Neurosci 20:185-215.

Medori R, Autilio-Gambetti L, Jenich H, Gambetti P (1988) Changes in axon size and slow axonal transport are related in experimental diabetic neuropathy. Neurology 38:597-601.

Menz HB, Lord SR, St George R, Fitzpatrick RC (2004) Walking stability and sensorimotor function in older people with diabetic peripheral neuropathy. Arch Phys Med Rehabil 85:245-252.

Messinger RB, Naik AK, Jagodic MM, Nelson MT, Lee WY, Choe WJ, Orestes P, Latham JR, Todorovic SM, Jevtovic-Todorovic V (2009a) In vivo silencing of the Ca(V)3.2 T-type calcium channels in sensory neurons alleviates hyperalgesia in rats with streptozocin-induced diabetic neuropathy. Pain 145:184-195.

Messinger RB, Naik AK, Jagodic MM, Nelson MT, Lee WY, Choe WJ, Orestes P, Latham JR, Todorovic SM, Jevtovic-Todorovic V (2009b) In vivo silencing of the Ca(V)3.2 T-type calcium channels in sensory neurons alleviates hyperalgesia in rats with streptozocin-induced diabetic neuropathy. Pain.

Milani D, Malgaroli A, Guidolin D, Fasolato C, Skaper SD, Meldolesi J, Pozzan T (1990) Ca2+ channels and intracellular Ca2+ stores in neuronal and neuroendocrine cells. Cell Calcium 11:191-199.

Mintz IM, Adams ME, Bean BP (1992) P-type calcium channels in rat central and peripheral neurons. Neuron 9:85-95.

Moolenaar WH, Spector I (1978) Ionic currents in cultured mouse neuroblastoma cells under voltage-clamp conditions. J Physiol 278:265-286.

Morley GK, Mooradian AD, Levine AS, Morley JE (1984) Mechanism of pain in diabetic peripheral neuropathy. Effect of glucose on pain perception in humans. Am J Med 77:79-82.

Nathan DM (1996) The pathophysiology of diabetic complications: how much does the glucose hypothesis explain? Ann Intern Med 124:86-89.

Nelson MT, Todorovic SM (2006) Is there a role for T-type calcium channels in peripheral and central pain sensitization? Mol Neurobiol 34:243-248.

Nichol K, Deeny SP, Seif J, Camaclang K, Cotman CW (2009) Exercise improves cognition and hippocampal plasticity in APOE epsilon4 mice. Alzheimers Dement 5:287-294.

Nilius B, Hess P, Lansman JB, Tsien RW (1985) A novel type of cardiac calcium channel in ventricular cells. Nature 316:443-446.

Nishimura C, Lou MF, Kinoshita JH (1987) Depletion of myo-inositol and amino acids in galactosemic neuropathy. J Neurochem 49:290-295.

Nothias JM, Mitsui T, Shumsky JS, Fischer I, Antonacci MD, Murray M (2005) Combined effects of neurotrophin secreting transplants, exercise, and serotonergic drug challenge improve function in spinal rats. Neurorehabil Neural Repair 19:296-312.

Nowycky MC, Fox AP, Tsien RW (1985) Three types of neuronal calcium channel with different calcium agonist sensitivity. Nature 316:440-443.

Oates PJ (2002) Polyol pathway and diabetic peripheral neuropathy. Int Rev Neurobiol 50:325-392.

O'Connor PJ, Cook DB (1999) Exercise and pain: the neurobiology, measurement, and laboratory study of pain in relation to exercise in humans. Exerc Sport Sci Rev 27:119-166.

Okada N, Aizawa T, Yokokawa N, Kobayashi M, Moriya T, Shigematsu S, Shirota T, Komatsu M, Shinoda T, Yamada T, et al. (1992) Abnormal molecular weight profile of urinary protein in rats with streptozotocin-induced diabetes. Diabetes Res Clin Pract 18:1-9.

Pan JQ, Lipscombe D (2000) Alternative splicing in the cytoplasmic II-III loop of the N-type Ca channel alpha 1B subunit: functional differences are beta subunit-specific. J Neurosci 20:4769-4775.

Pardridge WM, Boado RJ, Farrell CR (1990) Brain-type glucose transporter (GLUT-1) is selectively localized to the blood-brain barrier. Studies with quantitative western blotting and in situ hybridization. J Biol Chem 265:18035-18040.

Park JY, Jeong SW, Perez-Reyes E, Lee JH (2003) Modulation of Ca(v)3.2 T-type Ca2+ channels by protein kinase C. FEBS Lett 547:37-42.

Park K, Lee Y, Park S, Lee S, Hong Y, Kil Lee S (2010) Synergistic effect of melatonin on exercise-induced neuronal reconstruction and functional recovery in a spinal cord injury animal model. J Pineal Res.

Partanen J, Niskanen L, Lehtinen J, Mervaala E, Siitonen O, Uusitupa M (1995) Natural history of peripheral neuropathy in patients with non-insulin-dependent diabetes mellitus. N Engl J Med 333:89-94.

Patel J, Tomlinson DR (1999) Nerve conduction impairment in experimental diabetes-proximodistal gradient of severity. Muscle Nerve 22:1403-1411.

Pathirathna S, Brimelow BC, Jagodic MM, Krishnan K, Jiang X, Zorumski CF, Mennerick S, Covey DF, Todorovic SM, Jevtovic-Todorovic V (2005) New evidence that both T-type calcium channels and GABAA channels are responsible for the potent peripheral analgesic effects of 5alpha-reduced neuroactive steroids. Pain 114:429-443.

Perez-Reyes E (2003) Molecular physiology of low-voltage-activated t-type calcium channels. Physiol Rev 83:117-161.

Perez-Reyes E (2009) G protein-mediated inhibition of Cav3.2 T-type channels revisited. Mol Pharmacol 77:136-138.

Perez-Reyes E, Cribbs LL, Daud A, Lacerda AE, Barclay J, Williamson MP, Fox M, Rees M, Lee JH (1998) Molecular characterization of a neuronal low-voltage-activated T-type calcium channel. Nature 391:896-900.

Perkins BA, Greene DA, Bril V (2001) Glycemic control is related to the morphological severity of diabetic sensorimotor polyneuropathy. Diabetes Care 24:748-752.

Pirart J (1977) [Diabetes mellitus and its degenerative complications: a prospective study of 4,400 patients observed between 1947 and 1973 (3rd and last part) (author's transl)]. Diabete Metab 3:245-256.

Polo-Parada L, Pilar G (1999) kappa- and mu-opioids reverse the somatostatin inhibition of Ca2+ currents in ciliary and dorsal root ganglion neurons. J Neurosci 19:5213-5227.

Powers AC (2006) Diabetes Mellitus. In: Harrison's Endocrinology (J LJ, ed), pp 283-332. New York: McGraw-Hill Medical Publishing Division.

Rakieten N, Rakieten ML, Nadkarni MV (1963) Studies on the diabetogenic action of streptozotocin (NSC-37917). Cancer Chemother Rep 29:91-98.

Randall A, Tsien RW (1995) Pharmacological dissection of multiple types of Ca2+ channel currents in rat cerebellar granule neurons. J Neurosci 15:2995-3012.

Reaven GM (1988) Banting lecture 1988. Role of insulin resistance in human disease. Diabetes 37:1595-1607.

Rechthand E, Smith QR, Rapoport SI (1985) Facilitated transport of glucose from blood into peripheral nerve. J Neurochem 45:957-964.

Rees DA, Alcolado JC (2005) Animal models of diabetes mellitus. Diabet Med 22:359-370.

Reisi P, Babri S, Alaei H, Sharifi MR, Mohaddes G, Noorbakhsh SM, Lashgari R (2010) Treadmill running improves long-term potentiation (LTP) defects in streptozotocin-induced diabetes at dentate gyrus in rats. Pathophysiology 17:33-38.

Reuter H (1983) Calcium channel modulation by neurotransmitters, enzymes and drugs. Nature 301:569-574.

Richardson JK, Sandman D, Vela S (2001) A focused exercise regimen improves clinical measures of balance in patients with peripheral neuropathy. Arch Phys Med Rehabil 82:205-209.

Robbins MJ, Sharp RA, Slonim AE, Burr IM (1980) Protection against streptozotocin-induced diabetes by superoxide dismutase. Diabetologia 18:55-58.

Ross HR, Gilmore AJ, Connor M (2009) Inhibition of human recombinant T-type calcium channels by the endocannabinoid N-arachidonoyl dopamine. Br J Pharmacol 156:740-750.

Sabatini BL, Svoboda K (2000) Analysis of calcium channels in single spines using optical fluctuation analysis. Nature 408:589-593.

Saegusa H, Kurihara T, Zong S, Kazuno A, Matsuda Y, Nonaka T, Han W, Toriyama H, Tanabe T (2001) Suppression of inflammatory and neuropathic pain symptoms in mice lacking the N-type Ca2+ channel. Embo J 20:2349-2356.

Sarkey JP, Richards MP, Stubbs EB, Jr. (2007) Lovastatin attenuates nerve injury in an animal model of Guillain-Barre syndrome. J Neurochem 100:1265-1277.

Satoh H (1995) Role of T-type Ca2+ channel inhibitors in the pacemaker depolarization in rabbit sino-atrial nodal cells. Gen Pharmacol 26:581-587.

Schmalbruch H (1986) Fiber composition of the rat sciatic nerve. Anat Rec 215:71-81.

Schnedl WJ, Ferber S, Johnson JH, Newgard CB (1994) STZ transport and cytotoxicity. Specific enhancement in GLUT2-expressing cells. Diabetes 43:1326-1333.

Scroggs RS, Fox AP (1992) Calcium current variation between acutely isolated adult rat dorsal root ganglion neurons of different size. J Physiol 445:639-658.

Seal EE, Eaton DC, Gomez LM, Ma H, Ling BN (1995) Extracellular glucose reduces the responsiveness of mesangial cell ion channels to angiotensin II. Am J Physiol 269:F389-397.

Shankarappa SA, Piedras-Renteria ES, Stubbs EB, Jr. (2009) Small diameter DRG neurons exhibit increased low-voltage activated T-type calcium currents in experimental diabetes. J Periph Nerv Syst 14:135.

Shankarappa SA, Sarkey JP, Richards MP, Stubbs J, E.B. (2007) Forced-exercise protects against the development of early tactile hyperalgesia in experimental diabetes. J Periph Nerv Syst 12:79.

Sheetz MJ, King GL (2002) Molecular understanding of hyperglycemia's adverse effects for diabetic complications. Jama 288:2579-2588.

Shiba T, Inoguchi T, Sportsman JR, Heath WF, Bursell S, King GL (1993) Correlation of diacylglycerol level and protein kinase C activity in rat retina to retinal circulation. Am J Physiol 265:E783-793.

Shin JB, Martinez-Salgado C, Heppenstall PA, Lewin GR (2003) A T-type calcium channel required for normal function of a mammalian mechanoreceptor. Nat Neurosci 6:724-730.

Sima AA, Nathaniel V, Bril V, McEwen TA, Greene DA (1988a) Histopathological heterogeneity of neuropathy in insulin-dependent and non-insulin-dependent diabetes, and demonstration of axo-glial dysjunction in human diabetic neuropathy. J Clin Invest 81:349-364.

Sima AA, Zhang WX, Tze WJ, Tai J, Nathaniel V (1988b) Diabetic neuropathy in STZ-induced diabetic rat and effect of allogeneic islet cell transplantation. Morphometric analysis. Diabetes 37:1129-1136.

Simon GS, Dewey WL (1981) Narcotics and diabetes. I. The effects of streptozotocin-induced diabetes on the antinociceptive potency of morphine. J Pharmacol Exp Ther 218:318-323.

Singh R, Barden A, Mori T, Beilin L (2001) Advanced glycation end-products: a review. Diabetologia 44:129-146.

Singleton JR, Smith AG, Bromberg MB (2001) Increased prevalence of impaired glucose tolerance in patients with painful sensory neuropathy. Diabetes Care 24:1448-1453.

Smith AG, Russell J, Feldman EL, Goldstein J, Peltier A, Smith S, Hamwi J, Pollari D, Bixby B, Howard J, Singleton JR (2006) Lifestyle intervention for pre-diabetic neuropathy. Diabetes Care 29:1294-1299.

Smith MT, Cabot PJ, Ross FB, Robertson AD, Lewis RJ (2002) The novel N-type calcium channel blocker, AM336, produces potent dose-dependent antinociception after intrathecal dosing in rats and inhibits substance P release in rat spinal cord slices. Pain 96:119-127.

Splawski I, Yoo DS, Stotz SC, Cherry A, Clapham DE, Keating MT (2006) CACNA1H mutations in autism spectrum disorders. J Biol Chem 281:22085-22091.

Stanley EF, Mirotznik RR (1997) Cleavage of syntaxin prevents G-protein regulation of presynaptic calcium channels. Nature 385:340-343.

Stea A, Tomlinson WJ, Soong TW, Bourinet E, Dubel SJ, Vincent SR, Snutch TP (1994) Localization and functional properties of a rat brain alpha 1A calcium channel reflect similarities to neuronal Q- and P-type channels. Proc Natl Acad Sci U S A 91:10576-10580.

Stocker PJ, Bennett ES (2006) Differential sialylation modulates voltage-gated Na+ channel gating throughout the developing myocardium. J Gen Physiol 127:253-265.

Sugimura K, Windebank AJ, Natarajan V, Lambert EH, Schmid HH, Dyck PJ (1980) Interstitial hyperosmolarity may cause axis cylinder shrinkage in streptozotocin diabetic nerve. J Neuropathol Exp Neurol 39:710-721.

Talavera K, Nilius B (2006) Biophysics and structure-function relationship of T-type Ca2+ channels. Cell Calcium 40:97-114.

Talley EM, Cribbs LL, Lee JH, Daud A, Perez-Reyes E, Bayliss DA (1999) Differential distribution of three members of a gene family encoding low voltage-activated (T-type) calcium channels. J Neurosci 19:1895-1911.

Tanasescu M, Leitzmann MF, Rimm EB, Hu FB (2003) Physical activity in relation to cardiovascular disease and total mortality among men with type 2 diabetes. Circulation 107:2435-2439.

Tavee J, Zhou L (2009) Small fiber neuropathy: A burning problem. Cleve Clin J Med 76:297-305.

Tedford HW, Zamponi GW (2006) Direct G protein modulation of Cav2 calcium channels. Pharmacol Rev 58:837-862.

Tesfaye S, Harris ND, Wilson RM, Ward JD (1992) Exercise-induced conduction velocity increment: a marker of impaired peripheral nerve blood flow in diabetic neuropathy. Diabetologia 35:155-159.

Thorburn AW, Gumbiner B, Brechtel G, Henry RR (1990) Effect of hyperinsulinemia and hyperglycemia on intracellular glucose and fat metabolism in healthy subjects. Diabetes 39:22-30.

Todorovic SM, Lingle CJ (1998) Pharmacological properties of T-type Ca2+ current in adult rat sensory neurons: effects of anticonvulsant and anesthetic agents. J Neurophysiol 79:240-252.

Todorovic SM, Jevtovic-Todorovic V (2007) Regulation of T-type calcium channels in the peripheral pain pathway. Channels (Austin) 1:238-245.

Todorovic SM, Jevtovic-Todorovic V, Mennerick S, Perez-Reyes E, Zorumski CF (2001) Ca(v)3.2 channel is a molecular substrate for inhibition of T-type calcium currents in rat sensory neurons by nitrous oxide. Mol Pharmacol 60:603-610.

Tomlinson DR, Gardiner NJ (2008) Glucose neurotoxicity. Nat Rev Neurosci 9:36-45.

Trimarchi T, Pachuau J, Shepherd A, Dey D, Martin-Caraballo M (2009) CNTF-evoked activation of JAK and ERK mediates the functional expression of T-type Ca2+ channels in chicken nodose neurons. J Neurochem 108:246-259.

Tsakiridou E, Bertollini L, de Curtis M, Avanzini G, Pape HC (1995) Selective increase in T-type calcium conductance of reticular thalamic neurons in a rat model of absence epilepsy. J Neurosci 15:3110-3117.

Tsien RW, Lipscombe D, Madison DV, Bley KR, Fox AP (1988) Multiple types of neuronal calcium channels and their selective modulation. Trends Neurosci 11:431-438.

Turk J, Corbett JA, Ramanadham S, Bohrer A, McDaniel ML (1993) Biochemical evidence for nitric oxide formation from streptozotocin in isolated pancreatic islets. Biochem Biophys Res Commun 197:1458-1464.

U.K.prospective-diabetes-study (1995) U.K. prospective diabetes study 16. Overview of 6 years' therapy of type II diabetes: a progressive disease. U.K. Prospective Diabetes Study Group. Diabetes 44:1249-1258.

Uchigata Y, Yamamoto H, Kawamura A, Okamoto H (1982) Protection by superoxide dismutase, catalase, and poly(ADP-ribose) synthetase inhibitors against alloxan- and streptozotocin-induced islet DNA strand breaks and against the inhibition of proinsulin synthesis. J Biol Chem 257:6084-6088.

Umpierrez GE, Kitabchi AE (2003) Diabetic ketoacidosis: risk factors and management strategies. Treat Endocrinol 2:95-108.

Wachtel RE, Kraske SA, Yorek MA (1995) Sodium channels in cultured neuroblastoma cells grown in high glucose or L-fucose. J Membr Biol 145:187-192.

Wang S, Ma JZ, Zhu SS, Xu DJ, Zou JG, Cao KJ (2008) Swimming training can affect intrinsic calcium current characteristics in rat myocardium. Eur J Appl Physiol 104:549-555.

Wild S, Roglic G, Green A, Sicree R, King H (2004) Global prevalence of diabetes: estimates for the year 2000 and projections for 2030. Diabetes Care 27:1047-1053.

Williams J, Haller VL, Stevens DL, Welch SP (2008) Decreased basal endogenous opioid levels in diabetic rodents: effects on morphine and delta-9-tetrahydrocannabinoid-induced antinociception. Eur J Pharmacol 584:78-86.

Willow M, Carmody J, Carroll P (1980) The effects of swimming in mice on pain perception and sleeping time in response to hypnotic drugs. Life Sci 26:219-224.

Wilson GL, Patton NJ, McCord JM, Mullins DW, Mossman BT (1984) Mechanisms of streptozotocin- and alloxan-induced damage in rat B cells. Diabetologia 27:587-591.

Wittmack EK, Rush AM, Hudmon A, Waxman SG, Dib-Hajj SD (2005) Voltage-gated sodium channel Nav1.6 is modulated by p38 mitogen-activated protein kinase. J Neurosci 25:6621-6630.

Wolfe JT, Wang H, Howard J, Garrison JC, Barrett PQ (2003) T-type calcium channel regulation by specific G-protein betagamma subunits. Nature 424:209-213.

Woolf CJ, Mannion RJ (1999) Neuropathic pain: aetiology, symptoms, mechanisms, and management. Lancet 353:1959-1964.

Wu LG, Borst JG, Sakmann B (1998) R-type Ca2+ currents evoke transmitter release at a rat central synapse. Proc Natl Acad Sci U S A 95:4720-4725.

Xu X, Best PM (1992) Postnatal changes in T-type calcium current density in rat atrial myocytes. J Physiol 454:657-672.

Yagihashi S, Kamijo M, Watanabe K (1990a) Reduced myelinated fiber size correlates with loss of axonal neurofilaments in peripheral nerve of chronically streptozotocin diabetic rats. Am J Pathol 136:1365-1373.

Yagihashi S, Kamijo M, Ido Y, Mirrlees DJ (1990b) Effects of long-term aldose reductase inhibition on development of experimental diabetic neuropathy. Ultrastructural and morphometric studies of sural nerve in streptozocin-induced diabetic rats. Diabetes 39:690-696.

Yang Z, Chen M, Fialkow LB, Ellett JD, Wu R, Nadler JL (2003) The novel anti-inflammatory compound, lisofylline, prevents diabetes in multiple low-dose streptozotocin-treated mice. Pancreas 26:e99-104.

Zamponi GW, Lewis RJ, Todorovic SM, Arneric SP, Snutch TP (2009) Role of voltage-gated calcium channels in ascending pain pathways. Brain Res Rev 60:84-89.

Zhang Y, Hartmann HA, Satin J (1999) Glycosylation influences voltage-dependent gating of cardiac and skeletal muscle sodium channels. J Membr Biol 171:195-207.

Zhang Y, Proenca R, Maffei M, Barone M, Leopold L, Friedman JM (1994) Positional cloning of the mouse obese gene and its human homologue. Nature 372:425-432.

Zhong X, Liu JR, Kyle JW, Hanck DA, Agnew WS (2006) A profile of alternative RNA splicing and transcript variation of CACNA1H, a human T-channel gene candidate for idiopathic generalized epilepsies. Hum Mol Genet 15:1497-1512.

Zhou Z, January CT (1998) Both T- and L-type Ca2+ channels can contribute to excitation-contraction coupling in cardiac Purkinje cells. Biophys J 74:1830-1839.

Ziegler D, Luft D (2002) Clinical trials for drugs against diabetic neuropathy: can we combine scientific needs with clinical practicalities? Int Rev Neurobiol 50:431-463.

Ziv E, Shafrir E, Kalman R, Galer S, Bar-On H (1999) Changing pattern of prevalence of insulin resistance in Psammomys obesus, a model of nutritionally induced type 2 diabetes. Metabolism 48:1549-1554.

Zotova EG, Christ GJ, Zhao W, Tar M, Kuppam SD, Arezzo JC (2007) Effects of fidarestat, an aldose reductase inhibitor, on nerve conduction velocity and bladder function in streptozotocin-treated female rats. J Diabetes Complications 21:187-195.

Zuccollo A, Navarro M, Frontera M, Cueva F, Carattino M, Catanzaro OL (1999) The involvement of kallikrein-kinin system in diabetes type I (insulitis). Immunopharmacology 45:69-74.

VITA

The author, Sahadev Shankarappa, was born on October 21, 1976 in Shimoga, India to Gowthami and Shankar. In November 2000, Sahadev got his medical degree from Kempegowda Institute of Medical Sciences in Bangalore, India. After medical school, he travelled to the United States to join the School of Public Health at the University of North Carolina, Chapel Hill and obtained his Masters of Public Health (MPH) degree in July 2003.

In August of 2004, Sahadev entered the graduate program in Neuroscience at Loyola University Chicago. In spring of 2005, Sahadev joined the laboratory of Dr. Evan B. Stubbs, Jr. at the Edward Hines, Jr. VA Hospital. For his research project, Sahadev studied the effect of exercise on the onset and progression of pain in experimental diabetic neuropathy. In collaboration with Dr. Erika Piedras-Renteria, he studied how voltage gated calcium channels might play a role in exercise induced protection against painful diabetic neuropathy.

At Loyola, Sahadev met his wife Shivanee, also a gradate student at Loyola and they recently had a baby daughter, Aarika. After obtaining his Ph.D, Sahadev will move to Boston to work as a postdoctoral fellow in research involving drug delivery and biomaterials at the Massachusetts Institute of Technology in the laboratory of Dr. Daniel Kohane.